Copyright Undertaking

This thesis is protected by copyright, with all rights reserved.

By reading and using the thesis, the reader understands and agrees to the following terms:

1. The reader will abide by the rules and legal ordinances governing copyright regarding the use of the thesis.

2. The reader will use the thesis for the purpose of research or private study only and not for distribution or further reproduction or any other purpose.

3. The reader agrees to indemnify and hold the University harmless from and against any loss, damage, cost, liability or expenses arising from copyright infringement or unauthorized usage.

ROBUST OPTIMAL DESIGN OF HVAC SYSTEMS CONSIDERING UNCERTAINTY AND RELIABILITY

CHENG QI

Ph.D

The Hong Kong Polytechnic University

2017

The Hong Kong Polytechnic University

Department of Building Services Engineering

Robust Optimal Design of HVAC Systems

Considering Uncertainty and Reliability

Cheng Qi

A thesis submitted in partial fulfillment of the requirements

for the Degree of Doctor of Philosophy

September, 2016

CERTIFICATE OF ORIGINALITY

i

I hereby declare that this thesis is my own work and that, to the best of my knowledge and belief, it reproduces no materials previously published or written, nor material that has been accepted for the award of any other degree or diploma, except where due acknowledgment has been made in the text.

I also declare that the intellectual content of this thesis is the product of my own work, except to the extent that assistance from others in the project's design and conception or in style, presentation and linguistic expression is acknowledged.

Cheng Qi

Department of Building Services Engineering

The Hong Kong Polytechnic University

Hong Kong, China

September, 2016

ABSTRACT

Abstract of thesis entitled: Robust Optimal Design of HVAC Systems

            Considering Uncertainty and Reliability

Submitted by   : Cheng Qi

For the degree of   : Doctor of Philosophy at The Hong Kong Polytechnic

            University in September, 2016

This thesis presents a robust optimal design method of HVAC systems in buildings concerning the uncertainties of design inputs and the reliability of system components. The developed methods include uncertainty-based optimal design considering uncertainties only, robust optimal design concerning uncertainties and reliability, probabilistic approach for generating the cooling load distribution of required accuracy and reliability quantification methods (including Markov method and sequential Monte Carlo simulation).

Monte Carlo simulation is a broad class of computational algorithms that rely on repeated random sampling to obtain numerical results. In this thesis, Monte Carlo simulation is used for generating cooling load distributions. In order to represent the characteristics of the uncertainties of design input in cooling load distribution, sufficient number of Monte Carlo simulation is required. A probabilistic approach is developed to determine the minimum number of Monte Carlo simulations for accuracy.

Reliability analysis or assessment is necessary to avoid/reduce losses caused by both the normal situations and abnormal situations such as the failure of some components. Markov method and sequential Monte Carlo simulation are frequently used to conduct

the reliability assessment in other fields such as electrical engineering. In this thesis, both the two methods are used to conduct the reliability assessment of HVAC system. Availability risk cost is considered as the index to evaluate the system reliability.

An uncertainty-based optimal design is developed and used to optimize the chiller plant design. It ensures that the chiller plant operate at a high efficiency and the minimum annual total cost (including annual operational cost and annualized capital cost) could be achieved under various possible cooling load conditions, considering the uncertain variables in cooling load calculation (i.e., weather conditions). A case study on the chiller plant of a building in Hong Kong is conducted to demonstrate the design process and validate the uncertainty-based optimal design.

A robust optimal design method is proposed to optimize the design of chiller plants concerning impacts of uncertainty in the design input data and the system reliability in operation. Monte Carlo simulation is used to generate the cooling load distribution and Markov method is used to obtain the probability distribution of system states considering the different failure rates between constant-speed chillers and variable-speed chillers. A case study of a building in Hong Kong is conducted to demonstrate the design process and validate the robust optimal design method. Comparisons are made among the conventional design, uncertainty-based optimal design and robust optimal design. The results show that the system could operate at a relatively high efficiency and the minimum total annual total cost could be achieved under various possible cooling load conditions considering the uncertainties and system reliability.

A robust optimal design method is proposed to optimize the design of chilled water pump systems while concerning the uncertainties of design inputs and models as well as the component reliability in operation. Monte Carlo simulation is used to generate the cooling load distribution and hydraulic resistance distribution by quantifying the uncertainties. Markov method is used to obtain the probability distribution of the system state. Under different control methods, this proposed design method minimizes the annual total cost. A case study on a building in Hong Kong is conducted to demonstrate the design process and validate the robust optimal design method. Results show that the system could operate at a relatively high efficiency and the minimum total life-cycle cost could be achieved.

A robust optimal design based on sequential Monte Carlo simulation is proposed to optimize the design of cooling water system. Monte Carlo simulation is used to obtain accurate cooling load distributions, power consumptions and unmet cooling loads. Convergence assessment is conducted to terminate the sampling process of Monte Carlo simulation. Under different penalty ratios and repair rates, this proposed design minimizes the annual total cost of cooling water system. A case study of a building in Hong Kong is conducted to demonstrate the design process and test the robust optimal design method. The results show that the minimum total cost could be achieved under various possible cooling load conditions considering the uncertainties of design inputs and reliability of system components.

PUBLICATIONS ARISING FROM THIS THESIS

Journal Papers

2017   Qi Cheng, Shengwei Wang, Chengchu Yan. Sequential Monte Carlo Simulation for Robust Optimal Design of Cooling Water System with Quantified Uncertainty and Reliability. Energy 2017, 118: 489-501.

2017   Qi Cheng, Shengwei Wang, Chengchu Yan, Fu Xiao. Probabilistic approach for uncertainty-based optimal design of chiller plants in buildings. Applied Energy 2017, 185 (2): 1613-1624.

2016   Qi Cheng, Shengwei Wang, Chengchu Yan. Robust optimal design of chilled water systems in buildings with quantified uncertainty and reliability for minimized life-cycle cost. Energy and Buildings 2016, 126: 159-169.

Conference Papers

2016   Qi Cheng, Shengwei Wang, Wenjie Gang. Performance evaluation for the optimal design of chiller plants concerning uncertainty and reliability. *12th REHVA World Congress*, 22-25 May 2016, Aalborg, Denmark.

2015   Qi Cheng, Chengchu Yan, Shengwei Wang. Robust optimal design of chiller plants based on cooling load distribution. *7th International Conference on Applied Energy (ICAE2015)*, 28-31 March 2015, Abu Dhabi, United Arab Emirates.

2015   Qi Cheng, Shengwei Wang, Chengchu Yan, Fu Xiao. Investigation on the energy performance of air-handling units with rotatable cooling coil in an underground station. *The 2nd International Conference on Sustainable Urbanization*, 7-9 January 2015, Hong Kong.

ACKNOWLEDGEMENTS

I would like to express my sincerest appreciation to Professor Shengwei Wang, my supervisor, for his readily available supervision, valuable suggestions, patient encouragement and continuous support during the course of this research. Also, I would like to thank Professor Fu Xiao, my co-supervisor, for her support and encouragement to me over entire process of my PhD study.

I would also like to thank all colleagues in the research team, especially Dr. Diance Gao, Dr. Chengchu Yan, Dr. Xue Xue, Dr. Borui Cui and Dr. Weijie Gang. Their talents and diligence always inspire and encourage me to be better.

Finally, I would like to dedicate this thesis to my parents, Laiyou Cheng and Yanrong He, for their unconditional trust and support in my life. I also would like to express my appreciation to my girlfriend, Binbin Chen, for her comprehensively support and encouragement in the past year.

TABLE OF CONTENTS

LIST OF FIGURES

LIST OF TABLES

NOMENCLATURE

TC	total cost
OC	operation cost
CC	capital cost
RC	availability risk cost
EC	equipment cost
SC	space cost
COP	coefficient of performance
PLR	part load ratio
CL	cooling load
N	number
a	minimum number of simulations
b	minimum number of simulations
C	capacity
D	coefficient
e	coefficient
f	coefficient
g	coefficient
MTTF	mean time to failure
MTTR	mean time to repair
p	probability
m	water flow rate

H	pump head
t	temperature
c	specific heat of water
S	resistance coefficient
B	convergence band
i	number of simulations
k	The kth simulation
Σ	summation

Greek symbols

η	efficiency
μ	repair rate
α	coefficient
β	coefficient
γ	confidence level
λ	failure rate
Δ	variation

Subscripts

n	total number of components
T	total
op	operating
C	constant-speed chiller
V	variable-speed chiller

re	required
ava	available
pu	pump
ch	chiller
cwp	cooling water pump
cot	cooling tower
VFD	variable speed drive
set	set-point
in	inlet
out	outlet
wb	wet bulb
tot	total

CHAPTER 1 INTRODUCTION

1.1 Background and Motivation

The building sector is usually the largest energy consumer in most countries and districts worldwide, especially in the metropolis such as Hong Kong (EMSD 2014; CSD 1998). In commercial buildings, about 40-60% of the total electricity consumption is consumed by the Heating, Ventilation and Air-Conditioning (HVAC) system (Wang and Ma 2008). Effective measures to achieve the energy saving of HVAC systems are vital for alleviating the energy shortage and reducing the greenhouse gas emissions. It is found that a significant energy-saving potential could be achieved through the optimal design and energy efficient operation (Lee et al. 2001; Lee and Lee 2007).

Two main ways can be used to achieve the energy saving of HVAC systems. One is to use energy-efficient HVAC systems which can meet the thermal comfort requirement with less energy usage. The other is to use supervisory and optimal control of HVAC systems. The optimal control strategies, such as chiller sequence control (Wang and Ma 2008), pressure set-point resetting and demand control ventilation, are frequently used in the HVAC system.

Optimal design of HVAC systems needs to be investigated for avoiding or reducing the possible energy waste and adverse impacts in the design stage. Appropriate design of HVAC systems is significant because it not only relates to the capital cost, but also will

influence the operation cost of the entire cooling system throughout the life cycle. Determination of the design cooling capacity plays a significant role in the selection and sizing of HVAC systems, which depends on the cooling load. Three conventional methods are often used to calculate the cooling load and determine the size and configuration of the HVAC system (ASHRAE 2009; Lu 2008; Rudoy and Cuba 1979):

1) The simplest way is to estimate the cooling load based on an index for a typical building in typical climate zones. With the gross floor area and the index, the maximum cooling load can be determined and the capacity of the HVAC system can be obtained.

2) The cooling load of one design day or one hour is calculated, where the outdoor weather data are selected based on the statistical outdoor weather condition and maximum values are assigned for variables representing the internal heat sources such as the occupants, lighting, plug-in equipment, etc.

3) Professional simulation platforms such as EnergyPlus (2015), DOE-2 (2009), TRNSYS (2015) and DeST (2011) are employed to get the annual cooling load based on typical meteorological year (TMY) data and schedules of the occupants, lighting and plug-in equipment. TMY data for typical regions are used. Based on the peak cooling load and the cooling load distribution, the design cooling capacity and configuration of the HVAC system can be determined.

The cooling loads obtained from the above three methods are commonly subject to a deterministic model-based simulation. Even for the third method, parameters used in the calculation are constants for each time step, like the number of occupants and lighting, etc. However, in actual operations, these parameters are very likely to be different from

those used in the design calculation, which will cause the deviation between actual cooling load and the design cooling load. Due to the inevitable uncertainty of weather data, indoor occupants and internal heat gain, designers tend to select a much larger capacity than the peak duty (e.g., multiply a safety factor) so that the HVAC system can fulfil the cooling demand under any uncertain conditions for safety (Domínguez-Muñoz et al. 2010 and Sun et al. 2014). This may result in significant oversizing of HVAC system and thus a large amount of energy waste because the actual operating conditions are seldom the same as the design condition (Yik et al. 1999; Djunaedy et al. 2011 and Woradechjumroen et al. 2014). To reduce the oversizing of HVAC systems and the associated energy waste, some measures, such as using a detailed simulation method, statistic weather data, model calibration and even experiments, have been recommended (Domínguez-Muñoz et al. 2010). However, these methods cannot help to eliminate or minimize the oversizing due to the adoption of conservative criteria for estimating the cooling loads of buildings (Cheng et al. 2015). Besides, some engineers think they can grossly oversize the HVAC system and then use variable speed drives to maintain high efficiency and reduce operation cost during the part load period (Walski et al. 2003; Hartman 2001; Koury et al. 2001; Tassou and Qureshi 1998 and Ma and Wang 2011).

Reliability can be defined as the probability of successful operation or performance of systems and their related equipment, with minimum risk of loss or disaster (Stapelberg 2009). It is another very important issue in the design of HVAC system besides uncertainty. In conventional design and optimization methods, the components or subsystems of HVAC systems are always assumed to be healthy (i.e. they only have a system state).

However, in fact, they might be unavailable due to maintenance or failures. Failure of one component may result in the incapability to fulfill the cooling demands of users. The most commonly used way is to install a standby or backup component of equal capacity in addition to the basic working systems to supply sufficient cooling in case that the equipment fails to operate or needs to be maintained (ASHRAE Handbook 2012). Such a conventional design method is reasonable but not optimal. Without considering the uncertainty and reliability in a quantified way, the empirical method may result in serious oversizing problems, low efficiency and energy waste.

To address the above issues, the research in this thesis, therefore, focuses on developing a new optimal design method to obtain the appropriately sized and configured HVAC systems (including chillers, chilled water systems and cooling water systems) by considering uncertainties of design inputs and reliability of system component in quantified ways. The proposed design method could ensure that the HVAC system can always operate at high-energy performance even though the actual operating conditions deviate from the design conditions significantly due to uncertainties of design inputs and reliability of system components.

1.2 Aim and Objectives

The aim of this study is develop robust optimal design methods for the HVAC system. The new methods should render the designed systems to maintain good performance when uncertainty or failures occur in operation.

The objectives of this study can be summarized as follows:

1) To generate accurate cooling load distributions considering uncertainties of design inputs. Factors that contain uncertainty are classified and quantified. A probabilistic approach is developed to determine the minimum number of Monte Carlo simulations for achieving the required accuracy.

2) To quantify the reliability of system components by using Markov method and sequential Monte Carlo simulation. Comparison between Markov method and sequential Monte Carlo simulation is conducted.

3) To develop an uncertainty-based optimal design method of chiller plant when only considering uncertainties at design stage. By using the proposed design method, the design cooling capacity and configuration of chiller plant can be determined based on the minimized total life-cycle cost.

4) To develop a robust optimal design method of chiller plant when considering both the uncertainties of design inputs and reliability of system components. Different failure rates are considered for constant-speed chiller and variable-speed chiller.

5) To develop a robust optimal design method of chilled water system under different control methods considering the uncertainties of design inputs and reliability of system components. The chilled water pumps are assumed to be identical in parallel and have the same failure rate.

6) To develop a robust optimal design method of cooling water system based on sequential Monte Carlo simulation considering the uncertainties of design inputs and reliability of system components. Each individual cooling water pump and each

individual cooling tower are assumed to be independent from the other components.

1.3 Organization of this Thesis

In this thesis, Chapter 2 presents a comprehensive literature review on the conventional design method of HVAC systems. The oversizing problem of HVAC systems and subsystems is discussed. In addition, the uncertainty in HVAC fields is introduced in this chapter. The uncertainty analysis and reliability assessment of building energy systems are also discussed.

Chapter 3 presents the design optimization method of HVAC systems and the quantification methods of uncertainty and reliability. The concept of robust optimal design used in HVAC systems is presented. Four optimal design methods are proposed for handling different uncertainty and reliability conditions. The proposed methods contain the uncertainty-based optimal design, robust optimal design with different failure rates, robust optimal design with the same failure rate and robust optimal design based on sequential Monte Carlo simulation, which are used in Chapters 4, 5, 6 and 7 respectively for the design of HVAC subsystems.

Chapter 4 presents a probabilistic approach for generating the accurate cooling load distribution considering the uncertainties of inputs. In the design optimization of HVAC systems, generating the accurate cooling load distribution is the key process to determine the optimal configuration of HVAC systems. The proposed approach is used to evaluate the stability of cooling load distribution and determine the minimum

simulation number. In addition, the minimum Monte Carlo simulations corresponding to each threshold are determined.

Chapter 5 comprehensively presents the quantification methods of reliability. The probability distribution of system state is generated by the reliability assessment, which plays an important role in the robust optimal design of HVAC systems. In this chapter, both the Markov method and sequential Monte Carlo simulation are used to quantify the reliability. A comparison is made between Markov method and sequential Monte Carlo simulation.

Chapter 6 presents an uncertainty-based optimal design method of chiller plant based on probabilistic approach. Only uncertainties in the cooling load of a building are considered. A statistic method is developed to conduct the convergence assessment of generating accurate cooling load distributions. Design cooling capacity and configuration of the chiller plant are optimized based on the generated cooling load distributions. Total life-cycle cost of the chiller plant using the uncertainty-based optimal design method is analyzed and compared with that using the conventional design method.

Chapter 7 presents a robust optimal design method of chiller plant concerning both uncertainty and reliability simultaneously. Different from the Chapter 4, the reliability assessment of chiller plant is considered. Moreover, the failure rate difference between constant-speed chiller and variable-speed chiller is considered and quantified. The cooling load distribution is generated based on the quantified uncertainty. Searching

range of the cooling capacity of chiller plant is obtained based on the cooling load distribution. Based on the probability distribution of chiller plant state, design cooling capacity and configuration of the chiller plant are optimized. Total life-cycle cost of the chiller plant using the robust optimal design method is analyzed.

Chapter 8 presents a robust optimal design method of chilled water systems considering both uncertainty and reliability simultaneously. In this chapter, the chilled water pumps are assumed to have the same failure rate. Design chilled water flow rate and pump head are determined based on the cooling load distribution and hydraulic resistance distribution respectively. Under different control methods, the total pump flow capacity and number/size of pump are optimized. Total life-cycle cost of the chilled water system using the robust optimal design method is analyzed.

Chapter 9 presents a robust optimal design method of cooling water system based on sequential Monte Carlo simulation. Different from Chapters 5 and 6 which use the Markov method to quantify the reliability, in this chapter sequential Monte Carlo simulation is used for the quantification of reliability. Uncertainties in the cooling load and reliability of system components are quantified. A statistic method is used to conduct the convergence assessment of obtaining the accurate cooling load distribution, operation cost and unmet cooling load. Design cooling water flow rate and configurations of the condenser water pumps and cooling towers are optimized. Total life-cycle cost of the cooling water system using the robust design method is analyzed and compared with that using the conventional method and uncertainty-based optimal

design.

Chapter 10 presents the main conclusions and contributions. Shortcomings of this study

and recommendations for the future study are presented.

CHAPTER 2 LITERATURE REVIEW

2.1 An Overview

Since this study attempts to develop robust optimal design methods considering uncertainties of design inputs and reliability of system components, previous research efforts on the design and optimization of HVAC systems, uncertainty study and reliability assessment in building energy systems are reviewed.

Section 2.2 presents the conventional design methods of chillers, chilled water systems (i.e. chilled water pumps) and cooling water systems (i.e. cooling water pumps and cooling towers). In Section 2.3, applications of uncertainty analysis in building energy systems are reviewed, especially in the design of HVAC subsystems. In Section 2.4, reliability assessment and its application in building energy systems are reviewed. In Section 2.5, research on the above three sections is summarized. Limitations of existing studies and challenges for future work are also presented.

2.2 Conventional Design of HVAC Systems

A typical central air-conditioning system is usually comprised of a chilled water loop, a condenser water loop and indoor air loops (Lu et al. 2004), as shown in Fig.2.1. In this thesis, the research focuses on the chilled water loop and condenser water loop. The main components of a chilled water loop are comprised of chiller evaporators, chilled water pumps and AHUs. Chiller evaporators transfer the cooling generated by refrigerant into the chilled water. Chilled water pumps circulate chilled water from

chiller evaporators to AHUs. The main components of a condenser water loop consist of chiller condensers, cooling water pumps, cooling towers and fans (ASHRAE handbook 2009). Chiller condensers transfer the indoor cooling load and the heat generated by the compressors into the cooling water. Cooling water pumps circulate cooling water from chiller condensers to cooling towers. The heat load is rejected to the ambient through heat transfer and evaporation by cooling towers.
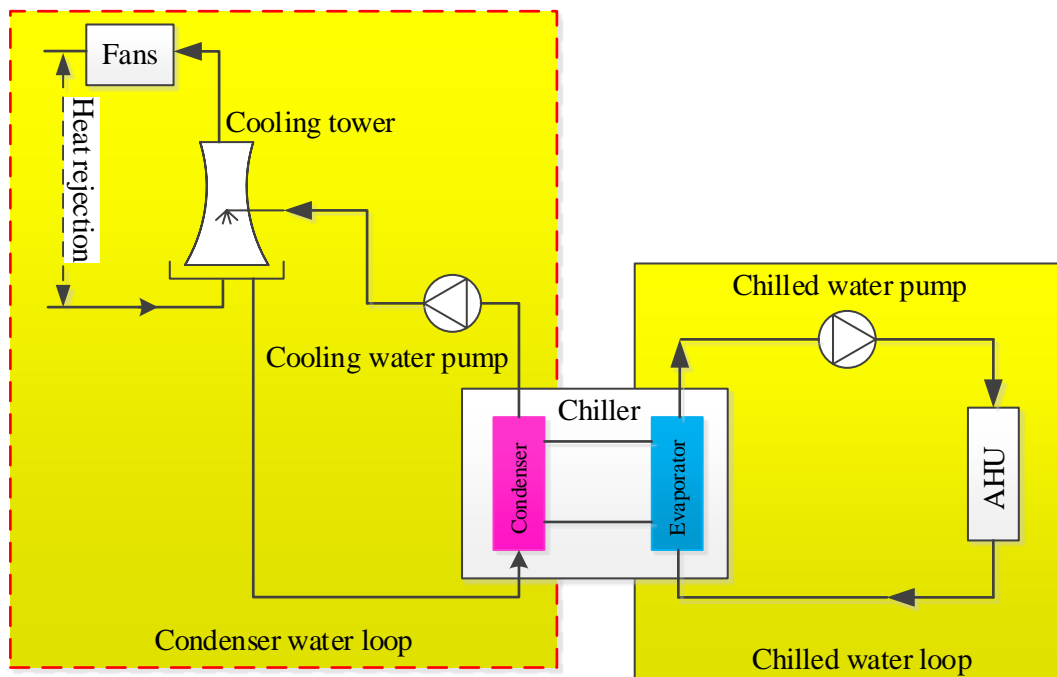
Fig. 2.1 A typical central air-conditioning system

2.2.1 Chiller plant

Among all HVAC components and equipment, chiller plant is usually the largest energy consumer, accounting for up to 50% of the total energy consumption of the entire HVAC systems (Sun et al. 2013). The sizing and selection of chiller plants play the most important role in determining the energy performance of the HVAC systems (Lee et al. 2001). The conventional design of chiller plant, proposed by ASHRAE (ASHRAE

handbook 2012), is usually based on sizing the components individually to meet a peak duty at a nominal operating point under the design conditions. Due to the inevitable uncertainty of weather data, indoor occupants and internal heat gain, designers tend to select a larger capacity than the peak duty (e.g., multiply a safety factor) in order that the plant can fulfil the cooling demand under any uncertain conditions for safety (Domínguez-Muñoz et.al 2010; Sun et al. 2014 and Cheng et al. 2015). This may result in significant oversizing of chiller plant and a large amount of energy wastes because the actual operating conditions are seldom the same as the design condition (Yik et al. 1999). Oversizing of chiller plants is usually encountered because of improper cooling load calculation method, predefined weather data, and internal heat-gain criteria (Lee et al. 2001; Yu and Chow 2000). Some measures, such as using a detailed simulation method, statistic weather data, model calibration and even the experiments, have been recommended to reduce the oversizing problems to a certain degree caused by uncertainties (Domínguez-Muñoz et.al 2010). However, these methods cannot help to minimize the oversizing due to the adoption of conservative criteria for estimating the cooling loads of buildings (Cheng et al. 2015).

Different from the early design methods that only address the peak cooling load of selected design day, some studies also have taken part load conditions into account in order to achieve a high efficiency in most of operating time of chiller plants (Trane 2005). There are several approaches available to improve the energy performance of chiller plants under part load conditions since such conditions frequently occur throughout the entire cooling season (Gorter 2012). In order to improve the systems

PLR (part load ratio) that affects the COP (coefficient of performance) strongly, optimal sequence control is considered as an effective approach for the chiller plant with multiple chillers (Braun et al. 1989; Gidwani 1987; Kaya 1991 and Chang et al. 2005). When the actual cooling load falls down from the peak duty, some of the chillers can be shut down so that each of the operating chillers can operate at a relatively higher PLR. Another important approach to ensure the performance of a chiller plant at high level is to use high efficiency chillers, particularly the chillers having good performance characteristics even under part load conditions (Yu and Chan 2007). For instance, variable-speed chillers may be employed to improve the energy efficiency when the chiller plant operate at part loads (Hartman 2001; Koury et al. 2001; Tassou and Qureshi 1998 and Ma and Wang 2011). In addition, some studies show that the high COP of chiller plants can also be achieved by using hybrid chillers with different types of compressors or different energy sources, which can ensure all operating chillers within the optimum loading ranges (Celuch 2001).

When the part load conditions are considered in conventional optimal chiller design methods, they are typically based on the annual cooling load under the predefined conditions, which is commonly subject to a deterministic model-based simulation (Sun et al. 2014; Ashouri et al. 2014). The system may achieve a satisfactory performance when the actual operating conditions are the same or similar as the predefined conditions. However, when the actual conditions are different from predefined conditions caused due to various uncertain factors, the chiller plant is very likely to operate at a low efficiency (Ashouri et al. 2014; Van Gelder et al. 2013).

2.2.2 Chilled water system

The sizing and selection of chilled water pump systems is the second most important aspects in determining the energy performance of the HVAC systems (Tirmizi et al. 2012; Nolte 2004). The conventional design of chilled water pump systems, proposed by ASHRAE Handbook (ASHRAE handbook 2012), mainly concerns the design flow required and design pressure head required. The intersection of the required head and flow on the pump curve should occur close to or perhaps a little to the left of best efficiency point (BEP), which may maintain the pumps operating at high efficiency and thus minimize the electricity cost of operating the pumps (Ahlgren 2001). Considering that pumps are only manufactured in certain sizes, selection range between 66% and 115% of design flow at the BEP are suggested (ASHRAE handbook 2008). In a central air-conditioning system, the designer tends to use identical pumps in parallel to share the system flow (ASHRAE handbook 2004). In addition, a standby or backup pump of equal capacity and pressure installed in parallel to the main pumps is recommended to operate to ensure continuous operation when a pump fails to operate or needs to be maintained (ASHRAE handbook 2004).

Oversizing of chilled water pump systems, which is a common problem in HVAC fields (Mansfield 2001), may result in high capital cost, high operation cost, and increased maintenance problems over the system life-cycle when compared to properly sized systems (Ahlgren 2001). Oversizing of pump systems contain the oversizing of design flow and oversizing of design pressure head (Cheng et al. 2016). Due to the inevitable uncertainty of input parameters (e.g., weather condition, occupancy) on cooling load

calculation (Ashouri et al. 2014), designers tend to select a larger design cooling capacity than the peak duty (e.g., multiply a safety factor) in order that the design cooling capacity can fulfil the cooling demand for safety (Domínguez-Muñoz et al. 2010; Sun et al. 2014). This may result in significant oversizing of cooling capacity and design flow (Yik et al. 1999). Based on the design flow rate and the design information of the chilled water loop, the component pressure drops are calculated for determining the assumed pump head. Additional design safety factors are added on the assumed pump head to get the design pump head to allow the changes of system load and to cover unknown or unforeseen pressure drop factors (Mansfield 2001). Sometimes an artificial aging factor (e.g., an extra 15%) is included to account for the decrease in pipe diameter as deposits build up on the inside surfaces of the pipes due to aging (Ahlgren 2001). Since part load conditions frequently occur throughout the entire cooling season (Gorter 2012), some engineers think they can grossly oversize a pump system and then use variable speed drives to maintain high efficiency and reduce operation cost during the part load period (Walski et al. 2003). However, the capital cost and operation cost are still high while the system is not properly designed even variable speed drives are used.

2.2.3 Cooling water system

The sizing and selection of cooling water systems plays a significant role in determining the energy performance of the HVAC systems (Jin et al. 2007; Bernier 1995 and Crowther et al. 2004). According to ASHRAE Handbook (ASHRAE handbook 2012), the thermal performance of cooling towers is determined by

following parameters, i.e. return and supply cooling water temperatures, inlet air wet-bulb temperature and design cooling water flow rate (Stanford 2011; United Nations Environment Program 2006; Cooling tower fundamentals 1983; Milosavljevic and Heikkilä 2001 and Mohiuddin et al. 1996). Design cooling water flow rate depends on the total heat rejection of condensers under the given working conditions. The total heat rejection contains the design cooling capacity and heat of compression (Cooling tower fundamentals 1983). Due to the inevitable uncertainty of weather data, indoor occupants and internal heat gain, designers tend to select a larger design cooling capacity than the peak duty (e.g., multiply a safety factor) in order that the plant can fulfil the cooling demand under any uncertain conditions for safety (Domínguez-Muñoz et al. 2010; Sun et al. 2014). At the same time, additional cooling tower capacity is added in case that the ambient temperature is off-design or heat rejection varies from the design condition (Stanford 2011). This may result in significant oversizing of design cooling capacity and cooling tower capacity and thus a large amount of energy wastes.

In selecting a pump for cooling water system, considerations are mainly given to the static pressure and the system friction loss (ASHRAE handbook 2012). The pump inlet must have an adequate net positive suction pressure (Mansfield 2001). In addition, continuous contact with air introduces oxygen into the water and concentrates minerals that can cause scale and corrosion on a continuing basis (ASHRAE handbook 2012). Fouling factors and an increased pressure caused by aging of the piping must be taken into account in the design of cooling water pump

(Ahlgren 2001).

However, research on cooling water systems has focused on the individual components of cooling systems, not the system as a whole (Kim and Smith 2001). In addition, very limited attention has been placed to the interactions among cooling towers, cooling water pumps and condensers of chillers (Panjeshahi et al. 2009), even though changes to operating conditions of cooling water systems frequently happen.

2.2.4 Concluding remarks

Conventional design methods and previous optimal design methods in HVAC field mainly address the design capacity and operational performance of systems under predefined conditions (without considering the uncertainties). However, the actual operating conditions may change significantly throughout the lifetime of the building energy system. Under the deterministic inputs (e.g., weather conditions, number of occupants), HVAC systems could be possibly ensured to operate at a high efficiency using the statistic and historic data. However, given the fluctuations of weather conditions and number of occupants, the optimal design alone cannot guarantee the HVAC systems operating at high efficiency. Based on the predefined conditions, conventional design and even optimal design would result in obvious deviations between the design and the actual system performance and thus a large amount of energy waste. Therefore, the uncertainties of variables in these condition should not be ignored in the engineering practice.

2.3 Studies on Uncertainty Issue in HVAC Fields

Uncertainty is a term used to encompass many concepts with different definitions (Morgan et al. 1992). It has been defined as a degree of ignorance (Beven 2010), a state of incomplete knowledge (Cullen and Frey 1999), insufficient information (Murray 2002), or a departure from the unattainable state of complete determinism (Walker et al. 2003). In building and structure field, the various sources and categories of uncertainty identified in the literature can be classified into four categories (Keith 2011): epidemic uncertainty, variability, linguistic uncertainty (Carey and Burgman 2008) and decision uncertainty (Finkel 1990). Epistemic uncertainty is the uncertainty associated with imperfect knowledge, which could be reduced by additional research and observation, i.e. model calibration and realistic data (Gillund et al. 2008). Variability is the uncertainty associated with diversity or heterogeneity, which cannot be minimized or eliminated with additional research or observation (Anderson and Hattis 1999; McCann et al. 2006). Since HVAC fields contain epidemic uncertainty and variability only, linguistic uncertainty and decision uncertainty are not considered in this study (Cheng et al. 2015).

According to engineering practice, the uncertainties in the HVAC field could be divided into two types, including design uncertainties and operation uncertainties. Fig.2.2 presents an outline of uncertainties in the HVAC domain (Cheng et al. 2015). Operation uncertainties mainly consist of information uncertainty and system reliability. Design uncertainties are mainly related to the cooling load uncertainty since the selection and sizing of HVAC subsystems (i.e., chillers, pumps, AHUs and cooling towers) mainly

depends on building cooling load. Cooling load uncertainty consists of the epidemic uncertainty and variability. Variability mainly consists of the number of occupants and weather conditions, which cannot be minimized or eliminated with additional research or observations. As for epidemic uncertainty, it concerns heat transfer performance of building envelopes and efficiency of air-conditioning equipment, which could be minimized and narrowed with additional research and observations, i.e. model calibration, realistic data and even correction factor.
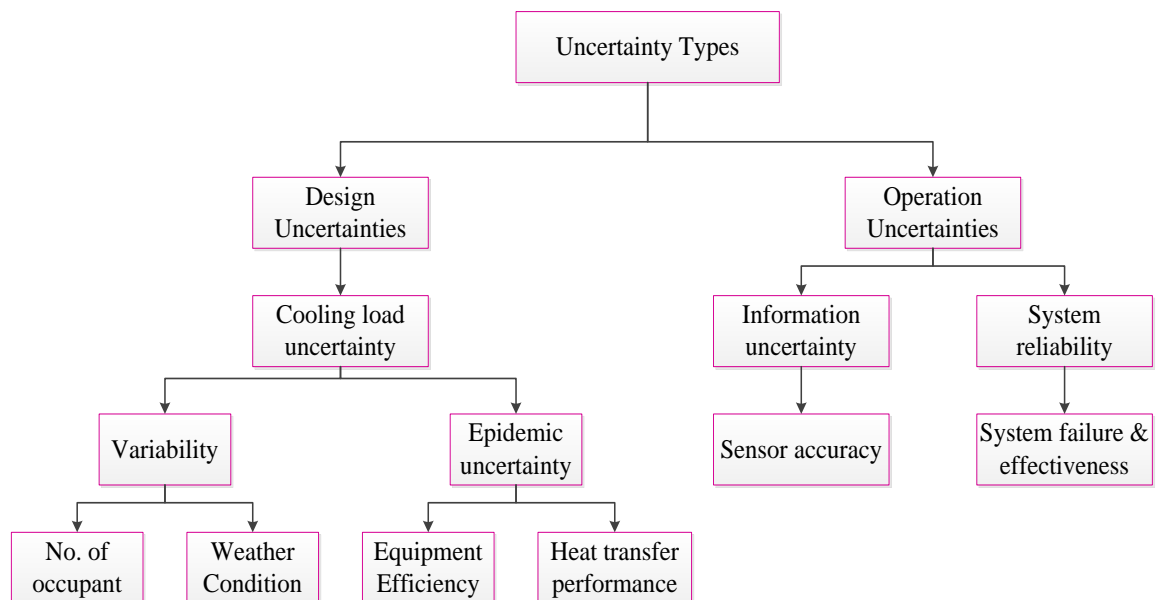
Fig.2.2 Types of uncertainties in HVAC field

By considering and quantifying the uncertainty, the configuration of building energy system can be determined with confidence. Extensive studies have been done regarding the uncertainty and sensitivity analysis of building energy systems, which is reviewed in this section.

2.3.1 Uncertainty analysis in HVAC fields

Conventional design of HVAC system is typically based on the annual cooling load

under the predefined conditions, which is commonly subject to a deterministic model-based simulation (Sun et al. 2014; Ashouri et al. 2014). The system may achieve a satisfactory performance when the actual operating conditions are the same or similar as the predefined conditions. However, when the actual conditions are different from predefined conditions due to various uncertain factors, the HVAC system is very likely to operate at a low efficiency (Ashouri et al. 2014; Van Gelder et al. 2013).

In order to address the problem caused by uncertainties, several studies have taken the impact of uncertain variables into account when designing building energy systems or assessing the performance of the systems (Brohus et al. 2011; Eisenhower et al. 2011; Heiselberg et al. 2009; Hopfe et al. 2011; Zhou et al. 2013). Energy consumption of dwellings considering uncertainties in climate, building construction and inhabitants was studied by Pettersen (1994). Results show that the energy consumption can vary with an uncertainty of ±25-40%. Smith et al. (2010) and Li et al. (2008) presented an analysis on a CCHP (combined cooling, heating and power) system model considering uncertainties of inputs and models. Case studies under different operating strategies were conducted to investigate the significance and sensitivity of uncertainties in predicting the CCHP system performance. The source of uncertainties in a housing stock model was studied and method to handle the uncertainties was proposed (Booth et al. 2012). Zhou et al. (2013) proposed a two-stage stochastic programming model for the optimal design of distributed energy systems. They use genetic algorithm to perform the search in the first stage and Monte Carlo simulation to deal with uncertainties in the second stage. Burhenne et al. (2013) developed a Monte Carlo based methodology for

uncertainty quantification to combine the building simulation and cost-benefit analysis.

Uncertainty analysis can be also used to assess the performance of retrofit of building energy systems. Eisenhower et al. (2011) conducted an uncertainty study in the intermediate processes by performing decomposition, aiming to find the most important subsystem in modelling. Lee et al. (2013) proposed a statistic method to conduct probabilistic risk assessment of the energy saving in energy performance contracting projects. Uncertainties in weather conditions, occupancy, operating hours, thermostat set-point, etc. were considered. Possible energy saving was obtained with quantified confidence. The necessity to decouple uncertainties in HVAC systems and building models was investigated by Augenbroe et al (2013). The coupled simulation method usually requires a higher level of expertise of system modeling and can be computationally intensive. Sun et al. (2014) proposed a design method to size building energy systems considering uncertainties in weather conditions, building envelope and operation. Menassa (2011) presented a quantitative approach to determine the investment value in sustainable retrofits for existing buildings considering different uncertainties associated with the life cycle costs and perceived benefits of the investment. The proposed methodology provided the decision maker with managerial flexibility to determine, prioritize and evaluate the required retrofits over time. O'Neill and Eisenhower (2013) used measured data to conduct model calibration and the uncertainty study was implemented to tune the models.

However, the above studies have recognized and analyzed the impact of uncertainties on system performance, but they did not consider or propose effective approaches to

30

overcome or reduce these impacts, which is most important for improving the operating efficiency and robustness since uncertainties exist inevitably.

2.3.2 Design of building energy systems involving uncertainty

Design inputs such as weather conditions are used in the calculation of annual cooling load and most of them contain uncertainties (Li et al. 2003; Sun et al. 2014; Yıldız and Arsan 2011). The peak cooling load distribution was studied by Domínguez-Muñoz et al. (2010) considering the uncertainties in the building material, heat transfer coefficients of external and internal wall, internal sources, etc. The impact of furniture and contents (i.e. internal mass) on zone peak cooling loads, which is not accounted in traditional simulations, is investigated (Raftery et al. 2014). Results show that involving internal mass can change the peak cooling load by a median value of -2.28% (-5.45% and -0.67% lower and upper quartiles respectively). Uncertainties in the peak load prediction are investigated (Huang et al. 2015), which is used for the determination of design cooling capacity of HVAC system. Multi-criteria optimization is conducted including the energy consumption, initial cost and failure time. The annual cooling and heating load considering the physical, design and scenario uncertainties was investigated by Hopfe et al. (2011). The distribution of the annual heating/cooling load, weighted overheating and under heating hours related to the thermal comfort was analyzed.

Uncertainty was also considered in the design optimization of building energy systems. The impact of uncertainties in the building performance evaluations was addressed by

De Wit and Augenbroe (2002). Results show that considering the uncertainties can change the decision maker's choice for the same project. Sun et al. (2014) proposed a new design method considering the uncertainty involved in the cooling/heating load calculation. Results recommend that using actual weather data in the load calculation helps to alleviate the oversize problem in the cooling/heating system design. Zhang and Augenbroe (2014) investigated that how to right size a photovoltaic system. Uncertainties in the building's physical properties, solar irradiance, efficiency and degradation rates of PV panels are considered. A method was proposed to estimate building energy performance in early design decisions (Rezaee et al. 2014). Design uncertainties involving in early design were quantified and their impact on design decisions was examined. Results using different models or software indicate different solutions. It indicates that uncertainties in the models have to be fully addressed.

2.3.3 Concluding remarks

From the above reviewed studies, it can be found that research on building energy systems involving uncertainty mainly focuses on presenting the result distribution, comparing with the deterministic results, finding the most important factors, calibrating models and analyzing the impact on system performance. However, they did not consider or propose effective approaches to overcome or reduce these impacts, which is most important for improving the operating efficiency and robustness since uncertainties exist inevitably. Even for the selection and sizing of HVAC system, the design considering uncertainties is rarely studied.

2.4 Reliability Assessment of Building Energy Systems

Reliability can be defined as the probability of successful operation or performance of systems and their related equipment, with minimum risk of loss or disaster (Stapelberg 2009). Reliability design has been widely applied and studied in the fields such as structure, military industry, power system, electronic hardware, etc. (Frangopoulos and Dimopoulos 2004; Heising 1991). Redundancy is usually adopted to improve the reliability of systems. Redundancy can be active where the additional components may also work under normal conditions, or passive where these components only are switched on during abnormal conditions or maintenance occurrence (Aguilar et al. 2008). Passive redundancy is usually used in building energy systems. It means that a standby or backup component of equal capacity is installed in parallel to the main work systems to ensure continuous operation in case of failure or maintenance, which is frequently used in the convention design method to ensure the system capability (ASHRAE handbook 2012).

Reliability analysis or assessment is necessary to avoid/reduce losses caused by both the normal situations and abnormal situations such as the failure of some components (Vanderhaegen 2001). Myrefelt (2004) used actual data collected from buildings of seven large real estate operators to analyze the reliability of the HVAC systems. Peruzzi et al. (2014) emphasized the importance of the reliability parameters considering financial (reduction of energy and maintenances costs), environmental and resources managing (both concerning the energy and staff) profits. Chinese et al. (2011) used a multi-criteria approach to select the space heating system for an industrial building,

where the criteria included reliability, operation cost, comfort, etc. Au-Yong et al. (2014) investigated the maintenance characteristics of HVAC systems that affect occupants' satisfaction, subsequently established a relationship between the characteristics and occupants' satisfaction through questionnaire surveys and interviews and finally develop a regression model for prediction purpose. Kwak et al. (2004) proposed a method to predict an optimal inspection period for condition-based preventive maintenance based on reliability assessment of air-conditioning systems in office buildings.

From the above studies, it shows that very limited studies are done considering reliability of system components using quantitative methods in the design process of HVAC systems. Therefore, study on design optimization considering both uncertainties of design inputs and reliability of system components needs to be continued and furthered.

2.5 Summary

This chapter presents a comprehensive review on the design of HVAC system (including chillers, chilled water systems and cooling water systems), uncertainty study and reliability assessment in building energy systems. From the above review, the following research gaps can be summarized:

I.   Based on the predefined conditions, conventional design and even optimal design would result in obvious deviations between the design and the actual system performance and thus a large amount of energy wastes.

II.   Oversizing of HVAC system is a prevalent problem for conventional design

        method due to the adoption of conservative criteria for estimating the cooling

        loads of buildings, which results in high capital cost, low operating efficiency

        and thus energy waste;

III.   Research on building energy systems involving uncertainty mainly focuses on

        analyzing the impact on system performance. However, there are few effective

        design methods developed to improve the operating efficiency and robustness

        since uncertainties exist inevitably. Even for the selection and sizing of HVAC

        system, the design considering uncertainties is rarely studied.

IV.   Reliability assessment, particularly quantitative assessment, is rarely considered

        in the design optimization of HVAC system.

Therefore, this study attempts to develop a new design method considering uncertainties

of design inputs and reliability of system component, aiming at providing the system

with the capability to operate at relatively high efficiency at various possible conditions

considering the uncertainties of design inputs and system reliability in operation. At the

same time, the minimum total life-cycle cost could be achieved through the design

optimization method.

CHAPTER 3 DESIGN OPTIMIZATION METHODS AND QUANTIFICATIONS OF UNCERTAINTY AND RELIABILITY

In order to achieve more flexible, resilient and cost-effective design of the HVAC system, a robust optimal design method is developed in this thesis. It can ensure that the HVAC system could operate at high energy performance and the minimum total life-cycle cost could be achieved under various possible cooling load conditions considering the uncertainties of design inputs and reliability of the components.

This chapter presents the concept of uncertainty-based optimal design (i.e. robust optimal design considering uncertainty only) and robust optimal design method (i.e. robust optimal design considering uncertainty and reliability). Then, four types of design optimization methods are introduced, which contains uncertainty-based optimal design, robust optimal design based on Markov method with the same failure rate, robust optimal design based on Markov method with the different failure rates and robust optimal design based on sequential Monte Carlo simulation. Finally, the quantifications of uncertainty and reliability are presented.

3.1 Concept of Robust Optimal Design

Robust optimal design is essential for improving engineering productivity (Zang et al. 2005). The typical definition of robust design is described as "*a product or process is said to be robust when it is insensitive to the effects of sources of uncertainties, even*

though the design parameters and the process variables have large tolerances for ease of manufacturing and assembly" (Fowlkes et al. 1995; Phadke 1995 and Park 2007). The aim of the robust optimal design is to achieve an optimal design option of minimized life-cycle cost, which provides the system with the capability to operate at relatively high efficiency at various possible conditions considering the uncertainties of design inputs and system reliability in operation. This proposed method takes into account the uncertainty and reliability compared with the conventional/optimal design method, which has the following features:

• Uncertainty being considered: the designed system has enough tolerance towards the deviation between the actual condition and the predefined information, associated to the design inputs such as weather conditions and number of occupants.

• Reliability being considered: the designed system has the capability to fulfill the cooling demands of users under the normal situations and abnormal situations (i.e., the failure of systems), associated to the uncertain heath situations of equipment.

The fundamental difference between the robust optimal design method and other design methods is illustrated in Fig. 3.1. *Conventional optimal design* in HVAC field guarantees the optimization over predefined conditions (without considering the uncertainties and reliability) (Sun et al. 2014). It can be seen that the conventional method determines the HVAC system without quantitative uncertainty and reliability analysis. *Uncertainty-based method* determines the size of the systems (Sun et al. 2014) or investigates the building performance (Hopfe et al. 2011) considering uncertainties in design. However, this design method may result in the insufficient cooling under the normal conditions

(i.e. the design capacity is small) or abnormal conditions (i.e. the failure and maintenance occur). *Reliability-based method* ensures the system capability by minimizing the effect of sources of design parameters or process variables, which is rarely studied in HVAC field (Gang et al. 2015). In addition, this method may result in the low efficiency due to the low load ratio (i.e. the nominal capacity of system component is large). *Robust optimal design method* concerns quantitative uncertainty and reliability analysis as well as quantitative performance optimization simultaneously. It provides the system with the capability to operate at relatively high efficiency at various possible conditions considering the uncertainties of design inputs and system reliability in operation.
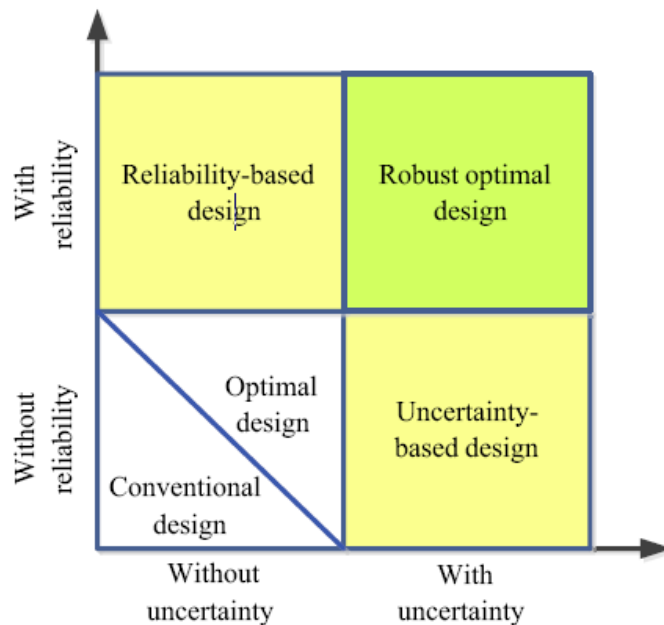
Fig.3.1 Illustration of different design methods (Gang et al. 2015)

3.2 Design Optimization Method Proposed

In this thesis, both the uncertainty-based optimal design and robust optimal design are used in the design of HVAC subsystems. Uncertainty-based optimal design method mainly focuses on improving the energy efficiency of HVAC system and achieving the

minimum total life-cycle cost considering uncertainties of design inputs only. Monte Carlo simulation is usually used for the quantification of uncertainty. To achieve the minimum total cost, there is a balance between the operation cost and capital cost. Besides, under the same cooling load distribution, the operation cost depends on the rated energy efficiency and part load ratio. The minimum operation cost can be achieved through the optimization of number and size of HVAC components. A detailed introduction of uncertainty-based optimal design will be given in the Chapter 4. Robust optimal design mainly focuses on improving the energy efficiency of HVAC system, ensuring the sufficient capacity to supply the cooling and achieving the minimum total life-cycle cost considering both the uncertainties of design inputs and the reliability of system components. There is a comprised level of reliability (i.e. system capacity) among availability risk cost, operation cost and capital cost. To achieve the minimum total cost, the total design capacity, number and size of system components are optimized.

Fig.3.2 illustrates the design optimization methods in this thesis, which contains conventional design, uncertainty-based optimal design and robust optimal design. Since many studies were conducted on the conventional design of HVAC system, this thesis will not focus on the conventional design. Table 3.1 shows the implementation methods of uncertainty and reliability under different design methods and the application of different design methods in this thesis.

Design optimization method

Conventional design

Uncertainty-based optimal design

Robust optimal design

Monte Carlo simulation

Analytical method (e.g. Markov method)

Sequential Monte Carlo simulation

The same failure rate

The different failure rates
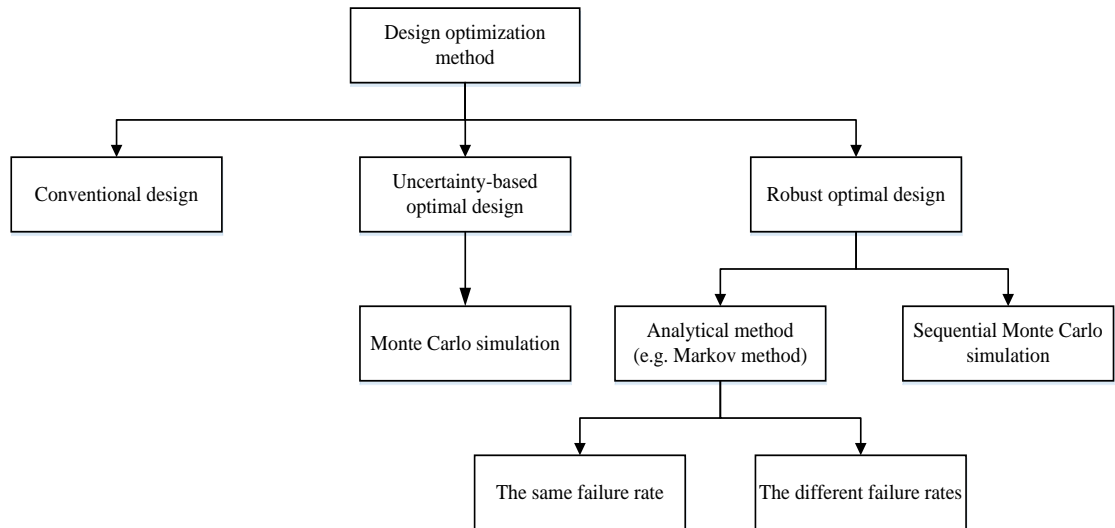
Fig.3.2 Proposed design optimization method

Table 3.1 Design methods and Application

Design method	Uncertainty	Reliability	Application
Conventional design	×	×	×
Uncertainty-based optimal design	Monte Carlo simulation	×	Chapter 6
Robust optimal design	Monte Carlo simulation	Markov Method (different failure rates)	Chapter 7
		Markov Method (the same failure rate)	Chapter 8
		Sequential Monte Carlo simulation	Chapter 9

The sequential Monte Carlo simulation method and the Markov method are two of the most commonly used methods for quantifying the reliability. Sequential Monte Carlo simulation is a simulation-based method, which provides a convenient and attractive approach to compute the posterior distributions. It is very flexible, easy to implement, parallelizable and applicable in very general settings. In HVAC subsystems, all the

components of each subsystem are parallel and independent. This method can be used in the reliability assessment of HVAC subsystems. Chapter 7 gives the detail introduction of sequential Monte Carlo simulation for robust optimal design.

Markov method is frequently used for conducting the reliability assessment of HVAC systems. It contains the Markov method with the same failure rate and Markov method with different failure rates. In this thesis, it is assumed that all the chillers, pumps and cooling towers with constant speed drives have the same failure rates and all the chillers, pumps and cooling towers with variable speed drives have different failure rates.

In HVAC subsystems, the chilled water pumps, cooling water pumps and cooling towers are usually identical in parallel. Therefore, robust optimal design with the same failure rate can be used for the design of chilled water pumps, cooling water pumps and cooling towers. Chapter 6 gives a detailed introduction of robust optimal design with the same failure rate.

In order to improve the energy efficiency of chiller plant, both the constant-speed chillers and variable-speed chillers are used in parallel to supply the cooling. The failure rate of constant-speed chillers is different from that of variable-speed chillers. Therefore, robust optimal design with different failure rates can be used for the design of chiller plant. Chapter 5 gives the detail introduction of robust optimal design with different failure rates.

3.3 Quantification of Uncertainty

The uncertainties in the building load calculation involve:

a) Number of occupants and weather conditions, which cannot be predicted accurately;

b) Infiltration flow rate between outdoor environment and indoor air, heat rejection by equipment, etc., which can be narrowed through some proper measures but cannot be eliminated.

As mentioned in Chapter 2.3, the uncertain variables are divided into two parts, i.e. variability and epidemic uncertainty. Variability including weather conditions and number of occupants may not be accurately predicted due to the irregular fluctuations. Weather conditions may be assumed to be subject to normal distribution, which is described by the mean value and standard deviation. The number of occupants may be assumed to be subject to triangular distribution (described by the mean value, minimum value and maximum value), which is selected based on the forecast of building management department. As for epidemic uncertainty (i.e., infiltration flow rate), it usually fluctuates around the mean value, and can be predicted according to the regular fluctuation. Uniform distribution is used to consider this type of uncertainties in cooling load calculation. Table 3.2 shows an example of the settings of uncertainties of the variables.

It is worth noting that the selection of uncertainties may also influence the sizing of a chilled water system. For example, if a larger range of uncertainties is used, the total design capacity of chilled water pumps may be larger to reduce the availability risk cost and thus the optimal option may be different. More details will be discussed in later chapters.

Table 3.2 Distributions of stochastic input parameters

Parameters	Distributions
Outdoor temperature (℃)	N(0,1)
Relative Humidity (%)	N(0,1.35)
Number of Occupants	T(0.3,1.2,0.9)
Infiltration rate (m^3/s)	U(2.7, 3.3)
Equipment rejection load (kW)	U(376, 464)
Remarks: $N(\mu, \sigma)$ - normal distribution with mean value μ and standard deviation σ; $U(a, b)$ - uniform distribution between a and b; $T(a, b, c)$ - triangular distribution with lower limit a, upper limit b and mode c.	

3.4 Quantification of Reliability

Fig.3.3 is a reliability and maintainability history chart of a three-state machine. The state "Operate" indicates that the equipment currently resides in a working state (i.e. State 1). The lengths of this state are the holding times of being in working state. The holding time is random and determined by analysis of historical reliability and maintainability data. In practice, the mean time to failure (MTTF, $1/\lambda$) is often used to represent this holding time, as shown in Equation (3.1) (Ge and Asgarpoor 2011). The state "Maintenance" and "Failure" (i.e. State 0) indicate that the equipment currently resides in an inoperative (i.e. failure or maintenance) state. The lengths of these state are the holding times of being in this state. In practice, the mean time to repair (MTTR, $1/\mu$) is often used to represent this holding time, as shown in Equation (3.2) (Ge and Asgarpoor 2011). Commonly, failure rate (λ) and repair rate (μ) are usually used as the

major parameters for conducting the reliability assessment.

$$MTTF = \frac{1}{\lambda} = \sum t_{operate} \qquad (3.1)$$

$$MTTR = \frac{1}{\mu} = \sum t_{main} + \sum t_{fail} \qquad (3.2)$$
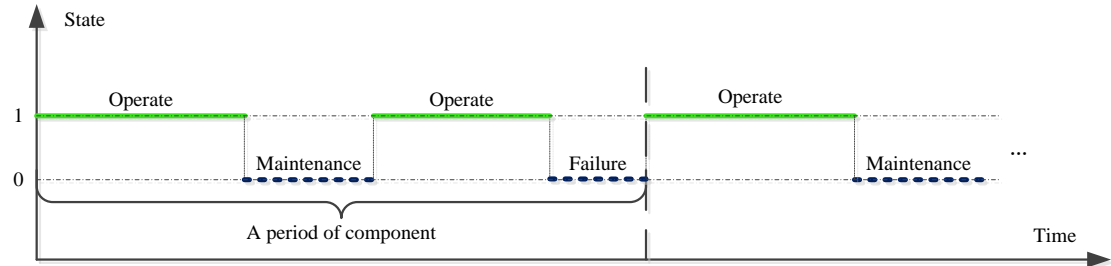
Fig.3.3 Health states of a component in the life cycle

Markov method

Conventional design and uncertainty-based optimal design usually assume that all equipment and components are at healthy states and a standby or backup component of equal capacity is used in case that one of the components fails to operate or needs to be maintained. Using the Markov method, the HVAC subsystems are usually regarded as multi-state systems. A multi-state system contains three states or situations: no failure of component, failure of one component and up to failure of all components. It is assumed that the state probabilities at a future instant do not depend on the states occurred in the past. The system either keeps current state or transfer to other states at the next time step.

It is assumed that each component of HVAC subsystems has two states only: normal (0) and failure (1). State 0 symbolizes that no component fail and state k symbolizes that k ($1 \leq k \leq n$) components fail (i.e. n is the total number of components). From state 0 to state n, the failure rate λ is used to represent the probability from one state to another. From

state *n* to state 0, the repair rate μ is used to represent the probability from one state to another. The transition probability is determined by a state transition density matrix. Then the steady state probabilities can be obtained by solving the linear algebraic equations.

Sequential Monte Carlo simulation

Sequential Monte Carlo simulation is based on the assumption that the components in parallel are independent and each component has no relationship with the other components. The reliability indices, such as availability, $p_{availability}$ (percentage of time staying in a working state) and unavailability, $p_{unavailability}$ (percentage of time staying in a failure and maintenance state) are used for the reliability assessment of system component, which can be calculated by Equation (3.3) & (3.4). With the assumption that each component is independent and it has no relationship with the other components, the system component is assumed to be subject to the binary distribution. Where, $t_{operate}$ is the total operation time in an entire period, t_{main} is the total maintenance time in an entire period, t_{fail} is the total failure time in an entire period, λ is failure rate, μ is repair rate.

$$p_{availability} = \frac{MTTF}{MTTF + MTTR} \tag{3.3}$$

$$p_{unavailability} = \frac{MTTR}{MTTF + MTTR} \tag{3.4}$$

3.5 Summary

This chapter presents the concept of robust optimal design, the methodologies to achieve robust optimal design and the quantification methods of uncertainty and reliability.

Compared with the other design methods, robust optimal design method concerns quantitative uncertainty and reliability analysis as well as performance optimization simultaneously. It allows the designed system with the capability to operate at relatively high efficiency at various possible conditions considering the uncertainties of design inputs and system reliability in operation.

Then, three design optimization methods are presented and compared. It contains uncertainty-based optimal design and robust optimal design. Monte Carlo simulation is used for the quantification of uncertainty. The methods for quantifying the reliability contain Markov method and sequential Monte Carlo simulation. Markov method includes Markov method with the same failure rate and Markov method with different failure rates.

Finally, the quantifications of uncertainty and reliability are presented. Three types of distributions (including normal distribution, triangular distribution and uniform distribution) are commonly used to describe the uncertainties of inputs. For reliability assessment, the settings under analytical method and sequential Monte Carlo simulation are introduced respectively.

CHAPTER 4 PROBABILISTIC APPROACH FOR GENERATING THE COOLING LOAD DISTRIBUTION OF REQUIRED ACCURACY

In the design optimization of HVAC systems, generating the accurate cooling load distribution is the key issue to determine the optimal configuration of HVAC systems. In this thesis, Monte Carlo simulation is used to generating the cooling load distribution. Monte Carlo simulation is a broad class of computational algorithms that rely on repeated random sampling to obtain numerical results. In order to represent the characteristics of the uncertainties of design input in cooling load distribution, sufficient number of Monte Carlo simulation is required. When using a Monte Carlo simulation, a question that usually arises in connection with such simulations is to ask how many iterations of a particular Monte Carlo simulation are sufficient for achieving the required accuracy. This chapter presents a probabilistic approach for determining the minimum number of Monte Carlo simulations for accuracy. This systematical approach is used to evaluate the stability of cooling load distribution and determine the minimum simulation number.

Section 8.1 presents an introduction of this probabilistic approach. Section 4.2 presents the criteria of determining the minimum simulation number. Section 4.3 presents the procedure for implementing this approach. Section 4.4 gives a case study to illustrate the process of this approach. A summary of this chapter is given in Section 4.5.

4.1 Introduction

In general, the required number of Monte Carlo simulation is related to the inputs including the sampling method adopted and uncertain parameters. However, in this study, the output of cooling load distribution is directly used to evaluate the variation of cooling load distribution and determine the minimum simulation number (Ata 2007; Sadeghi et al. 2014). Different from previous research that only used the mean value at one point to determine the number of simulations needed (Ata 2007), both cooling load distribution profile and the mean value at a specific point, i.e. the peak cooling load in 99.6 percentile which represents the peak cooling load, are used for determining the minimum number of simulations needed.

4.2 Criteria for Determining the Minimum Simulation Number

In this study, two types of deviations, called as convergence band width in Reference (Ata 2007), are used for determining the minimum simulation number. The single-step deviation means the deviation between the average of i simulations and the average of i-1 simulations. The validation deviation (multi-step deviation) means the deviation between the average of i simulations and the average of $i+j$ simulations ($0 < j \leq B_L$). The validation deviation at the "peak cooling load" is used to ensure the accuracy of the design capacity and the validation deviation of the cooling load distribution profile is used to ensure the accuracy of cooling load distribution for calculating the operation cost of different chiller plant configurations. Two criteria are defined as follows:

- The validation deviation of the cooling load distribution profile should be within

its threshold B_{w1} over a number of simulation trials defined as convergence band length B_L.

- The validation deviation of the "peak cooling load" should be within it threshold B_{w2} over a number of simulation trials defined as convergence band length B_L.

The band length is expressed as a minimum number of simulations to verify whether the trials of Monte Carlo simulations are sufficient or not (Ata 2007). To achieve a desired level of confidence (i.e., $100(1-\gamma)$ %), the minimum simulation number B_L can be determined using the stopping rule as shown in Equation (8.1) (Tanner et al. 2014). In reference (Sadeghi et al. 2014; Tanner et al. 2014), the minimum number is 50, corresponding to a confidence interval of 99. 5% ($\gamma=0.0001$).

$$0.9^{B_L}\left[-\text{In}(0.1)B_L\right]^{-1} \leq \gamma \tag{4.1}$$

It is important to notice that two criteria request deviations are not beyond their thresholds over a number of simulation trials, defined as convergence band length B_L, to ensure reliability of convergence as shown in Fig.4.1. For the Region I from 0 to n_0, the single-step deviation is used for obtaining the initial simulation number n_0. The initial simulation number n_0 is the minimum number of simulations allowing the single-step deviation to be within the threshold. For the Region II (A) from n_0 to n, the validation deviation is over the threshold after a number of simulation trials (less than B_L) and thus the simulation number from n_0 to n is not sufficient. For the Region II (B) from n to $(n+B_L)$, the validation deviations are within the threshold after B_L simulation trials and thus the minimum sufficient simulation number is n.
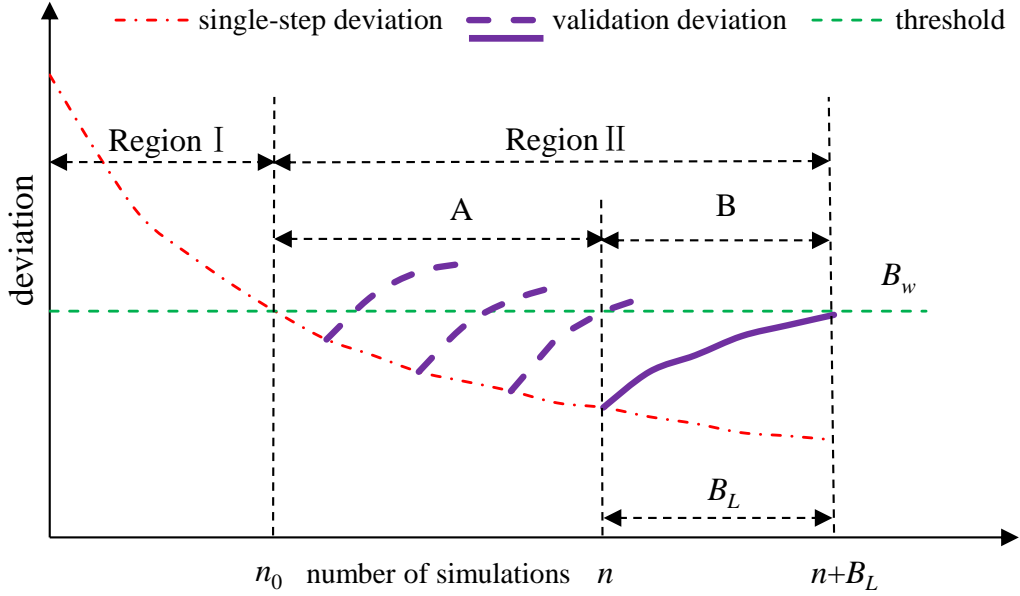
Fig.4.1 Scheme of threshold and convergence band length

4.3 Implementation Procedure of the Probabilistic Approach

A deviation index $f(n,m)$ is defined to represent the difference between average cooling load distribution profiles of n number of simulations and m number of simulations respectively, as shown in Equation (4.2) and Fig.4.2.

$$f(n,m) = \frac{\sum_1^k \left[|p_n(i) - p_m(i)| \cdot \Delta CL_i \right]}{\sum_1^k \left[p_m(i) \cdot \Delta CL_i \right]} \tag{4.2}$$

where, $p_n(i)$ is the probability at the load of CL_i of n trials of simulations, $p_m(i)$ is the probability at the load of CL_i of m trials of simulations, $\triangle CL_i$ is the cooling load interval and k is the total number of intervals. To validate if the number of simulations b is sufficient for obtaining accurate cooling load distribution profile, one should ensure that the deviation index $f(n,m)$ at each of B_L trials of simulations over the convergence band length falls within the threshold B_{w1}. Equation (4.3) presents this criteria in mathematic form, i.e. for all last B_L simulations, the deviation index is within the threshold B_{w1}.

$$f(b+j,b) \le B_{w1} \qquad \forall j, \; j = 1,2,..., B_L \qquad (4.3)$$
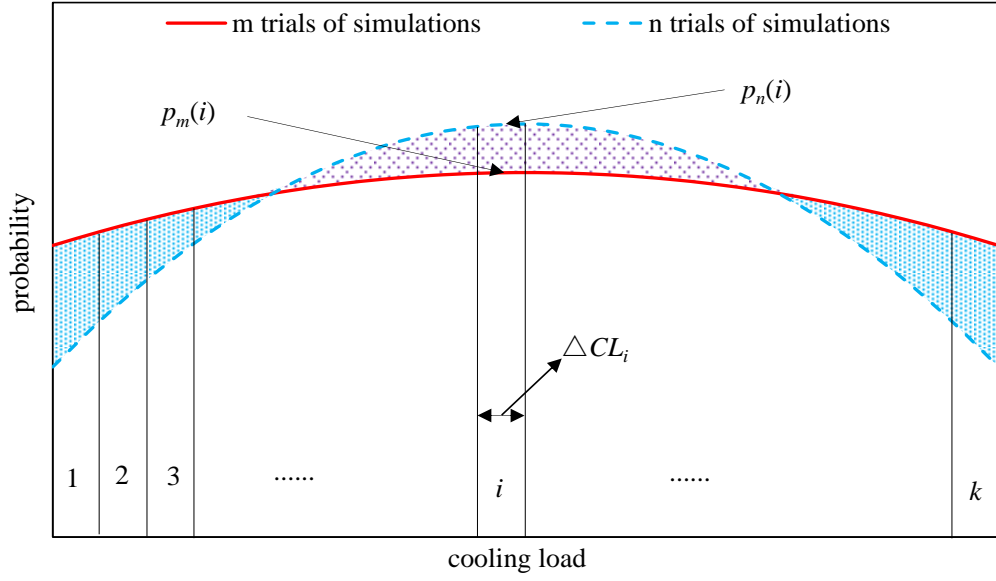
Fig.4.2 Difference of cooling load distribution with different simulation numbers

The second deviation index $g(x,y)$ is defined to represent the difference between the peak cooling load in 99.6 percentile of x number of simulations and y number of simulations respectively, as shown in Equation (4.4). It is worth noticing that the peak cooling load in 99.6 percentile is corresponding to the 30 unsatisfied hours per year.

$$g(x, y) = \frac{\left| CL_{x,99.6\%} - CL_{y,99.6\%} \right|}{CL_{y,99.6\%}} \qquad (4.4)$$

where, $CL_{x,99.6\%}$ is the peak cooling load in 99.6 percentile at x trials of simulations, $CL_{y,99.6\%}$ is the peak cooling load in 99.6 percentile at y trials of simulations. To validate that the number of simulations a is sufficient for obtaining accurate "peak cooling load", one should ensure that the deviation index $g(x,y)$ at each of B_L trials of simulations falls within the threshold B_{w2} over the convergence band length. Equation (4.5) presents the criteria in mathematic form, i.e. for all last B_L simulations, the deviation of the peak cooling load in 99.6 percentile is within the threshold B_{w2}.

$$g(a+j,a) \leq B_{w2} \qquad \forall j, \ j = 1,2,...,B_L \qquad (4.5)$$

Fig.4.3 illustrates the scheme for determining minimum efficient simulation number in practical design optimization computation. At first, it is essential to obtain the initial simulation number a_0 and b_0, which can be computed by Equation (4.6).

$$f(b_0 + i, b_0) < B_{w1} \quad and \quad g(a_0 + i, a_0) < B_{w2} \qquad (4.6)$$

where, i is the interval of simulation number. The initial numbers are increased further until the one-step deviations reach their thresholds. When the initial simulation number a_0 and b_0 are determined, the simulation number is validated from the initial value until the convergence condition is achieved. If the convergence condition is achieved, the larger one out of the two simulation numbers is chosen as the minimum sufficient simulation number.
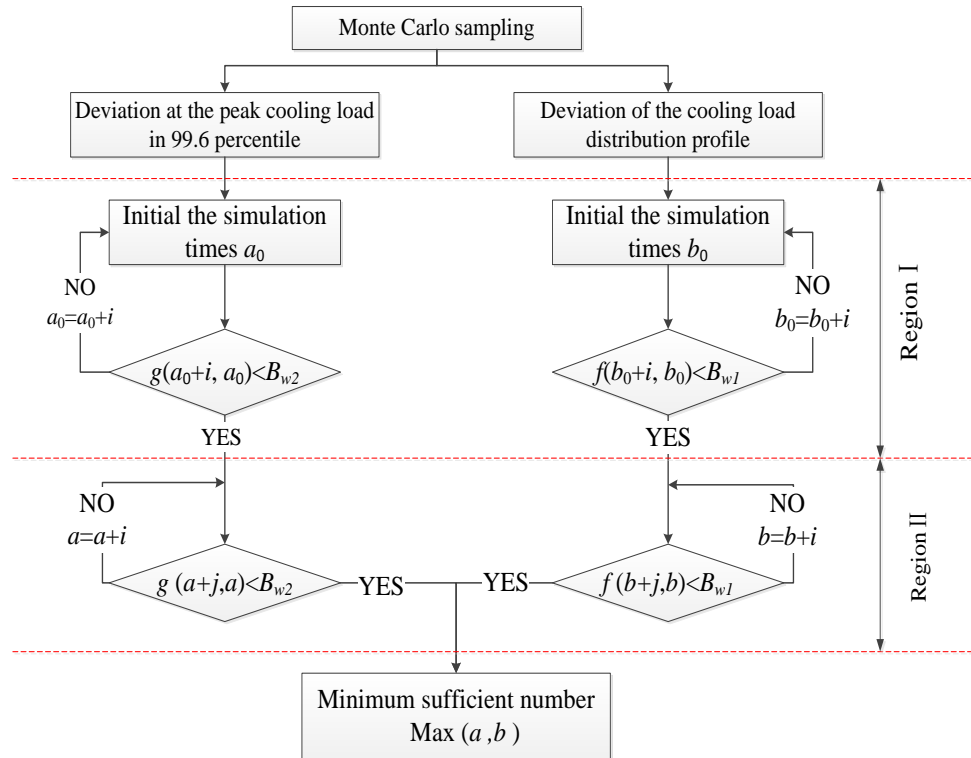
Fig.4.3 Scheme for determining minimum efficient simulation number

4.4 Case Study

To conduct the Monte Carlo simulations to obtain the cooling load distribution, it is essential to determine the settings of uncertainties of the variables. According to the settings in Table 3.2, the uncertainties of the input parameters are computed by Matlab. Combining the output uncertainties from Matlab, the TRNSYS building model is used to generate the building cooling load with considering of uncertainties.

In order to obtain the reasonable cooling load distribution, a sufficient simulation number should be selected for computational efficiency and accuracy. In this study, both validation deviation thresholds for the cooling load distribution profile and peak cooling load in 99.6 percentile are chosen to be 0.5%.

The test results show that the initial simulation number should be 20. Then the minimum simulation number can be obtained until the convergence condition is achieved, as shown in Table 4.1. It can be seen that 20 trials of simulations are sufficient as the corresponding validation deviation is within the threshold over 50 validation trials of simulations.

Table 4.1 Minimum simulation number for the "peak cooling load"

Simulation time	20	30	40	50	60	70
"Peak cooling load"	5177	5179	5179	5178	5177	5176
Deviation	-	0.0004	0.0004	0.0002	0	0.0002

In order to obtain the accurate operational cost, the validation deviation of cooling load distribution profile $f(n,m)$ is used to select the minimum simulation number. Fig.4.4

shows the results in determining the initial simulation number of cooling load distribution. It can be observed that the initial simulation number should be 350. Then the minimum simulation number can be obtained when the convergence condition is achieved, as shown in Table 4.2. It can be observed that 780 trials of simulations are sufficient for the cooling load distribution profile as the corresponding validation deviation is within the threshold over 50 validation trials of simulations.
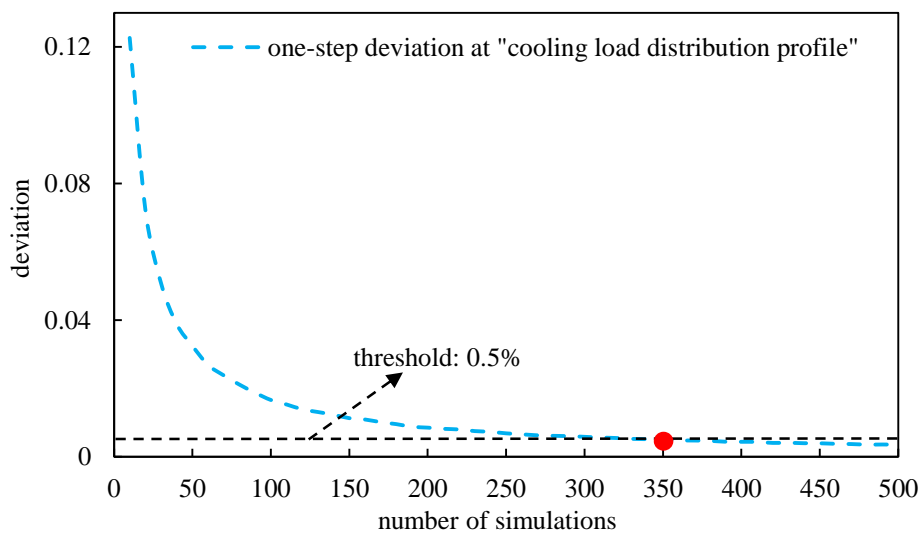
Fig.4.4 Determination of initial simulation number for cooling load distribution

Table 4.2 Minimum simulation number for the cooling load distribution

Simulation time	780	790	800	810	820	830
cooling load distribution	3231	3231	3231	3231	3231	3231
Deviation	-	0.0020	0.0032	0.0037	0.0041	0.0048

Compared with the minimum simulation number for accurate "peak cooling load", the minimum simulation number for accurate cooling load distribution is much larger. To obtain the accurate cooling load distribution and peak cooling load, at least 780 times

of Monte Carlo simulations are required to achieve the computational efficiency and accuracy. Table 4.3 shows the minimum simulation number of other thresholds for your reference. In some literatures (Gang et al. 2015), the researchers assumed that 1000 simulation trials are sufficient without a quantized index to evaluate the accuracy and attempted to use 1000 simulation trials to generate the required cooling loads.

Table 4.3 Minimum simulation number for the other thresholds

Thresholds	1%	0.9%	0.8%	0.7%	0.6%	**0.5%**	0.4%
Initial simulation number	180	190	220	250	300	**350**	440
Minimum simulation number	380	420	470	510	620	**780**	1020

4.5 Summary

This chapter presents a probabilistic approach to determine the minimum sufficient number of Monte Carlo simulation. This approach is used to obtain the cooling load distribution of required accuracy considering the uncertainties in inputs. A case study is given as an example to demonstrate the proposed method. Conclusions can be made as follows:

- Determining the minimum simulation number is very important for obtaining the accurate peak cooling load and cooling load distribution. 780 simulation trials are found and used and to achieve an accuracy of 0.5% for both of them.

- The minimum simulation required depends on the required accuracy.

CHAPTER 5 RELIABILITY QUANTIFICATION METHODS

Reliability analysis or assessment is necessary to avoid/reduce losses caused by both the normal situations and abnormal situations such as the failure of some components. However, very limited studies considering reliability of system components are found in the design process of HVAC systems. Markov method and sequential Monte Carlo simulation are frequently used to conduct the reliability assessment in the other fields such as electrical engineering. The probability distribution of system state is generated by the reliability assessment, which plays an important role in the robust optimal design of HVAC systems. According to the publication in other fields, in this chapter, both the two methods are compared to conduct the reliability assessment of HVAC system. Availability risk cost is considered as the indices to evaluate the system reliability.

Section 5.1 presents a brief introduction of Markov method and sequential Monte Carlo simulation. Section 5.2 presents the sequential Monte Carlo simulation to obtain the probability distribution of HVAC system. Section 5.3 presents the Markov method to obtain the probability distribution. Section 5.4 gives a case study to illustrate the process of the two methods and a comparison is made between Markov method and sequential Monte Carlo simulation. A summary of this chapter is given is Section 5.5.

5.1 Introduction

As mentioned in Chapter 3, the commonly used methods for quantifying the reliability

contains Markov method and sequential Monte Carlo simulation. The objective of Markov method is to obtain the probability distribution of each healthy state of a multi-state system at the steady period. According to the probability distribution, the capacity of the system under each state can be estimated. It is assumed that the state probabilities at a future instant do not depend on the states occurred in the past. The system either keeps current state or transfer to another state at the next time step. Markov method will be used for reliability modeling of aging equipment in Chapter 6 and Chapter 7. The advantages of the Markov method include high accuracy and relatively fast computation time; the disadvantages are the inability to provide more reliability information (i.e. this method can only provide the average probability distribution of steady state of system).

Sequential Monte Carlo simulation is a simulation-based method that provides a convenient and attractive approach to compute the posterior distributions. It is very flexible, easy to implement, parallelizable and applicable in very general settings. In HVAC subsystems, all the components of each subsystem are parallel and independent. Based on the characteristics of the HVAC subsystems, this method can be used in the reliability assessment of HVAC subsystems. Compared with Markov method, the sequential Monte Carlo simulation is capable of providing more comprehensive results than Markov method. Chapter 7 gives an example to show the application of robust optimal design based on sequential Monte Carlo simulation.

5.2 Sequential Monte Carlo Simulation

As mentioned above, availability risk cost, which depends on the unmet cooling load directly, is considered as the indices to evaluate the system reliability. Unmet cooling

load is the load difference between the required cooling load and the available cooling supply capacity. Fig. 5.1 shows the simulation loop for obtaining the accurate cooling load distribution and average "unmet cooling load". Cooling load distribution is generated by the TRNSYS building energy model based on the uncertainties of design inputs. Available cooling capacity is the maximum cooling capacity corresponding to the capacity under the design weather conditions. Available cooling capacity is determined by the health state of system components and nominal capacity. Convergence assessment is conducted to justify the cooling load distribution and average "unmet cooling load".
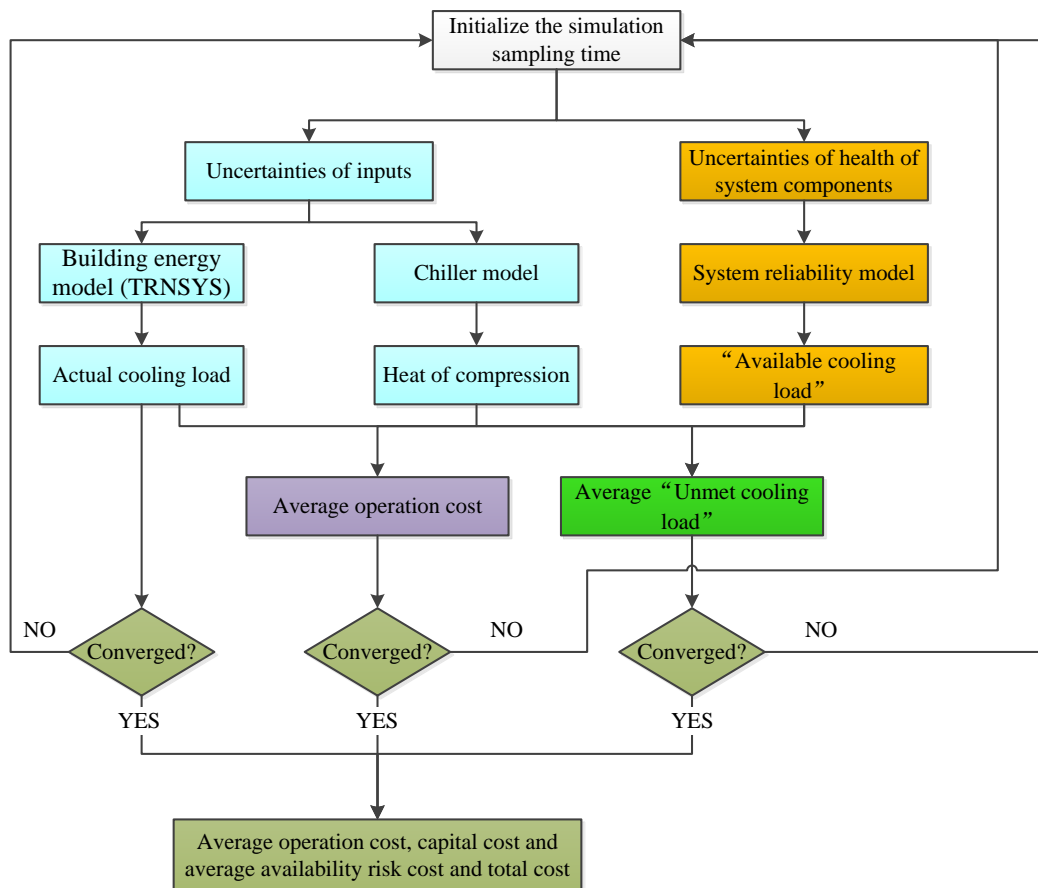
Fig.5.1 Simulation loop for obtaining the accurate cooling load distribution and average "unmet cooling load"

Monte Carlo simulation is employed to obtain the cooling load conditions considering uncertainties. The calculation process can be illustrated by Equation (5.1). With the inputs x_1, x_2,…, x_n (e.g., the outdoor temperature, ventilation rate), the output y (the cooling load) can be obtained.

$$Y = [y_1, y_2,..., y_{8760}] = f(x_1, x_2,..., x_n)$$ (5.1)

Two reliability indices, which includes the availability, $p_{availability}$ (percentage of time staying in a working state) and unavailability, $p_{unavailability}$ (percentage of time staying in a failure and maintenance state) can be calculated from the reliability and maintainability history chart above by Equation (5.2) and (5.3). Where, *MTTF* is mean time to failure, *MTTR* is mean time to repair.

$$p_{availability} = \frac{MTTF}{MTTF + MTTR}$$ (5.2)

$$p_{unavailability} = \frac{MTTR}{MTTF + MTTR}$$ (5.3)

With the assumption that each component is independent and it has no relationship with the other components, the probability of each component is assumed to be subject to the binary distribution. Monte Carlo simulation is used to obtain the state (i.e. normal or failure) of system component under each cooling load condition, as shown in Equation (5.4). The total available cooling capacity is calculated by Equation (5.5). The unmet cooling load is calculated by Equation (5.6). Where, f is the availability of system capacity, CL_{ind} is the nominal capacity, $CL_{available}$ is the available cooling capacity, $CL(i)$ is the cooling load, CL_{unmet} is the unmet cooling load.

$$f(i) = B(1, p_{availability})$$ (5.4)

$$CL_{available} = CL_{ind} \cdot \sum_{i=1}^{n} f(i)$$ (5.5)

$$CL_{unmet} = Max[CL(i) - CL_{available}, 0] \qquad (5.6)$$

As mentioned above, the cooling load distribution and available cooling capacity can be generated by a sequential Monte Carlo simulation. For the purpose of checking the convergence and terminating the sampling process, the threshold is used to evaluate the uncertainty and reliability in this study.

A deviation index $f(n+i,n)$ is defined to represent the difference between average cooling load distribution profiles of $(n+i)$ number of simulations and n number of simulations respectively, as shown in Equation (5.7) and Fig. 4.2.

$$f(n+i,n) = \frac{\sum_{1}^{k}\left[\left|p_{n+i}(j) - p_n(j)\right| \cdot \Delta CL_j\right]}{\sum_{1}^{k}\left[p_n(j) \cdot \Delta CL_j\right]} \qquad (5.7)$$

where, $p_n(j)$ is the probability at the load of CL_j of n trials of simulations, $p_{n+i}(j)$ is the probability at the load of CL_j of $n+i$ trials of simulations, $\triangle CL_j$ is the cooling load interval and k is the total number of intervals. Equation (5.8) presents this criteria in mathematic form, i.e. for all last B_L simulations, the deviation index is within the threshold B_w. Where, b is the required sampling time.

$$f(b+j,b) \le B_w \qquad \forall j, \; j = 1, 2, ..., B_L \qquad (5.8)$$

The second deviation index $g(n+i,n)$ is defined to represent the difference between average unmet cooling load of $(n+i)$ number of simulations and n number of simulations respectively, as shown in Equation (5.9).

$$g(n+i,n) = \frac{\left|CL_{un,(n+i)} - CL_{un,n}\right|}{CL_{un,n}} \qquad (5.9)$$

where, $CL_{un,n}$ is the average unmet cooling load at n trials of simulations, $CL_{un,(n+i)}$ is the average unmet cooling load at $(n+i)$ trials of simulations. Equation (5.10) presents the

criteria in mathematic form, i.e. for all last B_L simulations, the deviation of the unmet cooling load is within the threshold B_w. Where, c is the required sampling time.

$$g(c+j,c) \leq B_w \qquad \forall j, j = 1,2,...,B_L \qquad (5.10)$$

5.3 Markov Method

Markov method is used in this thesis because of its wide application in reliability analysis of multi-state systems. A system is comprised of n components in parallel. It is assumed that each component has two states only: normal (0) and failure (1). As shown in Fig. 5.2, from failure condition to normal condition, the repair rate μ is used to represent the probability from one state to another. From normal condition to failure condition, the failure rate λ is used to represent the probability from one state to another. Totally the system has n states (i.e., each states contains several situations) considering the reliability of each component, as shown in Fig.5.3. It can be observed that state 0 symbolizes that no component fail and state k symbolizes that k ($1 \leq k \leq n$) components fail. The transition probability between each two states is represented by a state transition density matrix A (Equation (5.11)), which only involves the repair rate and failure rate of components. It can be deduced from the initial state by Equation (5.12) and Equation (5.13). When the time approaches to infinity, $P(\infty)$ will keep stable (Equation (5.14)). Then the steady state probabilities can be obtained by solving the linear algebraic equations (Equation (5.15) and Equation (5.16)). The mean steady system performance under each state thus can be calculated. In addition, it is worth noticing that how much time is required to reach the steady condition is significant in the method. If the time is very long such as two years, it should be considered in the

reliability assessment. If the time is very short such as one month, then it will not be considered in this method. Probability of state 0 is selected as the standard to assess the time achieving the steady state, as shown in Fig. 5.4.
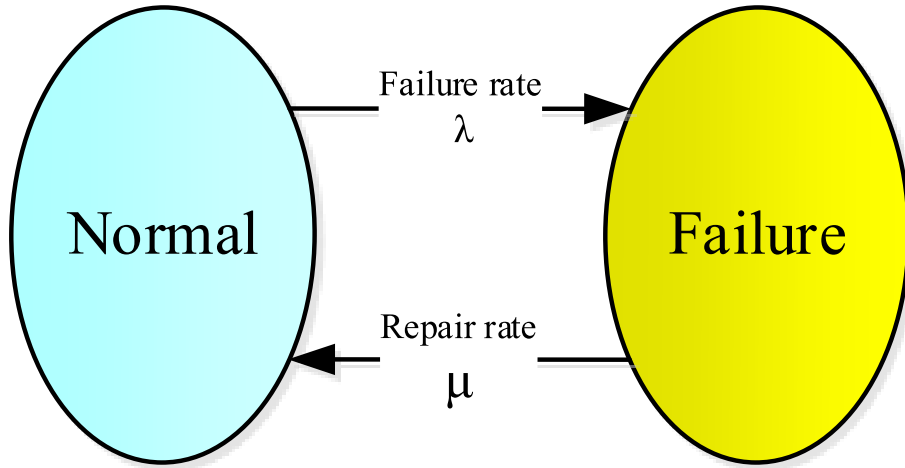
Fig.5.2 Two-state Markov process
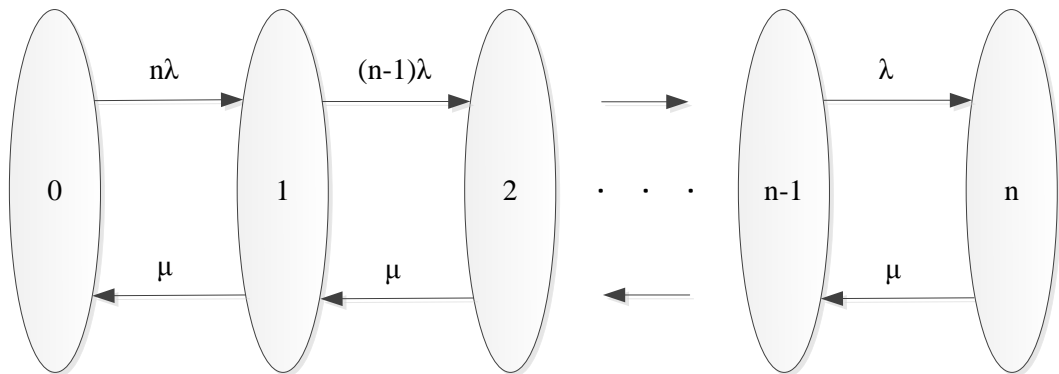
Fig.5.3 States of a *n*-parallel system and possible transitions

$$A = \begin{bmatrix} (1-n\lambda) & n\lambda & 0 & 0 & 0 \ldots 0 & 0 & 0 \\ \mu & (1-\mu-(n-1)\lambda) & (n-1)\lambda & 0 & 0 \ldots 0 & 0 & 0 \\ 0 & \mu & (1-\mu-(n-2)\lambda) & (n-2)\lambda & 0 \ldots 0 & 0 & 0 \\ \ldots & \ldots & \ldots & \ldots & \ldots \\ 0 & 0 & 0 & 0 & 0 \ldots \mu & (1-\lambda-\mu) & \lambda \\ 0 & 0 & 0 & 0 & 0 \ldots 0 & \mu & (1-\mu) \end{bmatrix} \quad (5.11)$$

$$P(0) = [1, 0, 0, ..., 0] \quad (5.12)$$

$$P(n) = P(n-1)A = P(0)A^n \quad (5.13)$$

$$P(\infty) = \lim_{n \to \infty} P(n) = \lim_{n \to \infty} P(0)A^n \tag{5.14}$$

$$P(\infty) = P(\infty - 1)A = P(\infty)A \tag{5.15}$$

$$\begin{cases} p(0) = a_{00}p(0) + a_{10}p(1) + \cdots + a_{n0}p(n) \\ p(1) = a_{01}p(0) + a_{11}p(1) + \cdots + a_{n1}p(n) \\ \quad\vdots \qquad\qquad\qquad\vdots \\ p(n) = a_{0n}p(0) + a_{1n}p(1) + \cdots a_{nn}p(n) \\ \quad \sum_{i=0}^{n} p(i) = 1 \end{cases} \tag{5.16}$$
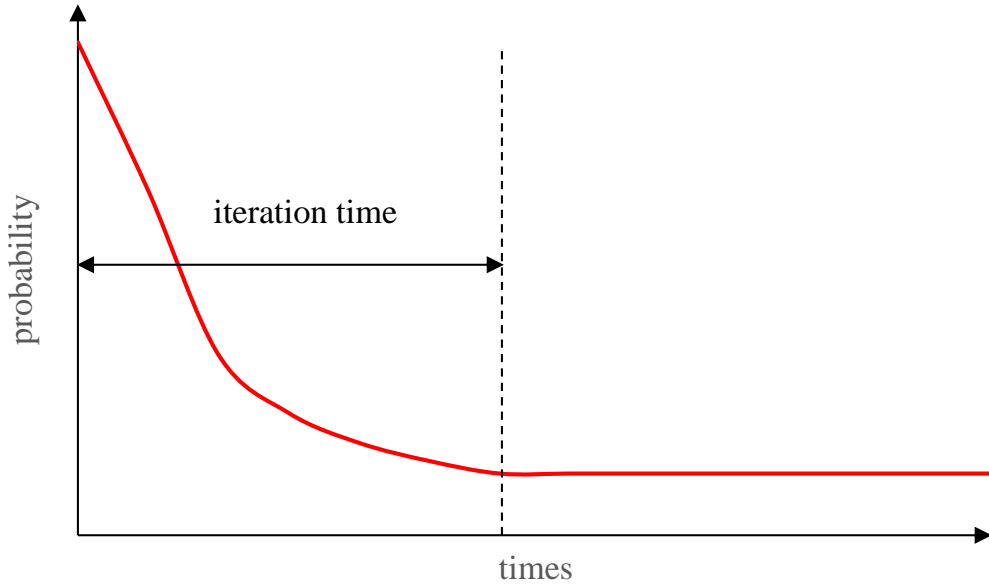
Fig.5.4 Scheme of the time achieving the steady condition

5.4 Comparison Case Study

5.4.1 Convergence assessment of iteration time of Markov method

As mentioned above, Markov method is used to obtain the probability of each (health) state of the pump system and to calculate the mean steady performance and capability under each state. In this chapter, the system is assumed to be comprised of about 2~8 chilled water pumps and the system there have 2~8 states accordingly. The failure rate is assumed to be 0.0001/hour (Blanchard et al. 1998), the repair rate is assumed to be

0.002/hour (Gang et al. 2015) and the ratio of repair rate/failure rate is 20. Fig. 5.5 shows the iteration time achieving the steady state 0 under different pump numbers. It is worth noticing that the system comprised of less pumps needs more time to achieve the steady state 0. The probabilities of state 0 under 2, 3, 4, 5 and 6 pumps are 0.9222, 0.8906, 0.8494, 0.7951 and 0.7289 respectively. For the system comprised of two pumps, about 1500 hours (i.e., 83 days if the system works 18 hours daily) is required to achieve the steady state 0, which could be ignored during the life cycle of system.
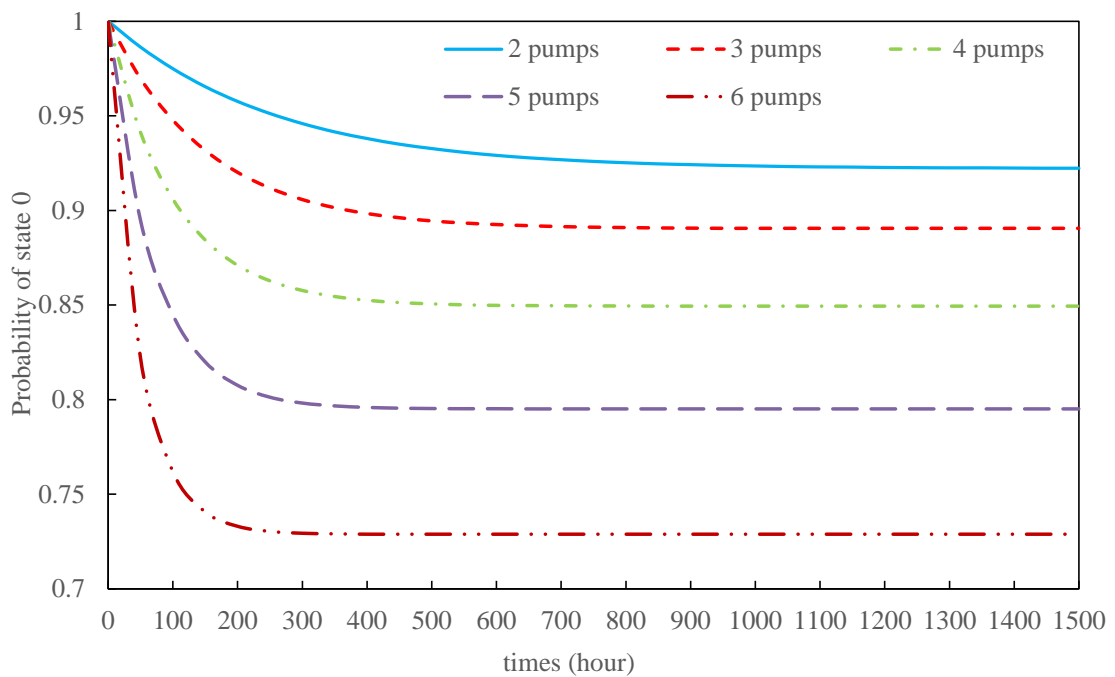
Fig.5.5 Iteration time achieving the steady state 0 under different pump numbers

It is worth noticing that the failure rate and repair rate may have significant impact on the iteration time. When the repair rate varies from 0.001 to 0.005, the ratio of repair rate to failure rate (i.e. repair rate/failure rate) varies from 10 to 50. Fig. 5.6 shows the impact of the ratio of repair rate to failure rate on the iteration time under the system comprised of three pumps. It can be seen that the iteration time is shorter when the ratio of repair rate to failure rate increases. When the ratio increases from 10 to 50, about

1750, 900, 750, 600 and 400 hours are required to reach the steady state 0 respectively. At the same time, the probabilities of state 0 are 0.79, 0.88, 0.93, 0.95 and 0.96 respectively when the ratio increases from 10 to 50 with an increment of 10. Therefore, when the ratio of repair rate to failure rate increases, less iteration time is required to reach the steady state, and the probability of state 0 increases to higher level. In this study, the ratio is assumed to be 20, which has high robustness concerning the system reliability.
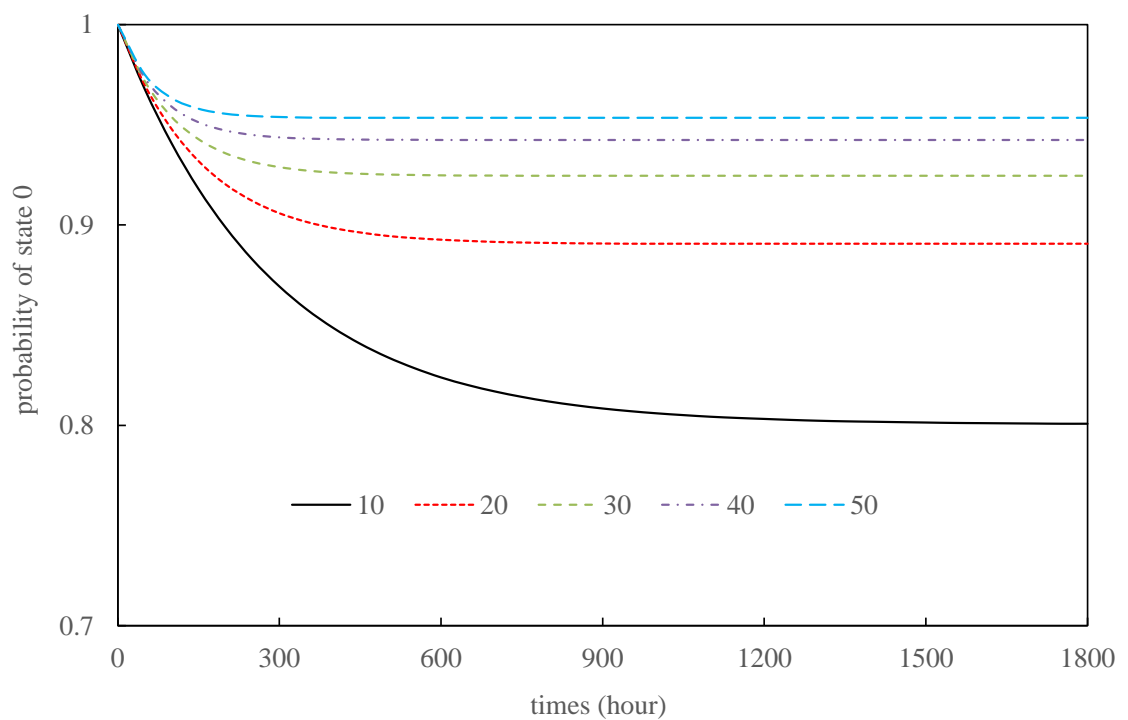
Fig.5.6 Iteration time under different ratios of repair rate to failure rate

5.4.2 Comparison between the two methods

In this chapter, the cooling towers are used as an example to illustrate the two methods. About 2-8 cooling towers are employed in the cooling water system. The design cooling water flow rate is 330L/s. The failures rate of cooling tower is 0.00001/hour, which means that the total working time of cooling towers is 100,000 hours during a period.

The repair rate of cooling towers is 0.002/hour, which means that it totally needs 500 hours to repair or maintain the cooling towers. Therefore, the availability of cooling towers is 0.995 respectively.

According to the Markov methods, Table 5.1 shows the probability distribution of each steady state under different cooling tower numbers. It can be observed that the probability of state 0 decreases as the increase of cooling tower number. It also can be observed that only the failure of one component and the failure of two components are required to be considered.

Table 5.1 Probability distribution of steady states of cooling towers

state	2	3	4	5	6	7
0	0.9900	0.9851	0.9801	0.9751	0.9702	0.9652
1	0.0099	0.0148	0.0196	0.0244	0.0291	0.0338
2	0	0.0001	0.0003	0.0005	0.0007	0.0010
3	-	0	0	0	0	0
4	-	-	0	0	0	0
5	-	-	-	0	0	0
6	-	-	-	-	0	0
7	-	-	-	-	-	0

Fig.5.7 shows the average unmet cooling loads of 3 cooling towers using sequential Monte Carlo simulation and Markov method. It is obvious that the average unmet cooling load is smaller when the number of cooling tower increases. It can be seen that the average unmet cooling load varies greatly when the simulation trial is less than 250. It can be also seen that about 530 sampling times are needed to obtain the accurate average unmet cooling load and the average unmet cooling load fluctuates around the

converged value 7330kW. The unmet cooling load using analytical method is equal to about 7314kW, which is almost equal to that using sequential Monte Carlo simulation.

Fig.5.8 shows the average unmet cooling loads of 5 cooling towers using sequential Monte Carlo simulation and Markov method. It can be seen that about 530 sampling times are needed to obtain the accurate average unmet cooling load and the average unmet cooling load fluctuates around the converged value 814kW. It can be also observed that the unmet cooling load based on the Markov method is almost equal to the converged average unmet cooling load based on the sequential Monte Carlo simulation.
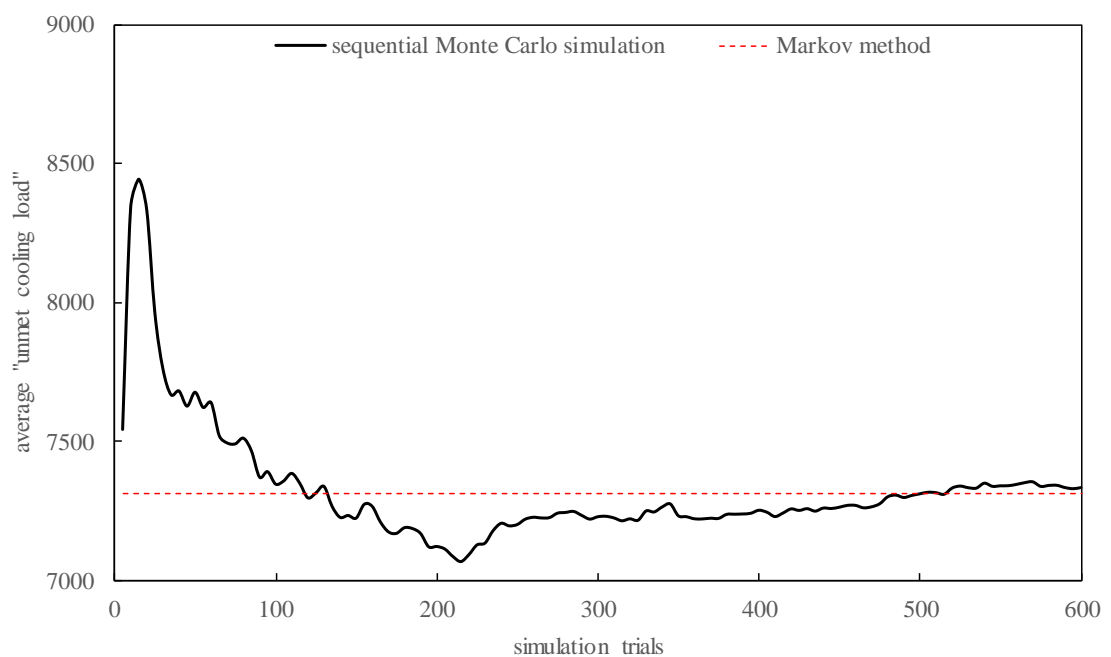
Fig.5.7 Unmet cooling load of 3 cooling towers
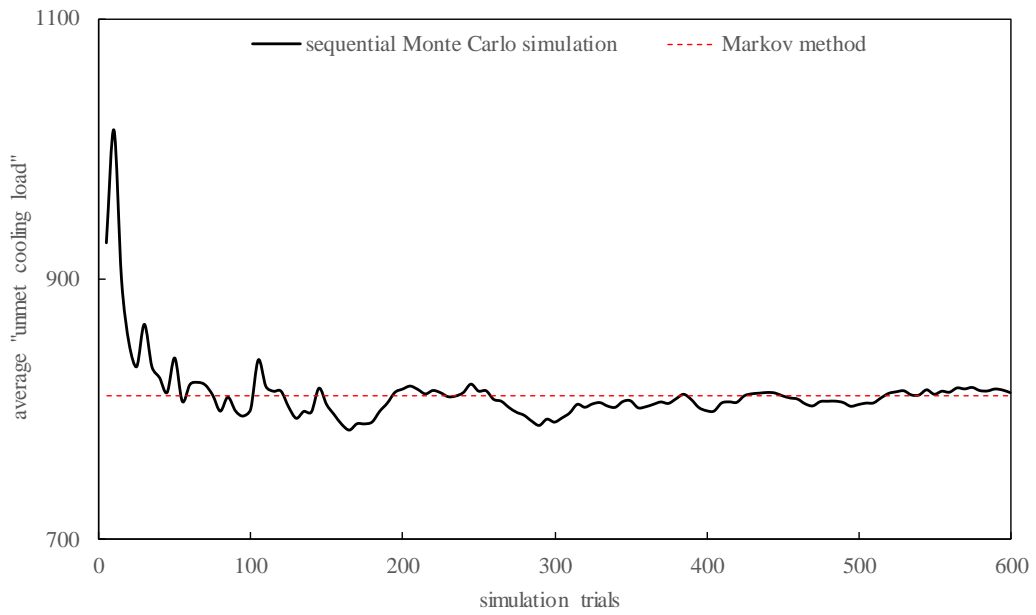
Fig.5.8 Unmet cooling load of 5 cooling towers

Fig.5.9 shows the average unmet cooling loads of 7 cooling towers using sequential Monte Carlo simulation and Markov method. It shows the average unmet cooling load of 7 cooling towers under different simulation trials. It can be seen that about 480 sampling times are needed to obtain the accurate average unmet cooling load and the average unmet cooling load fluctuates around the converged value 100kW.
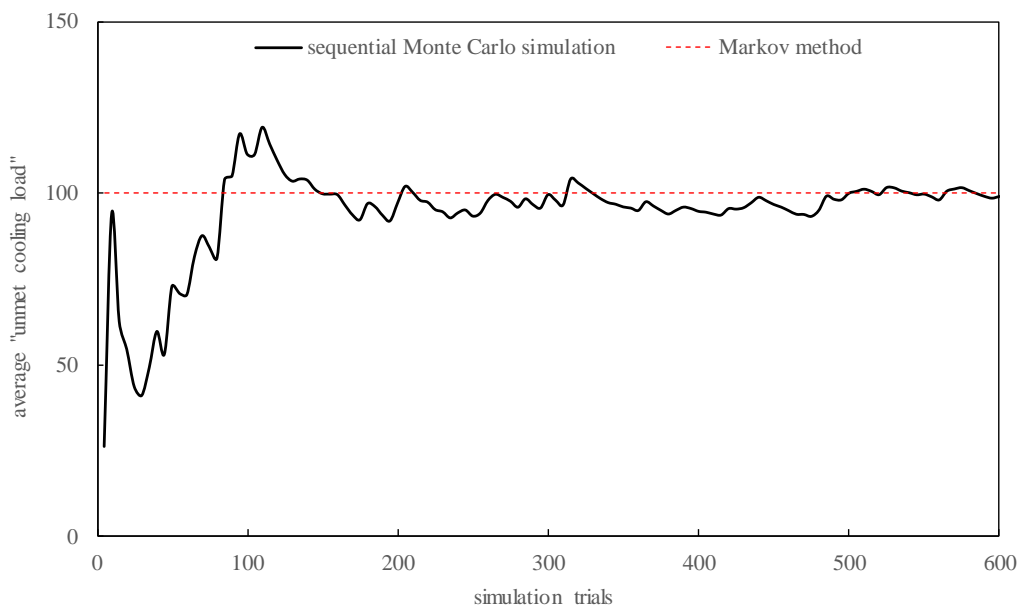
Fig.5.9 Unmet cooling load of 7 cooling towers

Table 5.2 shows the converged average unmet cooling load under different options of cooling towers. It can be seen that the converged average unmet cooling load decreases rapidly when the number of cooling towers increases. When the number of cooling towers is large, the average unmet cooling load does not change greatly.

Table 5.2 Converged average unmet cooling load and average operation cost of different cooling tower options

Options (Size (L/s) ×number)	165×2	110×3	83×4	66×5	55×6	47×7	41×8
Average unmet cooling load (kW)	26504	7341	1961	814	325	100	60

From the above three cases, using Markov method can obtain accurate unmet cooling load and consume less computation time compared with sequential Monte Carlo simulation. However, Monte Carlo simulation approach is capable of providing more comprehensive results than Markov methods such as the detailed changes of unmet cooling load.

5.5 Summary

This chapter presents two quantification methods of reliability. It contains the Markov method and sequential Monte Carlo simulation. Both the two methods are commonly used to conduct reliability assessment. The details of how to implement these two methods are presented in this chapter. A case study is given as an example to demonstrate the proposed methods. Conclusions can be made as follows:

- The transition hours of Markov method could be ignored during the lifespan of system. About 1500 hours (i.e., 83 days if the system works 18 hours daily) is required to achieve the steady state 0 when the Markov method is used.

- The advantages of the Markov method include high accuracy and relatively fast computation time; the disadvantages are the inability to provide more reliability information (i.e. this method can only provide the average probability distribution of steady state of system).

- Compared with Markov method, the sequential Monte Carlo simulation is capable of providing more comprehensive results than Markov method. However, the computation time using sequential Monte Carlo simulation is much longer than that using Markov method.

CHAPTER 6 UNCERTAINTY-BASED OPTIMAL DESIGN OF CHILLER PLANT

This chapter presents an uncertainty-based optimal design method of chiller plant using a probabilistic approach. It can ensure high chiller performance and achieve the minimum operation cost under various possible cooling load conditions, even though the load conditions deviating from the design conditions significantly due to various uncertainties of design information. In contrast to previous research, a probabilistic approach, which contains a wide range of so-called uncertainty "scenarios" generated by Monte Carlo simulation, is used for evaluating the performance of uncertainty-based optimal design. This design is based on two statistical objectives, i.e., a maximization of the expected COP and a minimization of the expected value of the annual total cost. Meanwhile, an uncertainty-based optimization is conducted to identify the best combination of number, sizes and types of chillers to achieve high operating efficiency and minimum total cost (including the operational cost and capital cost) under any cooling load conditions.

Section 6.1 gives a brief introduction about the uncertainty-based optimal design of chiller plant based on probabilistic approach. Section 6.2 presents the method of the uncertainty-based optimal design for chiller plants in detail. Section 6.3 shows a case study on the uncertainty-based optimal design of the chiller plant of a building in Hong Kong. A summary of this chapter is given in Section 6.4.

6.1 Introduction

The uncertainty-based optimal design is performed in three steps as follows:

- *First step: generate the cooling load distribution involving uncertainties;*

- *Second step: determine the total design capacity of the chiller plant based on the cooling load distribution;*

- *Third step: determine optimal chiller plant configuration, i.e. number and sizes of chillers, types of chillers (constant speed chiller/variable speed chiller), by minimizing the life-cycle total cost of the chiller plant at the cooling load involving uncertainties.*

6.2 Uncertainty-based Optimal Design Method

6.2.1 Cooling load distribution of required accuracy involving uncertainties

To conduct the proposed uncertainty-based optimal design, the first step is to obtain the cooling load distribution involving uncertainties. In order to consider various possible cooling load conditions under uncertainties (including variability and epidemic uncertainty), how to deal with the certain and uncertain factors is critical. Fig.6.1 illustrates the schematic of a stochastic cooling load simulation. In this scheme, some input factors (e.g., building characteristics and equipment characteristics) are considered to be well-known or non-influential factors. Therefore, the values are represented by scalar numbers (Domínguez-Muñoz et al. 2010). In addition, some input factors (e.g., weather conditions, occupants and heat transfer coefficients of building envelopes) are uncertain, and they are therefore described by probability distributions

of different types (Saltelli et al. 2004). When the certain and uncertain factors are determined, a more accurate model among alternative cooling load models is selected to calculate the cooling load in each scenario (Gentle 2003).
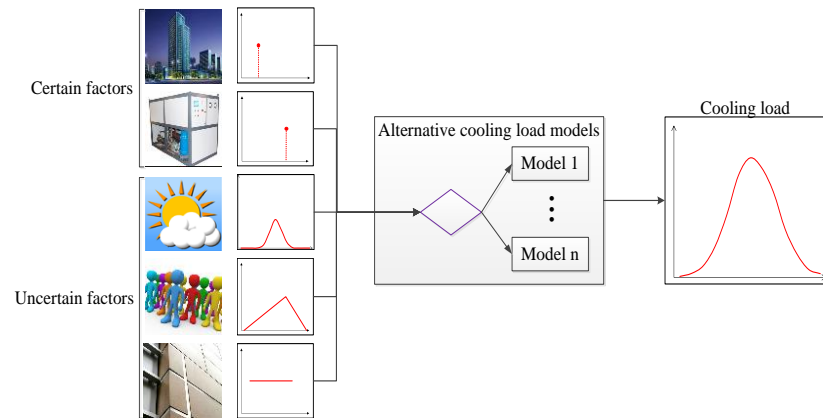
Fig.6.1 Scheme of the framework for cooling load simulation

In order to generate the cooling load considering uncertainties, Monte Carlo simulation is employed. Monte Carlo simulation is a sampling-based technique that performs multiple model runs with random samples generated from the input distributions (Gentle 2003). These simulations provide a series of possible results, which involve uncertainties in the variables. In this thesis, the uncertainties of the input parameters are computed by Matlab.

Combining the output uncertainties from Matlab, the TRNSYS building model is used to generate the building cooling load distribution considering the uncertainties based on the determined simulation number. After conducting the minimum trials of Monte Carlo simulations of required accuracy, the cooling load distribution involving uncertainties is determined. The peak cooling load is used for the determination of design capacity and cooling load distribution is used for calculating the operation cost of different chiller plant configurations. When using a Monte Carlo simulation, it is essentially important

to determine the minimum number of Monte Carlo simulation, which is presented in detail in Chapter 4.

6.2.2 Total design capacity determination

The second step is to determine the total design cooling capacity, which plays a significant role in the design of chiller plant. To determine the total design cooling capacity, it is essential to obtain the design capacities with numbers of hours when the cooling demand cannot be met (marked as unmet hours). Based on the cooling load distribution, the "mean" design capacity of the total simulation trials are calculated and shown in Figure 6.2. The "mean" value represents the design capacity of chiller plant, corresponding to different unmet hours per year, based on the average cooling load distribution profile. The "max" value represents the maximum value among all the simulation trials. The "reference" value represents the design capacity determined using conventional method, i.e. based on the cooling load distribution of typical year. The peak cooling load in typical year is presented for comparison. It can be observed that when all the cooling load conditions are met, the design capacities based on average annual load profile ("mean") and maximum load among all the simulation trials ("max") are much higher than the peak cooling load in typical year. However, when certain number of unmet hour is allowed (as required in design guide), the design capacities based on the average annual load profile and the maximum load profile become significantly lower than the peak cooling load in typical year. Therefore, using the peak cooling load in typical year as the design capacity may lead to the oversizing of chiller plant. At most of the unmet hours, the design capacities based on the average annual

cooling profile and that in typical year are very close.
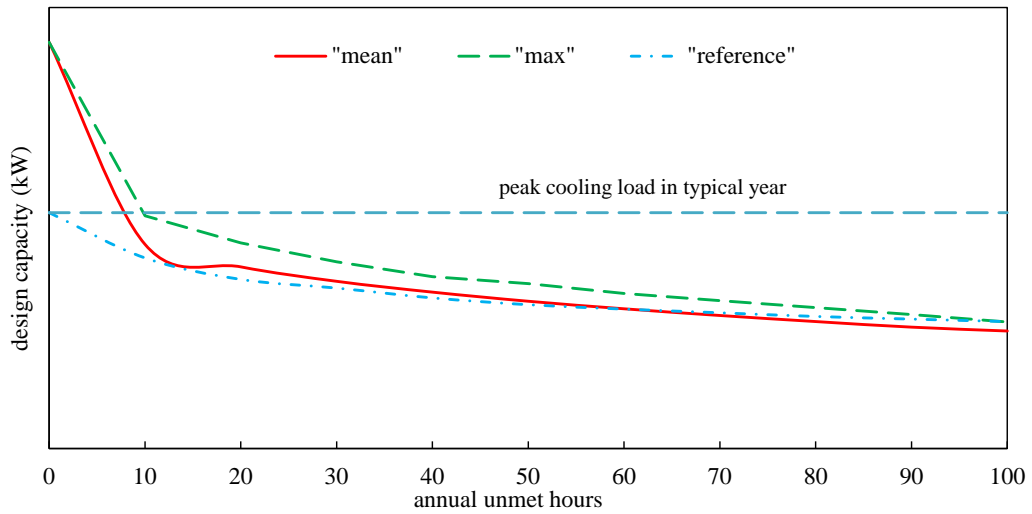
Fig.6.2 Design capacity vs. annual unmet hours

6.2.3 Chiller plant configuration optimization

When the total design capacity is determined, the other key issue is to determine the optimal number, sizes and types of chillers in order to achieve minimum annual total cost. The annual total cost TC_n contains two parts, i.e. annual capital cost CC_n and annual operational cost $OC_n(N)$, as shown in Equation (6.1).

$$TC_n = OC_n(N) + CC_n(N) \qquad (6.1)$$

The annual capital cost is the fixed expense in purchasing and installing the chillers and associated components, which is influenced by the number, sizes and types of chillers. As for the annual operational cost, it is mainly related to the annual cooling load distribution and the energy efficiency. The energy efficiency is subject to the number, sizes and types of chillers.

The optimization of the chiller plant configuration is achieved, as shown in Fig.6.3,

mainly based on three major modules. The optimization process and main assumptions are summarized as follows.

I. *Calculate the operating COP of chiller plant with different chiller numbers. At least two chillers are employed for convenient control and maintenance.*

II. *Under different number, optimize the sizes of chillers to maximize the operating COP. In practice, two types of sizes are preferred for convenient maintenance and control. Besides, more (or same number) chillers with larger capacity and fewer (or same number) chillers with smaller capacity are reasonable and therefore assumed in the optimization trials.*

III. *Under different number and associated optimal sizes of chillers, optimize the types of chillers (e.g. constant speed chiller/variable speed chiller).*

IV. *Having optimal sizes and types of chillers for different chiller numbers, select the optimal chiller number to achieve the minimum total cost when the capital cost is considered.*

The operating COP mainly relates to the number, size and type of chillers. In general, these three factors should be optimized together to achieve a high operating COP, which may result in that the calculations may be very complex. However, it is worth noticing that the number and size of chillers is subject to the total design capacity and the type of chillers mainly affects the operation efficiency of the chiller plant. To enhance the computation efficiency, the number and size of chillers are optimized together and then the type of chillers is optimized later, which may have no obvious impact on the optimization results compared with the situation that these three factors are considered

together.
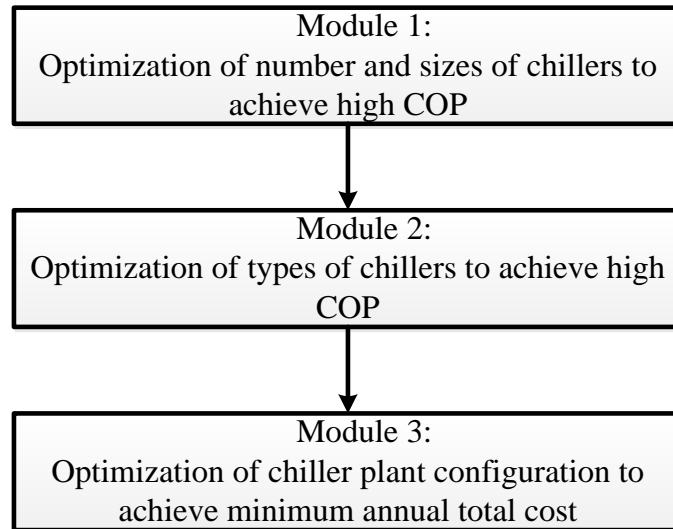
Fig.6.3 Determination of optimal chiller plant configuration

Module 1 – Optimization of number and sizes of chillers concerning energy efficiency

As mentioned above, the annual operational cost is mainly related to the annual cooling load distribution and system energy efficiency. The energy efficiency of chiller plants, usually evaluated by COP, strongly depends on the operating PLR. It is well known that the larger the PLR, the higher COP once the impact of other operating parameters (e.g. condensing and evaporating temperatures) are separated (Hong et al. 2014; Wang et al. 2012), as shown in Equation (6.2).

$$COP_i = D_0 + D_1 \cdot PLR_i + D_2 \cdot PLR_i^2 + D_3 \cdot PLR_i^3 \tag{6.2}$$

where, D_0-D_3 are the coefficients that can be identified from chiller catalogue or field measurement data. The PLR is usually determined by the number and size of chillers. Therefore, the optimization of number and size of chillers is conducted to improve the operating PLR and thus COP.

PLR is simply defined as the ratio of the required cooling load (CL_{re}) to the available

cooling capacity (CL_{ava}) (i.e. that of operating chillers) as shown in Equation (6.3).

$$PLR = \frac{CL_{re}}{CL_{ava}} = \frac{CL_{re}}{N_{op} \cdot CL_{Nominal}} \tag{6.3}$$

where, $CL_{Nominal}$ is the nominal cooling capacity of each chiller. Nop is the number of

operating chillers. It means that the more chillers are selected, the higher operating PLR

can be achieved through more flexible sequence control. On the other hand, selecting

more chillers means that the size of individual chillers is smaller. Generally, the rated

COP of chiller decreases when the nominal capacity of chillers reduces in certain extent

(Harvey 2012). Therefore, the operating COP increases when the number of chillers

increases to certain value and it reduces when the number of chillers increases further,

as shown in Fig.6.4. Since at least two chillers are used for convenient maintenance and

control, the calculation of the chiller number starts from two until the operating COP

begins to decrease.
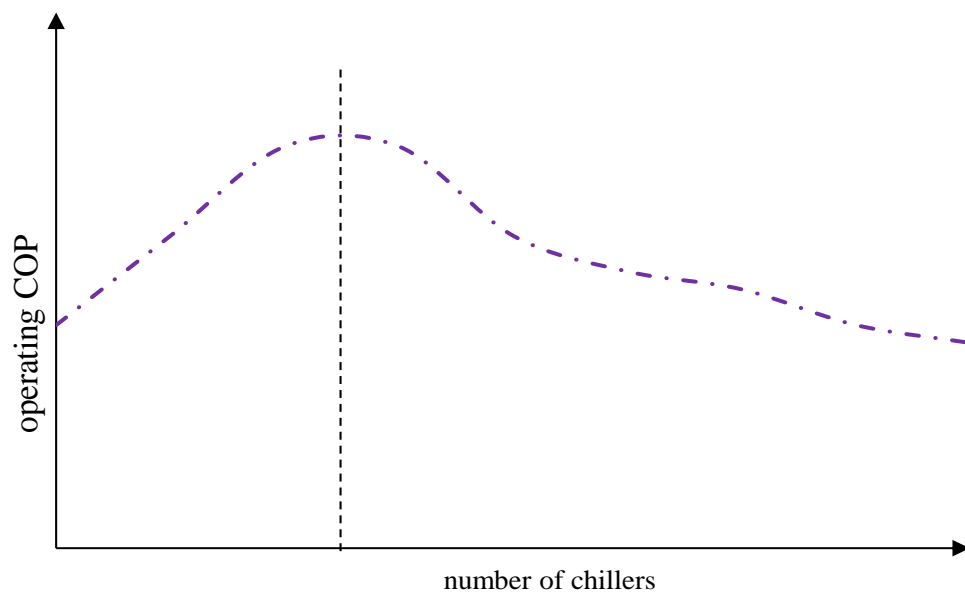
Fig.6.4 Effects of number of chillers on the operating COP

The sizes of individual chillers, which determine the rated COP, influence the PLR and operating COP of the chiller plant. In practice, two types of sizes of chillers are proper for the convenient maintenance and control. Besides, the number of chillers of larger capacity is selected to be at least the same as that of smaller capacity in the optimization trials. To determine the optimal sizes of chillers at a given chiller number, the larger size increases gradually from the mean value (i.e., all the chillers are equally sized) until the operating COP achieves the maximum value in the optimization trials. At the same time, the smaller size decreases accordingly. The constraint of chiller plant configuration is shown in Equation (6.4).

$$n_1 \cdot C_1 + n_2 \cdot C_2 = CL_T$$
$$C_1 \geq C_2, \ n_1 \geq n_2$$

(6.4)

where, C_1 and n_1 are the nominal design capacity and number of the larger chillers respectively. C_2 and n_2 are the nominal design capacity and number of the smaller chillers respectively. CL_T is the total design capacity of the chiller plant. Equation (6.5) formulates the optimization problem for selecting the chiller number/sizes.

$$
\begin{aligned}
\text{find} \quad & C_1, C_2, n_1, n_2 \\
\text{that maximizes} \quad & COP_{op}(C_1, C_2, n_1, n_2) \\
\text{subject to} \quad & n_1 \cdot C_1 + n_2 \cdot C_2 = CL_T \\
& n_1 + n_2 \geq 2 \\
& C_1 \geq C_2, n_1 \geq n_2
\end{aligned}
$$

(6.5)

where, COP_{op} is the operating COP based on annual cooling load distribution.

Module 2 – Optimization of types of chillers

It is well known that the chiller plant usually operates at part load condition for most of time. Under the same operating PLR conditions (with the same cooling load

distribution), chillers with better part load performance are preferred to be used. Fig.6.5 presents the COP profile of two typical types of chillers (i.e., variable-speed chiller and constant-speed chiller). The COP of constant-speed chillers may be the same as or even larger than that of the variable-speed chillers near the full load conditions while the variable-speed chiller performs much better under other load conditions, particularly the low PLR conditions. Therefore, both the constant-speed chillers and variable-speed chillers could be used to achieve a high operating COP.

In order to achieve high operating COP while minimizing the initial cost, more constant-speed chillers and fewer variable-speed chillers are used. In actual operation, the constant-speed chillers are maintained to operate at full load to achieve high COP. The insufficient cooling load, which is larger than the total capacity of operating constant-speed chillers, is covered by variable-speed chillers for their stable COP at part load condition. Equation (6.6) formulates the optimization problem for selecting chiller types. Where, N_c is number of constant-speed chillers, N_v is number of variable-speed chillers.
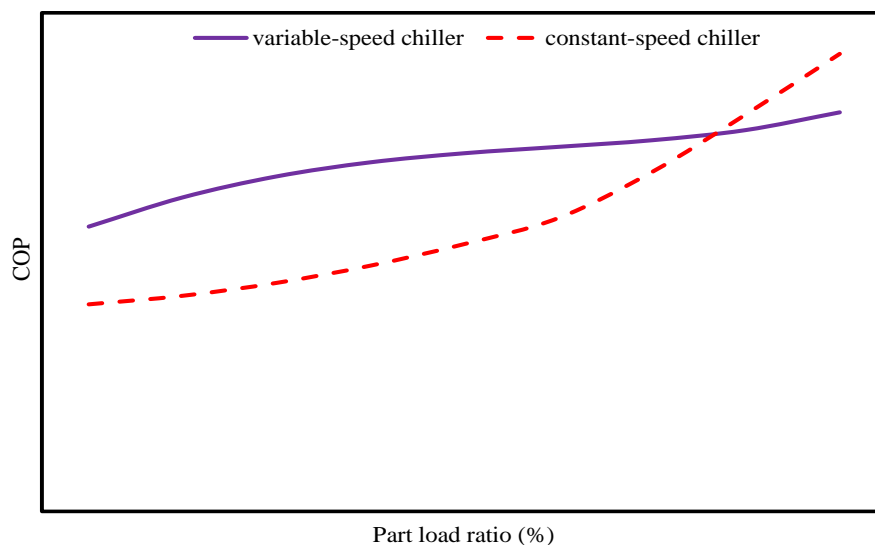
Fig.6.5 COP of constant-speed chiller and variable-speed chiller

$$\begin{aligned}
\text{find} \quad & N_C, N_V \\
\text{that maximizes} \quad & COP_{op}(N_C, N_V) \\
\text{subject to} \quad & N_C \geq N_V \geq 1 \\
& N_C + N_V = n_1 + n_2
\end{aligned} \tag{6.6}$$

Module 3 – Optimization of chiller plant configuration to achieve minimum total cost

As mentioned above, when number of chillers increases up to certain extent, the operating COP of operating chillers increases and the operation cost reduces. Normally, the capital cost of the chiller plant of given total capacity increases when more chillers are used. Therefore, there should be a compromised number of chillers when both the operating cost and the capital cost are considered.

Fig.6.6 illustrates the effects of number of chillers on minimum total cost. If the selected number of chillers is too small, the limited number of chillers will result in low energy efficiency and thus high operational cost while the capital cost of the chiller plant will be high if the selected number of chillers is too large. The optimal number of chillers is determined when the minimum total cost is achieved.
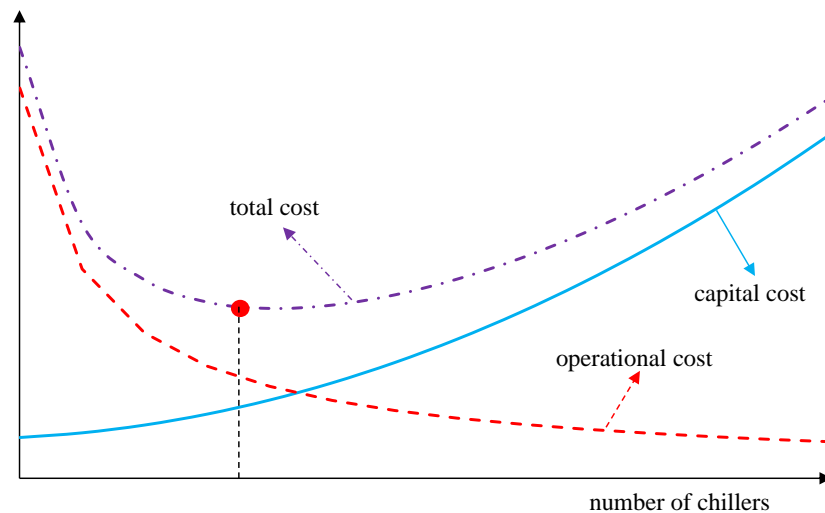
Fig.6.6 Effects of number of chillers on minimum total cost

6.3 Implementation and Evaluation of Uncertainty-based Optimal Design Method

A case study on the chiller plant design for a building in Hong Kong is conducted to test and evaluate the proposed uncertainty-based optimal design. At first, Monte Carlo simulation is used to generate the cooling load distribution profile for the assessment of proposed uncertainty-based optimal design. Then, the total design capacity is determined according to the cooling load distribution profile. Finally, optimal chiller plant configuration is conducted to achieve the minimum total cost.

6.3.1 Cooling load distribution and design cooling capacity

To conduct the Monte Carlo simulations to obtain the cooling load distribution, it is essential to determine the settings of uncertainties of the variables. According to the settings in Table 3.2, the uncertainties of the input parameters are computed by Matlab. Combining the output uncertainties from Matlab, the TRNSYS building model is used to generate the building cooling load considering the uncertainties.

After conducting 780 times of Monte Carlo simulations, the cooling load distribution is obtained, as shown in Fig.6.7. The reference case is the cooling load distribution without considering the uncertainties. It can be seen that the cooling load distribution profile of 780 simulation trials is smoother than that of reference case because more cooling load conditions are considered. The cooling load distribution mostly locates between about 2200kW and 4500kW.
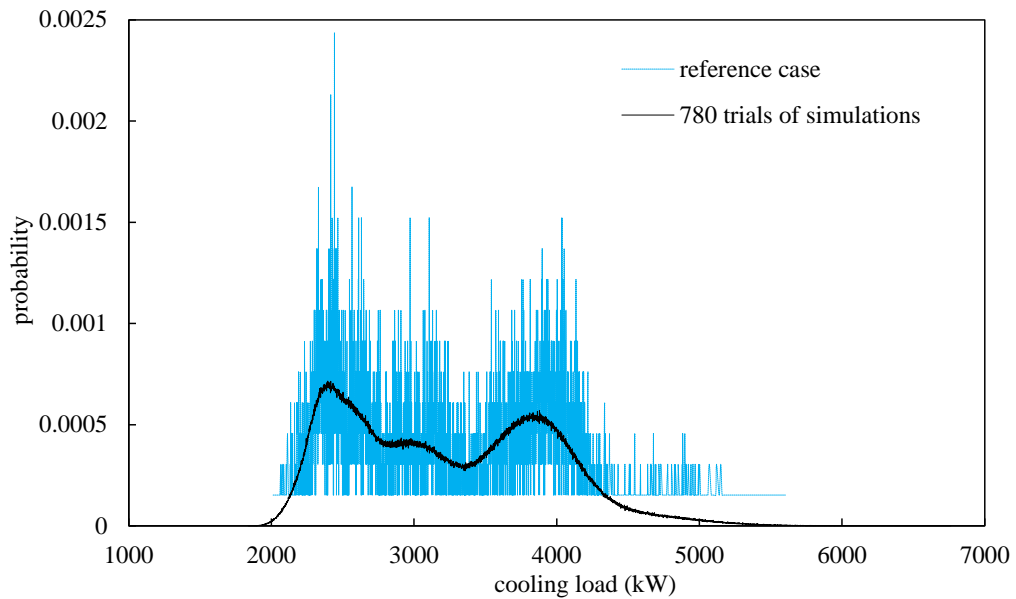
Fig.6.7 Distribution of cooling load considering uncertainties

Then, it is essential to determine the total design capacity of the chiller plant. The design capacities corresponding to different unmet hours are presented in Fig.6.8. The meanings of the symbols can be found in Section 6.2.2. It can be seen that using the peak cooling load of typical year (i.e. 5600kW) as design capacity may lead to the oversizing of chiller plant. When the annual unmet hours are equal to 0, the design capacity of the "mean" and the "max" can be much higher than the peak cooling load of typical year in conventional design, which could result in the serious oversizing of chiller plant. It can be also observed that the profile of "mean" is close to that of the reference case. The decision makers can size the chiller plant based on their specific requirements. In this study, the number of unmet hours should be no more than 50. The chiller plant can be sized based on the load of 5121 kW according to the "max". If the requirement is very strict, smaller number of unmet hours can be used in determining the design capacity.
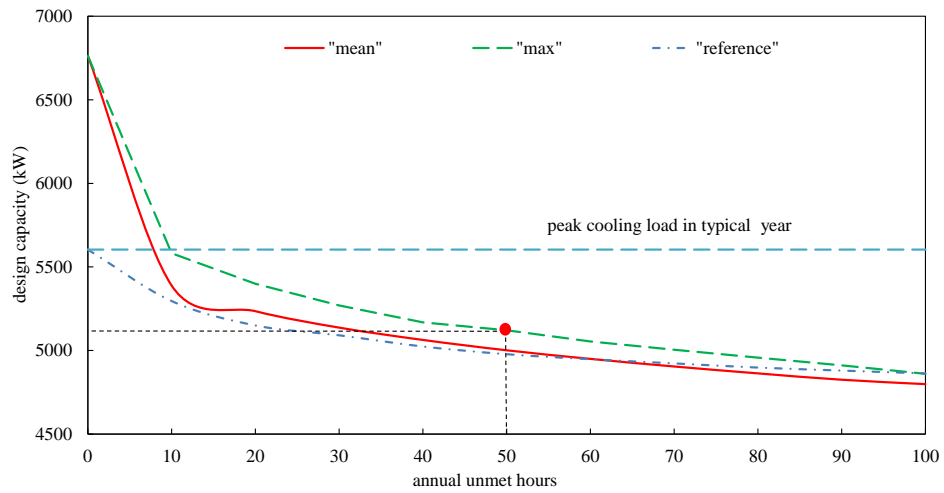
Fig.6.8 Design capacity vs. number of annual unmet hours

6.3.2 Optimal configuration of chiller plant

The capacity of all the chillers should be equal to the design capacity 5100kW. As shown in Fig.6.4, the operating COP increases when the number of chillers increases in certain extent. It decreases when the number of chillers increases further. To facilitate the operation and control, at least two chillers are employed for practical reasons. The tried number of chillers starts from 2 until the number where the operating COP begins to decrease. The sizes of chillers are also optimized under each given chiller number based on the rated chiller COP of different capacities, as shown in Fig.6.9.
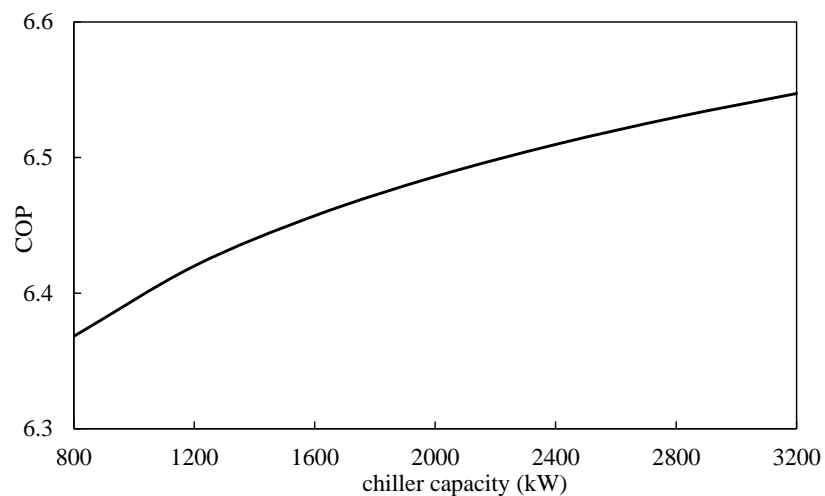
Fig.6.9 Rated COP vs. chiller capacity

Using Module 1 described in Section 6.2.3, the optimization of number and sizes of chillers is conducted. The results are listed in Table 6.1. It can be observed that the operating PLR increases when the number of chillers increases and the operating COP increases when the number of chillers increases from 2 to 5. When the number of chillers increases up to 6, the operating COP reduces. Therefore, the number of chillers is tried between 2 and 6. Combining the chiller plant options from 5 to 8, the chiller plant options consisting of some chillers of larger capacity and one chiller of smaller capacity have a larger operating COP compared with the other options. It means that the optimal chiller plant option consists of more chillers with larger capacity and one chiller with smaller capacity. Among these options, the option 6 has the largest operating COP (6.09) although its PLR (0.91) is not the largest among options. The options 4, 6 and 8 have the better energy performance than options 3, 5 and 7 correspondingly under their chiller numbers. Therefore, the options 3, 5 and 7 will not be considered and the options 1, 2, 4, 6 and 8 are selected for the optimization of types of chillers.

After the number and sizes of chillers are determined, what needs to do is to optimize the types of chillers to improve the COP at part load conditions. Fig.6.10 presents the typical COP profiles of a constant-speed chiller (1200kW) and a variable-speed chiller (1200kW) according to the data from the chiller manufacturer. In this study, under the same PLR, the COPs of constant-speed chillers are assumed to be proportional to their capacities.

Table 6.1 optimization of number and sizes of chillers

Option No.	Chiller Number	Chiller plant option	PLR_{op}	COP_{op}
1	2	1*3200+1*1900	0.790	5.56
2	3	2*2050+1*1000	0.863	5.84
3	4	2*1500+2*1050	0.919	5.89
4	4	3*1400+1*900	0.921	5.95
5	5	3*1200+2*750	0.941	5.95
6	5	4*1100+1*700	0.910	6.09
7	6	4*950+2*650	0.956	6.05
8	6	5*900+1*600	0.932	6.07
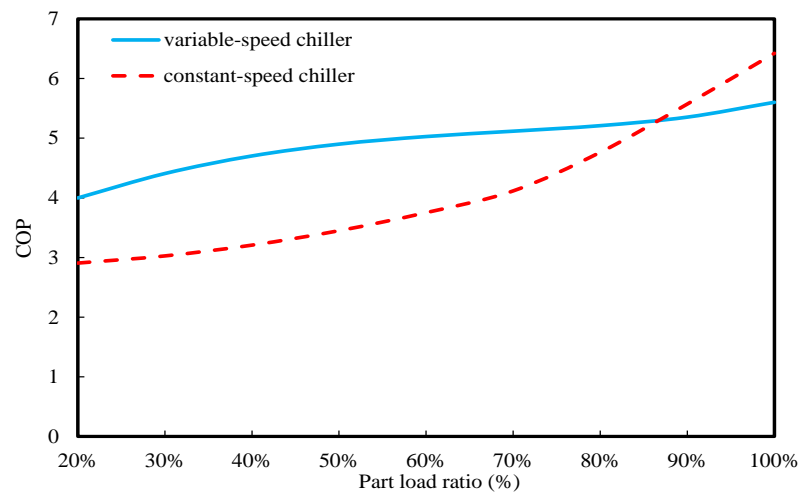
Fig.6.10 COP of constant-speed chiller and variable-speed chiller (1200kW)

Using module 2 described in Section 6.2.3, the optimization of chiller types is conducted to achieve a higher COP. Table 6.2 summarizes the optimization results of types of chillers. The COP distribution is shown in Fig.6.11. The result of conventional design is also presented for the comparison. It can be observed that the option consisting

of four constant-speed chillers (1100kW) and one variable-speed chiller (700kW) has the largest operating COP (6.15) compared with other options. The option consisting of six chillers has a more concentrated COP distribution (from 5.45 to 6.4) than that consisting of two chillers. From Table 6.2, the optimal chiller plant option consists of more constant-speed chillers and one variable-speed chillers to achieve minimum operation cost.

Table 6.2 Optimization of types of chillers

Chiller Number	Chiller plant option	COP_{op}
2	1*3200*CSD+1*1900*VSD	5.65
3	2*2050*CSD+1*1000*VSD	5.91
4	3*1400*CSD+1*900*VSD	5.98
5	**4*1100*CSD+1*700*VSD**	**6.15**
6	5*900*CSD+1*600*VSD	6.12
3	3*1700*CSD (conventional design)	4.75
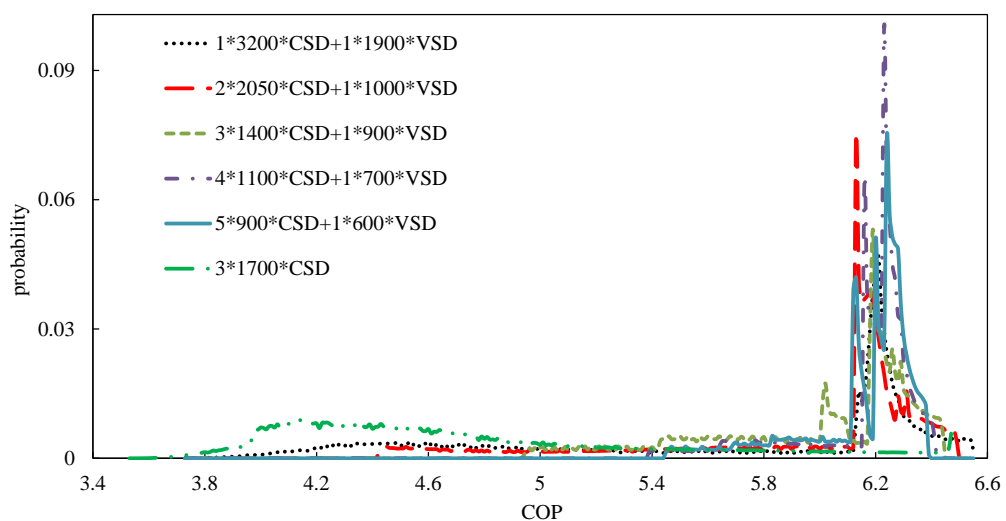
Fig.6.11 Distribution of COP

According to the cooling load distribution shown in Fig.6.7 and the COP distribution shown in Fig.6.11, the annual operation costs of the chiller plants are computed, as listed in Table 6.3. It can be seen that the chiller plant of four constant-speed chillers (1100kW) and one variable-speed chiller (700kW) has the lowest annual operation cost (3,474,483kW) compared with that of other options, while the design option with one constant-speed chiller and one variable-speed chiller has the highest annual operation cost (4,501,630kW). Considering the electricity price (0.8 HK$/kWh), Table 4.6 also shows the annual electricity cost.

Table 6.3 Annual operation cost and electricity cost of different design options

Types	Annual operation cost (kW)	Electricity cost (k HK$)
1*3200*CSD+1*1900*VSD	3,729,780	3,006
2*2050*CSD+1*1000*VSD	3,627,834	2,902
3*1400*CSD+1*900*VSD	3,512,582	2,810
4*1100*CSD+1*700*VSD	**3,474,483**	**2,780**
5*900*CSD+1*600*VSD	3,492,110	2,794
3*1700*CSD (conventional design)	4,501,630	3,601

The annual total cost also contains the annual capital cost of chiller plants. The capital cost contains the equipment, relevant accessories and space rent fees. The lifespan of the chiller plant is assumed to be 10 years. The capital cost of 900kW variable-speed chiller is HKD 1.2M and the capital cost of 900kW constant-speed chiller is HKD 0.9 M, referring to the data from a manufacture. As for the capital cost of other constant-

speed chillers and variable-speed chillers, they are computed by Equation (6.7) (Guthrie 1969; Biegler et al. 1997).

$$CC = CC_0 \cdot (C/C_0)^\alpha \qquad (6.7)$$

where, CC_0 is the capital cost of a reference chiller with the capacity C_0. CC is capital cost of chiller with the capacity C. α is the coefficient, which set to be 0.4 in this study (Biegler et al. 1997; Seider et al. 2009). The annual total costs under the different options are computed using Equation (6.8) and presented in Table 6.4. It can be seen that the option consisting of one constant-speed chiller and one variable-speed chiller has the lowest annual capital cost ($311k$ HK\$). From Table 6.4, the annual capital cost increases when chiller number increases at given total capacity.

Table 6.4 Capital cost of constant-speed chillers and variable-speed chillers

Types	Annual capital cost (k HK\$)
1*3200*CSD+1*1900*VSD	311
2*2050*CSD+1*1000*VSD	375
3*1400*CSD+1*900*VSD	442
4*1100*CSD+1*700*VSD	499
5*900*CSD+1*600*VSD	552
3*1700*CSD (conventional design)	348

Combining the annual operational cost shown in Table 6.3 and the capital cost shown in Table 6.4, the annual total costs under the different options are computed and presented in Table 6.5. It can be observed that the option with three constant-speed

chillers (1400kW) and one variable-speed chiller (900kW) is the optimum design option.

Table 6.5 Annual total costs of the chiller plants

Types	Annual operation cost (k HK$)	Annual capital cost (k HK$)	Annual total cost (k HK$)
1*3200*CSD+1*1900*VSD	3,006	311	3,317
2*2050*CSD+1*1000*VSD	2,902	375	3,277
3*1400*CSD+1*900*VSD	**2,810**	**442**	**3,252**
4*1100*CSD+1*700*VSD	2,780	499	3,279
5*900*CSD+1*600*VSD	2,794	552	3,346
3*1700*CSD (**conventional design**)	3,601	348	3,949

6.3.3 Comparison between conventional design and uncertainty-based design

From Table 6.5, the plant option with one constant-speed chiller (3200kW) and one variable-speed chiller (1900kW) has the least annual capital cost while the option with four constant-speed chillers (1100kW) and one variable-speed chiller (700kW) has the least annual operation cost. To achieve a compromised annual operational cost and annual capital cost and thus the minimum annual total cost, the chiller plant option with three constant-speed chillers (1400kW) and one variable-speed chiller (900kW) can be considered as the optimum selection for the design, and the minimum annual total cost is reduced by 17.7% compared with the conventional design option (3*1700kW

constant-speed chiller).

6.4 Summary

This chapter presents an uncertainty-based optimal design method considering uncertainties to ensure the high performance of chiller plants and achieve the minimum annual total cost under various possible cooling load conditions by optimize the capacity and configuration of chiller plants. A case study is given as an example to demonstrate the proposed method. Conclusions can be made as follows:

- Annual average cooling load varies largely when considering uncertainties. It can be seen that the cooling load distribution profile of 780 simulation trials is smoother than that of reference case because more cooling load conditions are considered.

- Having the quantitative relation between unmet hours and the design capacity, decision makers can properly size the chiller plant with quantified confidence according to their specific requirements.

- The configuration of the chiller plant can be selected by achieving the minimum total cost when considering uncertainties. The selected chiller plant can perform well under various possible cooling load conditions. The results of the case study show that the total cost of optimized chiller plant can be reduced significantly (i.e. 17.7%) compared with the conventional design.

The test results and experiences from the case study show that the proposed optimization method can determine the optimal design of the chiller plant effectively in

terms of the human effort of programming for implementing the method and the computing effort in using the method for optimizing a chiller plant design. The optimization is conducted by separating optimizing trials into three steps, i.e. plant cooling capacity, number and size of chillers and type of chillers. The computation efficiency is dramatically improved and the computation for the optimization of a chiller plant can be completed within about 10 minutes performed completed execution. It is worth noticing that the optimization output may not the perfect one as not all options/combinations are tested.

CHAPTER 7 ROBUST OPTIMAL DESIGN OF CHILLER PLANT

Different from the Chapter 6 which presents an uncertainty-based optimal design of chiller plant considering uncertainty only, this chapter presents a robust optimal design method of chiller plant considering both uncertainty and reliability simultaneously. A series of so-called uncertainty "scenarios" generated by Monte Carlo simulation are used for obtaining the accurate cooling load distribution. Considering that the failure rate of constant-speed chillers is different from that of variable-speed chillers, robust optimal design with different failure rates is used to obtain the steady probability distribution of each state of the chiller plant considering the reliability. The searching range of total cooling capacity is determined based on the cooling load distribution. In order to achieve the minimum total cost, trials of simulations on different total cooling capacities and different numbers/sizes of chillers are conducted to obtain the optimum chiller plant.

Section 5.1 presents an introduction of design optimization of chiller plant. Section 7.2 describes the objective of robust optimal design for chiller plant. Section 7.3 presents the method of the robust optimal design for chiller plant. Section 7.4 presents a case study on the implementation of the proposed robust optimal design of the chiller plant of a building in Hong Kong. A summary of this chapter is given in Section 7.5.

7.1 Introduction

A chiller plant is usually comprised of constant-speed chillers and variable-speed chillers. Regarding the reliability issue, most of the previous studies are based on the assumption that all the components in parallel have the same failure rate. In this study, different failure rates of constant-speed chillers and variable-speed chillers are considered.

According to the conclusion of Chapter 6, the optimum chiller plant option using uncertainty-based optimal design method should consist of more constant-speed chillers with larger capacity and one variable-speed chiller with smaller capacity, which could ensure that the selected option operate at high efficiency. In order to achieve high operating COP, more constant-speed chillers and fewer variable-speed chillers are used due to the higher COP of constant-speed chillers at nearly full load. For taking both the uncertainty and reliability into account of chiller plant design, following assumptions are made:

- a chiller plant consists of two or more constant-speed chillers and no more than two variable-speed chillers.

- the number of constant-speed chillers is no less than that of variable-speed chillers;

- the failure rate of constant-speed chiller is smaller than that of variable-speed chillers;

- all the constant-speed chillers are identical and they have the same failure rate under each nominal capacity;

- all the variable-speed chillers are identical and they have the same failure rate under each nominal capacity.

The robust optimal design aims at ensuring the high operating efficiency and sufficient cooling capacity to fulfill the cooling demands.

7.2 Objective of Robust Optimal Design of Chiller Plant

The objective the proposed method is to ensure that the chiller plant operates at high efficiency over the entire cooling season and achieve the minimum annual total cost considering uncertainties of design inputs and reliability of chillers. In this study, the annual total cost (TC_n) consists of three parts: annualized capital cost (CC_n), annual operation cost (OC_n) and annual availability risk cost (RC_n). Annualized capital cost includes the expense in purchasing/installing chillers and associated components and the space cost, which is determined by the number of and capacity of equipment. Annual operational cost is the cost charging for the electricity consumption of the chiller plant in operation, which is mainly associated to the annual cooling load, the rated COP of chillers and the part load ratio of chillers in operation. Availability risk cost is a virtual "expense" for accounting the service sacrifice due to insufficient cooling supply, which is considered only when the cooling demands cannot be fulfilled. Fig.7.1 illustrates the conceptual relationship between the costs and cooling capacity of chiller plant. Generally speaking, larger cooling capacity means higher reliability. The capital cost increases as the total cooling capacity increases. Under the optimal configuration of chiller plant, the operation cost may change slightly as the total cooling capacity increases. On the other hand, the availability risk cost decreases as the total cooling

capacity increases. The total life-cycle cost is comprised of the capital cost, operation cost and availability risk cost, as shown in Equation (7.1). According to Fig. 7.1, there should be a comprised total cooling capacity to achieve the minimum total life-cycle cost, at which the optimal capacity is achieved.

$$TC_n = CC_n + OC_n + RC_n \tag{7.1}$$
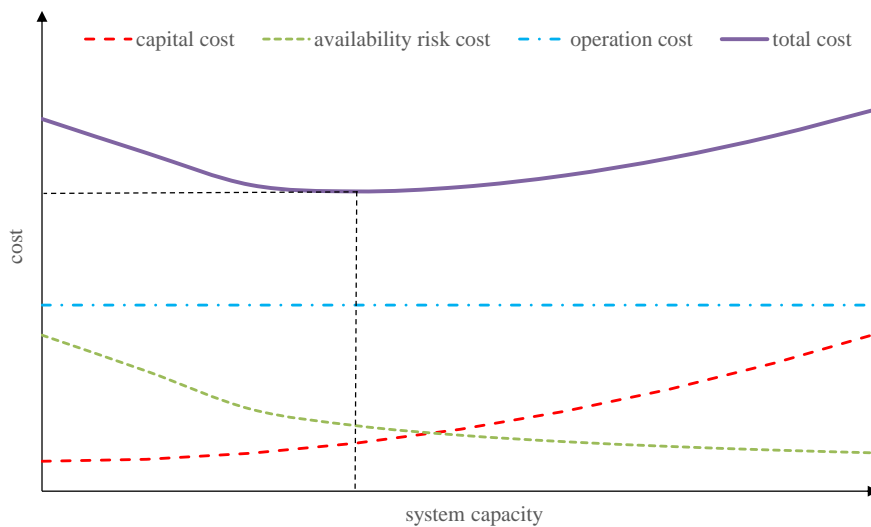
Fig.7.1 Total cost vs total cooling capacity

7.3 Design Optimization Method of Chiller Plant

As shown in Fig. 7.2, the robust optimal design is performed by three steps as follows.

- Uncertainty quantification: Monte Carlo simulation is used to generate the cooling load distribution considering the uncertainties of design inputs; According to the cooling load distribution, the searching range of total cooling capacity of chiller plant is determined;

- Reliability quantification: obtain the probability distribution of each state of chiller plant considering the failure rate difference between constant-speed chiller and variable-speed chiller;

- Trials of simulations on the total cooling capacity and number/size of chillers: conduct the trials on each total cooling capacity step by step; obtain the operation cost, capital cost and availability risk cost under different number/size of chillers on each total cooling capacity; obtain the optimal chiller plant option under each total cooling capacity.
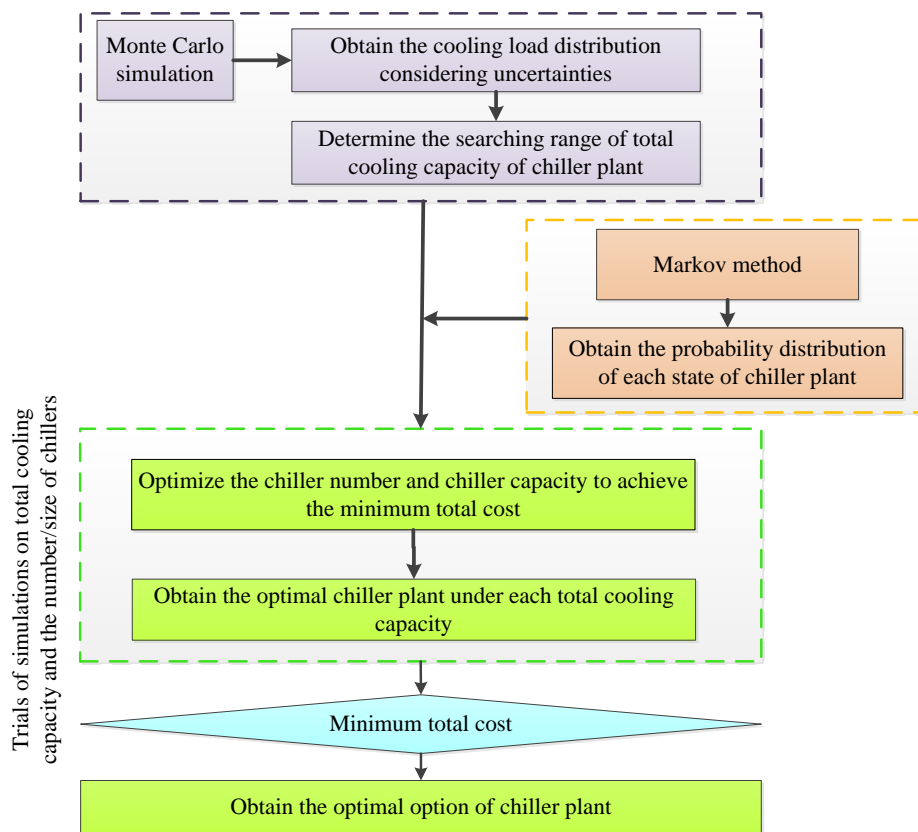
Fig.7.2 Procedure of the proposed robust optimal design

7.3.1 Quantification of cooling load distribution

To conduct the proposed robust optimal design, it is essential to obtain the cooling load distribution of required accuracy considering the uncertainties of design inputs. Monte Carlo simulation is employed to generate the cooling load distribution of required accuracy. Three types of distributions (including normal distribution, tri-angular distribution and uniform distribution) are commonly used to describe the uncertainties

of inputs. Table 3.2 shows an example of the settings of uncertainties of the inputs. Combining the output uncertainties from Matlab, the TRNSYS building model is used to generate the building cooling load distribution considering the uncertainties based on the determined simulation number. The required trials of Monte Carlo simulations are determined by a statistic method [26]. After conducting the required trials of Monte Carlo simulations, the cooling load distribution involving uncertainties is determined. In this study, about 780 times of Monte Carlo simulations are used to generate the cooling load distribution.

The selection of uncertainties may influence the final sizing of chiller plant. If a larger range of uncertainties is used, the total cooling capacity of chiller plant may be larger to reduce the availability risk cost and thus the optimal option may be different. Considering that this paper focuses on the design method, it will be discussed in later chapter.

7.3.2 Quantification of total cooling capacity

Then, it is necessary to determine the searching range of total cooling capacity of chiller plant, which plays a significant role in the design of chiller plant. If an inappropriate (overlarge in most cases) total cooling capacity is selected, it may result in that a chiller plant is significantly oversized in actual operation and it thus causes significant energy and cost wastes.

To determine the searching range of total cooling capacity of chiller plant, it is essential to obtain the cooling capacities with numbers of hours when the cooling demand cannot

be met (marked as unmet hours). Based on the cooling load distribution, the "mean" capacity of the total simulation trials are calculated and shown in Figure 7.3. The "mean" value represents the cooling capacity corresponding to different unmet hours per year, based on the average cooling load distribution profile. The "reference" value represents the cooling capacity based on the cooling load distribution of typical year. The peak cooling load in typical year is presented for comparison. It can be observed that the cooling capacities based on the average annual load profile are significantly lower than the peak cooling load in typical year, when certain number of unmet hour is allowed (as required in design guide). Therefore, using the peak cooling load in typical year as the design capacity may lead to the oversizing of chiller plant. At most of the unmet hours, the cooling capacities based on the average annual cooling profile and that in typical year are very close.
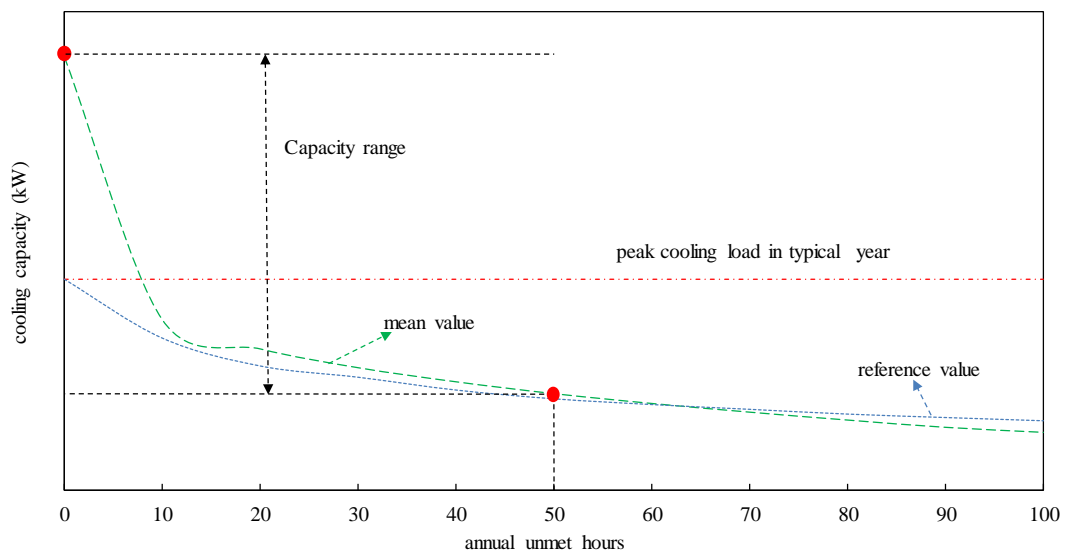
Fig.7.3 Cooling capacity vs. unmet hours

According to ASHRAE Standard 90.1, the total cooling capacity of chiller plant should be the capacity corresponding to 50 unmet hours. In this study, the minimum cooling

capacity is assumed to be the capacity corresponding to 50 unmet hours. The maximum

cooling capacity is assumed to be the capacity when all the cooling load conditions are

met. The interval of each trial is 2.5% of the minimum cooling capacity.

7.3.3 Quantification of probability distribution of chiller plant

Markov method is used in this study because of its wide application in reliability

analysis of multi-state systems (Lisnianski and Levitin 2003). The aim of using Markov

method is to obtain the probability of each state of a multi-state system at a specific

period and then the performance of the system and capability can be estimated. It is

assumed that the state probabilities at a future instant do not depend on the states

occurred in the past.

The life cycle of each component in this study contains the operating period,

maintenance period and failure period. The mean time to failure (MTTF, $1/\lambda$) is often

used to represent the operating time, as shown in Equation (7.2). The mean time to

repair (MTTR, $1/\mu$) is often used to represent the maintenance time and failure time, as

shown in Equation (7.3). Commonly, failure rate (λ) and repair rate (μ) are usually used

as the major parameters for conducting the reliability assessment.

$$MTTF = \frac{1}{\lambda}$$

(7.2)

$$MTTR = \frac{1}{\mu}$$

(7.3)

It is assumed that each chiller has two states only: normal (0) and failure (1). The

variable-speed chillers have no more than three states (i.e. no chillers fail, one chiller

fails and two chillers fail) considering the reliability of variable-speed chillers. The probability of the states of variable-speed chillers can be easily obtained through the calculation of transition matrix. The constant-speed chillers have (n_1+1) states (i.e., each states contains several situations) considering the reliability of constant-speed chillers, as shown in Fig.7.4 (Lisnianski et al. 2012). Totally, the chiller plant has $3(n_1+1)$ states, as shown in Equation (7.4) - (7.6). Where, n_1 is the number of constant-speed chillers, n_2 is the number of variable-speed chillers. $p_{2,n2}$ is equal to 0 when only one variable-speed chiller is used.

$$(p_{0,n_1} + p_{1,n_1} + \cdots + p_{n_1-1,n_1} + p_{n_1,n_1}) \cdot (p_{0,n_2} + p_{1,n_2} + p_{2,n_2}) = 1 \tag{7.4}$$

$$p_{0,n_1} + p_{1,n_1} + \cdots + p_{n_1-1,n_1} + p_{n_1,n_1} = 1 \tag{7.5}$$

$$p_{0,n_2} + p_{1,n_2} + p_{2,n_2} = 1 \tag{7.6}$$

According to Fig.7.4, it can be observed that state 0 symbolizes that no constant-speed chillers fail and state k symbolizes that k ($1 \leq k \leq n$) constant-speed chillers fail. From state 0 to state n_1, the failure rate λ_1 is used to represent the probability from one state to another. From state n_1 to state 0, the repair rate μ is used to represent the probability from one state to another. The transition probability is determined by a state transition density matrix A (Equation (7.7)), which only involves the repair rate and failure rate of constant-speed chillers. Probability distribution of the constant-speed chillers at each state at time t can be represented with a vector P(t) (Equation (7.8)). It can be deduced from the initial state by Equation (7.9) and Equation (7.10). When the time approaches to infinity, P(∞) will keep stable (Equation (7.11)). Then the steady state probabilities can be obtained by solving the linear algebraic equations (Equation (7.12) and Equation

(7.13)).
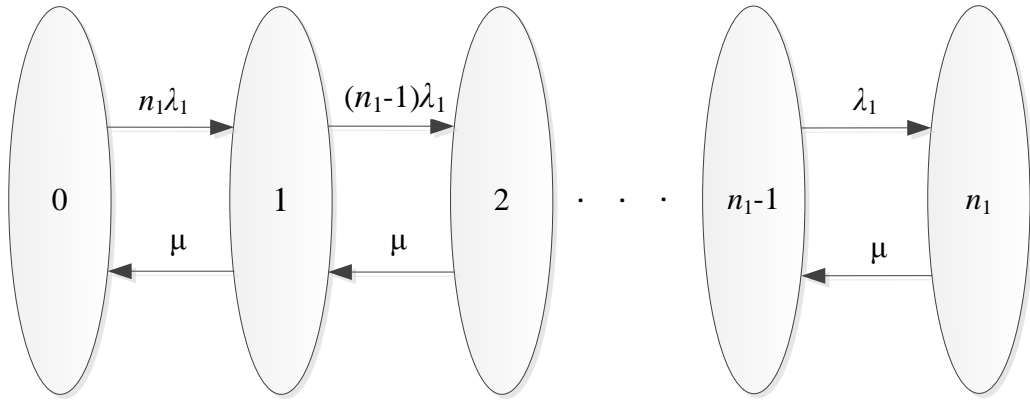
Fig.7.4 States of n_1 constant-speed chillers and possible transitions

$$A = \begin{bmatrix} (1-n_1\lambda_1) & n_1\lambda_1 & 0 & 0 & 0 \ldots 0 & 0 & 0 \\ \mu & (1-\mu-(n_1-1)\lambda_1) & (n_1-1)\lambda_1 & 0 & 0 \ldots 0 & 0 & 0 \\ 0 & \mu & (1-\mu-(n_1-2)\lambda_1) & (n_1-2)\lambda_1 & 0 \ldots 0 & 0 & 0 \\ \ldots & \ldots & \ldots & \ldots & \ldots \\ 0 & 0 & 0 & 0 & 0 \ldots \mu & (1-\lambda_1-\mu) & \lambda_1 \\ 0 & 0 & 0 & 0 & 0 \ldots 0 & \mu & (1-\mu) \end{bmatrix} \quad (7.7)$$

$$P(t) = \left[p_0(t), \, p_1(t), \, ..., \, p_n(t) \right] \tag{7.8}$$

$$P(0) = \left[1, 0, 0, ..., 0 \right] \tag{7.9}$$

$$P(n) = P(n-1)A = P(0)A^n \tag{7.10}$$

$$P(\infty) = \lim_{n\to\infty} P(n) = \lim_{n\to\infty} P(0)A^n \tag{7.11}$$

$$P(\infty) = P(\infty-1)A = P(\infty)A \tag{7.12}$$

$$\begin{cases} p(0) = a_{00}p(0) + a_{10}p(1) + \cdots + a_{n0}p(n) \\ p(1) = a_{01}p(0) + a_{11}p(1) + \cdots + a_{n1}p(n) \\ \quad \vdots \qquad\qquad\qquad\qquad \vdots \\ p(n) = a_{0n}p(0) + a_{1n}p(1) + \cdots a_{nn}p(n) \\ \quad \sum_{i=0}^{n} p(i) = 1 \end{cases} \tag{7.13}$$

7.3.4 Quantification of configuration of chiller plant

Different from previous design method that mainly focused on the optimal configuration on a typical total cooling capacity (e.g., the cooling capacity corresponding to 50 unmet hours), in this study, a series of total cooling capacities within the searching range are selected to determine the optimal chiller plant option, which could operate at high energy efficiency and have sufficient capacity to fulfill the cooling demands. Considering that the chillers are only manufactured in certain discrete size, trials of simulations on different total cooling capacities and different and discrete number/size of chillers are conducted to select the optimal chiller plant option.

Figure 7.5 presents the implementation of trials of simulation on each total cooling capacity. It contains two parts, i.e. the trials under the condition that only one variable-speed chiller is used and the trials under the condition that two variable-speed chillers are used. For the trials under the condition that only one variable-speed chiller is used, the number of constant-speed chillers are calculated from one (minimum two chillers, including the variable-speed chiller, is assumed concerning the basis requirement for reliability and maintenance) until the operation cost begins to increase. The option which has the lowest total cost under each total cooling capacity is selected. Equation (7.14) formulates the optimization problem for selecting the number/size of constant-speed chillers when only one variable-speed chillers is used.

$$
\begin{aligned}
\text{find} \quad & C_1, \ n_1, \ C_2 \\
\text{minimize} \quad & TC_{all}(C_1, \ n_1, \ C_2) \\
\text{constraint} \quad & n_1C_1 + C_2 = CL_T \\
& C_1 > C_2, \ n_1 \geq 1
\end{aligned}
\tag{7.14}
$$

For the trials under the condition that two variable-speed chillers are used, the number of constant-speed chillers are calculated from two (i.e. the number of constant-speed chillers is not less than that of variable-speed chillers) until the operation cost begins to increase. The option that has the lowest total cost under each total cooling capacity is selected. Equation (7.15) formulates the optimization problem for selecting the number/size of constant-speed chillers when only one variable-speed chillers is used.

$$
\begin{aligned}
&\texttt{find} && C_1,\ n_1,\ C_2 \\
&\texttt{minimize} && TC_{all}(C_1,\ n_1,\ C_2) \\
&\texttt{constraint} && n_1 C_1 + 2C_2 = CL_T \\
& && C_1 > C_2,\ n_1 \geq 2
\end{aligned}
\tag{7.15}
$$

A comparison is made between the optimal option with one variable-speed chillers and the optimal option with two variable-speed chillers. Eventually, among the options corresponding to various total cooling capacities, the option that has the minimum total cost is selected as the optimum design for a building.
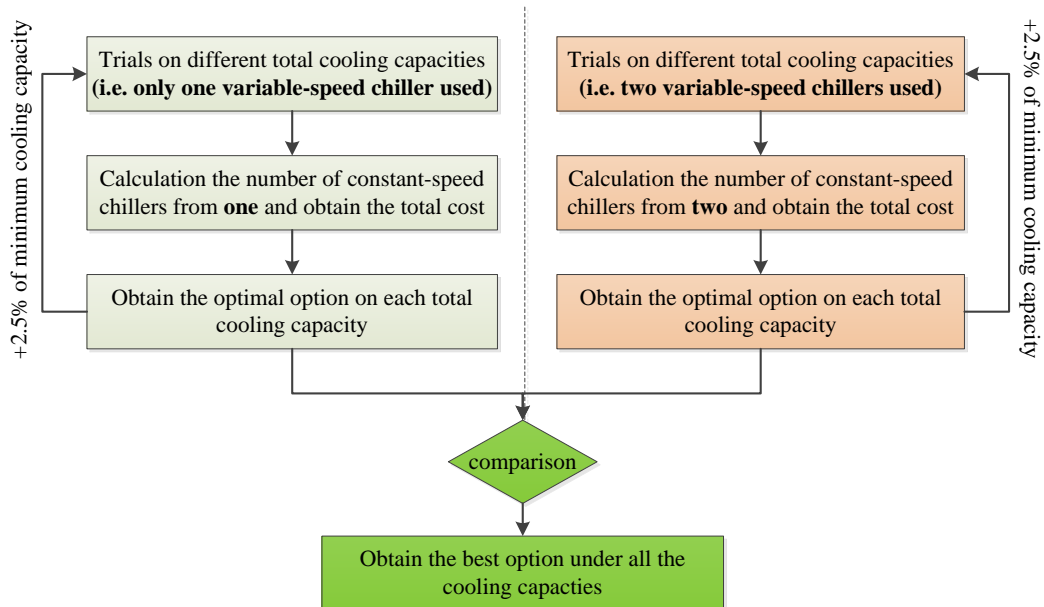
Fig.7.5 Trials of simulation to select optimum chiller plant design

The annual operational cost is mainly related to the annual cooling load distribution and energy efficiency of chiller plant. The energy efficiency of chiller plant, usually evaluated by COP, strongly depends on the operating PLR. It is well known that the larger the PLR, the higher COP once the impact of other operating parameters (e.g. condensing and evaporating temperatures) are separated, as shown in Equation (7.16).

$$COP_i = D_0 + D_1 \cdot PLR_i + D_2 \cdot PLR_i^2 + D_3 \cdot PLR_i^3 \tag{7.16}$$

where, D_0-D_3 are the coefficients that can be identified from chiller catalogue or field measurement data. The PLR is usually determined by the number and size of operating chillers. It is simply defined as the ratio of the required cooling load (CL_{re}) to the available cooling capacity (CL_{ava}) (i.e. that of operating chillers) as shown in Equation (7.17).

$$PLR = \frac{CL_{re}}{CL_{ava}} = \frac{CL_{re}}{N_{op} \cdot CL_{Nominal}} \tag{7.17}$$

where, $CL_{Nominal}$ is the nominal cooling capacity of each chiller. N_{op} is the number of operating chillers. It means that the more chillers are selected, the higher operating PLR can be achieved under appropriate sequence control strategies. On the other hand, selecting more chillers means that the size of individual chillers is smaller. Generally, the rated COP of chiller decreases when the nominal capacity of chillers reduces in certain extent. Therefore, the operating COP increases when the number of chillers increases to certain value and it reduces when the number of chillers increases further, as shown in Fig.7.6 (Harvey 2012).
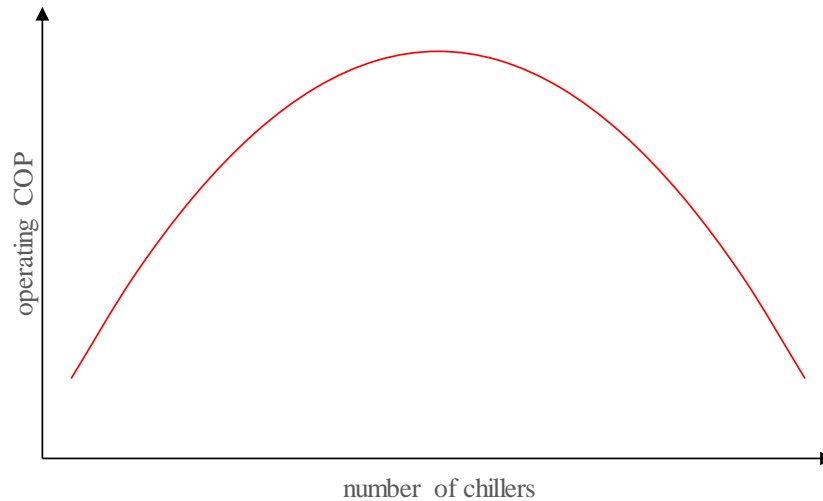
Fig.7.6 COP vs. number of chillers

The sizes of individual chillers, which determine the nominal COP, influence the PLR and operating COP of the chiller plant. In practice, two types of sizes of chillers are proper for the convenient maintenance and control. Besides, the number of chillers of larger capacity is selected to be at least the same as that of smaller capacity in the optimization trials. To determine the optimal sizes of chillers at a given chiller number, the larger size increases gradually from the mean value (i.e., all the chillers are equally sized) until the operating COP achieves the maximum value in the optimization trials. At the same time, the smaller size decreases accordingly.

7.4 Case Study and Results

A case study on the chiller plant design for a building in Hong Kong is conducted to test and evaluate the proposed robust optimal design. At first, Monte Carlo simulation is used to generate the cooling load distribution of required accuracy. Then, the searching range of total cooling capacity of chiller plant is determined according to the cooling load distribution. Reliability assessment of the chiller plant is conducted to

obtain the probability of each state considering the failure rate difference between constant-speed chiller and variable-speed chiller. Finally, the trials of simulations on different total cooling capacities and numbers/sizes of chillers are conducted to select the optimum chiller plant which has the minimum total cost.

7.4.1 Cooling load distribution and searching range of design cooling capacity

To conduct the Monte Carlo simulations in order to obtain the cooling load distribution, it is essential to select the parameters of uncertainties of the design inputs. Combining the output uncertainties from Matlab, the TRNSYS building model is used to generate the building cooling load involving the uncertainties. After conducting 780 times of Monte Carlo simulations, the cooling load distribution is obtained, as shown in Fig.7.7. The reference case is the normal cooling load distribution without considering the uncertainties. It can be seen that the cooling load distribution profile of 780 simulation trials is smoother than that of reference case because more cooling load conditions are considered.

Then, it is essential to determine the searching range of the total cooling capacity of the chiller plant. The cooling capacities corresponding to different unmet hours are presented in Fig.7.8. The meanings of the symbols can be found in Section 7.3.2. It can be observed that the profile of "mean" is close to that of the reference case. It can be seen that the peak cooling load of typical year (i.e. 5600kW) is higher than the minimum cooling capacity (i.e. about 5100kW). When the annual unmet hours are equal to 0, the maximum cooling capacity (i.e. 6600kW) is much higher than the peak cooling load of typical year in conventional design. The searching range of the total cooling capacity is

between 5100 kW and 6600 kW and the interval is assumed to be 100kW.
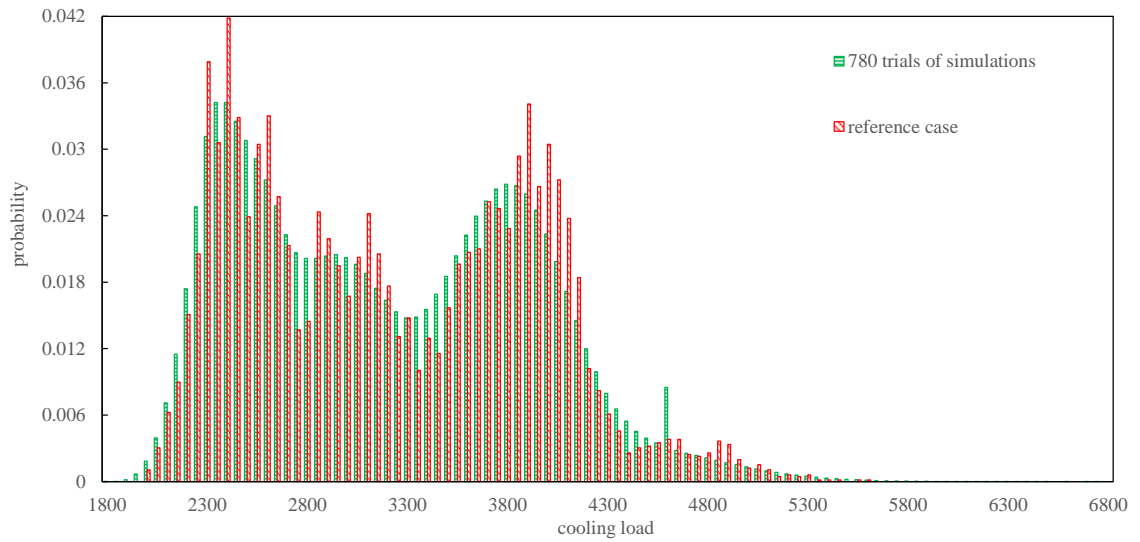
Fig.7.7 Distribution of cooling load considering uncertainties
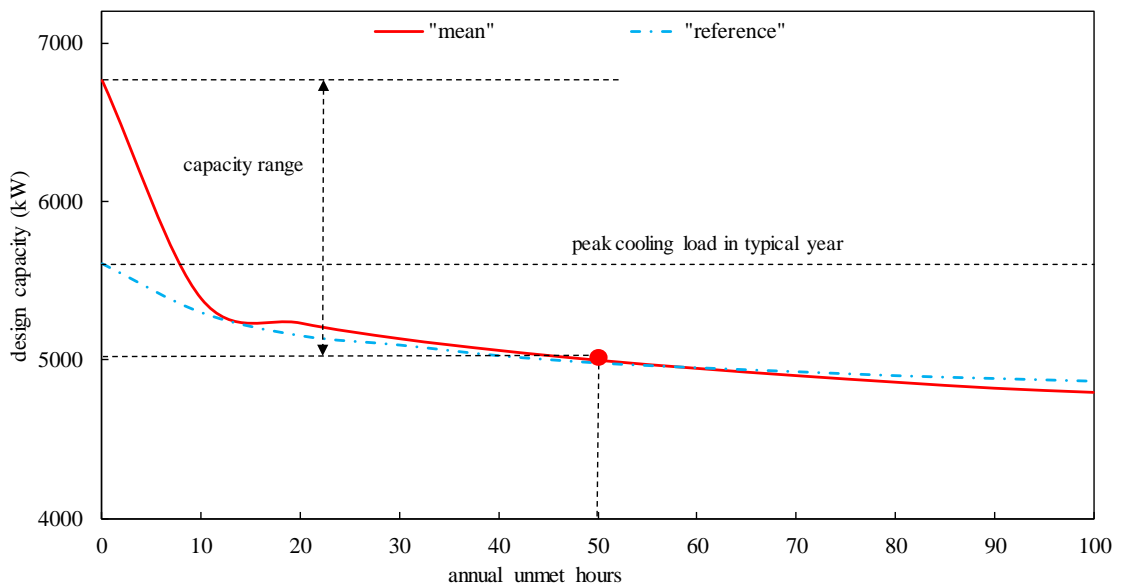
Fig.7.8 Cooling capacity vs. number of annual unmet hours

7.4.2 Probability distribution of each state of the chiller plant

As mentioned above, Markov method is used to obtain the probability of each (health) state of the chiller plant and to calculate the mean steady performance and capability under each state. In this study, the chiller plant is assumed to be comprised of about 2~6

chillers totally. The failure rate of constant-speed chillers is assumed to be 0.0001/hour and the failure rate of variable-speed chillers is assumed to be 0.000125/hour. Both their repair rates are assumed to be 0.002/hour.

Then, it is essential to obtain the probability distribution of each steady state under various numbers of constant-speed chillers. As mentioned above, the chiller plant consists of one or two variable-speed chillers. According to Equation (7.6), the probability distribution of variable-speed chillers can be obtained. Table 7.1 shows the probability distribution of each steady state of variable-speed chillers. It can be observed that the probability of state 0 is 0.9412 and the probability of state 1 is 0.0588 when only one variable-speed chiller is used. The probabilities of state 0, 1 and 2 are 0.8828, 0.1103 and 0.0069 respectively when two variable-speed chiller are used.

Table 7.1 Probability distribution of steady states of variable-speed chillers

State	Variable-speed chillers	
	1	2
0	0.9412	0.8828
1	0.0588	0.1103
2	-	0.0069

According to Equation (7.5), the probability distribution of constant-speed chillers can be obtained. Table 7.2 shows the probability distribution of each steady state of under different number of constant-speed chillers. It can be observed that the probability of state 0 decreases when the number of constant-speed chillers increases.

Table 7.2 Probability distribution of steady states of constant-speed chillers

State	Number of constant-speed chillers				
	1	2	3	4	5
0	0.9524	0.9050	0. 8578	0.8109	0.7644
1	0.0476	0.0905	0.1278	0.1622	0.1911
2	-	0.0045	0.0129	0.0243	0.0382
3	-	-	0.0006	0.0024	0.0057
4	-	-	-	0.0001	0.0006
5	-	-	-	-	0

According to Equation (7.4), the probability distribution of the chiller plant can be obtained. Table 7.3 shows an example of the probability distribution of chiller plant, which consists of five constant-speed chillers and two variable-speed chillers. This chiller plant has 18 states totally, i.e. three states of variable-speed chillers and six states of constant-speed chillers. The probability of the chiller plant under the state 0 of constant-speed chillers and state 0 of variable-speed chillers is 0.67481, and the probability of the chiller plant under state 5 of constant-speed chillers and state 2 of variable-speed chillers is 0.

Table 7.3 An example of the probability distribution of chiller plant

Probability distribution of chiller plant		State of variable-speed chillers		
		0	1	2
State of constant-speed chillers	0	0.67481	0.08431	0.00527
	1	0.16870	0.02108	0.00132
	2	0.03372	0.00421	0.00026
	3	0.00503	0.00063	0.00004
	4	0.00053	0.00007	0
	5	0	0	0

7.4.3 Trials on the total cooling capacities and numbers/sizes of chillers

As mentioned above, the searching range of total cooling capacity is assumed to be 5100-6600 kW and the searching interval is selected to be 100 kW in this study. Trials of simulations are conducted on the 16 total cooling capacities respectively (i.e. 5100 kW, 5200 kW, …, 6500 kW and 6600 kW).

For example, it is assumed that total cooling capacity of chiller plant is 6000 kW. According to Fig.7.6, the operating COP increases when the number of chillers increases in certain range and it decreases when the number of chillers increases further. According to Section 7.3.4, the evaluation of the number of constant-speed chillers on the operation cost is conducted. Meanwhile, the nominal capacities of constant-speed chillers and variable-speed chillers are optimized. The electricity price used in this study is 1 HKD/kW, which is the typical rate in Hong Kong. The results are shown in Table

7.4. It can be observed that the operation costs decrease when the number of chillers increases. It can also be observed that the operation cost of the chiller plant option with two variable-speed chillers is lower than that with one variable-speed chiller. Compared with the chiller plant option with two variable-speed chillers, the chiller plant with one variable-speed chiller might operate at lower efficiency at part load conditions when the variable-speed chiller could not work. The design option comprised of 4 constant-speed chillers (1050 kW) and 2 variable-speed chillers has the lowest operation cost compared with the other options.

Table 7.4 Annual operation cost and annualized capital cost of different design options

Chiller Number	Chiller plant option (Size (kW) ×number)	Operation cost (10^3 HKD)	Capital cost (10^3 HKD)
2	3200×1CSD+2800×1VSD	3,502	373
3	2100×2CSD+1800×1VSD	3,478	461
4	1550×3CSD+1350×1VSD	3,461	542
4	1600×2CSD+1400×2VSD	3,446	580
5	1250×4CSD+1000×1VSD	3,436	616
5	1300×3CSD+1050×2VSD	3,403	653
6	1050×5CSD+750×1VSD	3,435	685
6	1050×4CSD+900×2VSD	3,392	723

Remarks: CSD – constant-speed chiller, VSD – variable-speed chiller

Annualized capital cost contains the equipment cost and space cost. The lifespan of the chiller plant is assumed to be 10 years. The annual space costs of constant-speed chillers

and variable-speed chillers are assumed to be 15,000 HKD and 20, 000 HKD respectively. Equipment costs of constant-speed chiller (900 kW) and variable-speed chiller (900 kW) are 0.9 MHKD and 1.2 MHKD respectively, referring to the data from a manufacture. As for the equipment cost of other chillers, they are estimated using Equation (7.18) (Guthrie 1969; Biegler et al. 1997).

$$EC = EC_0 \cdot (C/C_0)^{\alpha} \tag{7.18}$$

where, EC_0 is the equipment cost of a reference chiller with the capacity C_0. EC is equipment cost of chiller with the capacity C. α is the coefficient, which set to be 0.15 in this study. The annualized capital costs under the different design options are estimated using Equation (7.18) and shown in Table 7.4.

Availability risk cost is the "expense" or service sacrifice which should be considered when the cooling demands cannot be fulfilled. Table 7.5 shows the annual availability risk costs and total costs of different design options under three penalty ratios (i.e., 1, 10 and 100 HKD/kW). It can be seen that, when the number of chillers is small, the annual availability risk cost decreases rapidly when the chiller number increases. It can also be observed that the total cost decreases when the number of chillers increases in certain range and it decreases when the chiller number increases further. Since the availability risk cost is high when the chiller number is small and the capital cost is high when the chiller number is large, there is a comprised numbers/sizes of chillers which has the minimum total cost. In this study, the penalty ratio is assumed to be 10HKD/kW. Among these options, the option with 4 constant-speed chillers (1250 kW) and 1 variable-speed chiller (1000 kW) has the minimum total cost $4,237 \times 10^3$HKD, which

has good robustness towards the uncertainties and reliability. Therefore, it can be considered as the best option under the total cooling capacity 6000 kW. If the penalty ratio is 1HKD/kW, the best option under the total cooling capacity is the option with 2 constant-speed chillers (2100 kW) and 1 variable-speed chiller (1800kW). The designers can select the best option based on their specific requirement of penalty ratio.

Table 7.5 Annual availability risk cost (10^3HKD) and total cost (10^3HKD) of different design options

Penalty ratio (HKD/kW)	1		10		100	
Option (size(kW)×number)	*RC*	*TC*	*RC*	*TC*	*RC*	*TC*
3200×1CSD+2800×1VSD	102	3,978	1,021	4,897	10,210	14,085
2100×2CSD+1800×1VSD	39	3,977	387	4,326	3871	7,810
1550×3CSD+1350×1VSD	25	4,140	247	4,362	2,468	6,583
1600×2CSD+1400×2VSD	25	4,053	254	4,282	2,542	6,570
1250×4CSD+1000×1VSD	19	4,070	**185**	**4,237**	1,851	5,903
1300×3CSD+1050×2VSD	28	4,084	275	4,331	2,755	6,811
1050×5CSD+750×1VSD	15	4,135	145	4,265	1,451	5,571
1050×4CSD+900×2VSD	22	4,165	216	4,331	2,161	6,276
Remarks: RC- availability risk cost, *TC*- total cost.						

Table 7.6 Best design options under different total cooling capacities (penalty

ratio:10HKD/kW)

Total cooling capacity (kW)	Best option (size (kW) × number)	Availability risk cost (10^3HKD)	Operation cost (10^3HKD)	Total cost (10^3HKD)
5,100	1050×4CSD+ 900×1VSD	490	3,397	4,469
5,400	1100×4CSD+ 1000×1VSD	343	3,412	4,350
5,700	1150×4CSD+ 1100×1VSD	246	3,421	4,274
6,000	1250×4CSD+ 1100×1VSD	185	3,436	4,237
*6,300**	*1300×4CSD+ 1100×1VSD*	*131*	*3,463*	*4,222*
6,600	2300×2CSD+ 2000×1VSD	253	3,501	4,231

After conducting the trials on other total cooling capacities, the minimum total costs are

computed and presented in Table 7.6. When the total cooling capacity increases from

5100 kW to 6300 kW, the availability risk costs of the best options decrease rapidly and

the total costs are also reduced. When the total cooling capacity is over 6300 kW, the

total cost increases. It can be observed that the best option of each total cooling capacity

has only one variable-speed chillers. Although the chiller plant with two variable-speed

chillers may operate at higher efficiency at part load conditions, the variable-speed

chiller is more expensive than the constant-speed chiller. Therefore, using one variable-

speed chiller is economical in spite of the lower operating efficiency. It can be seen that

the option with 4 constant-speed chillers (1300 kW) and 1 variable-speed chiller (1100

kW) has the minimum total cost $4,222 \times 10^3$ HKD compared with other options. It means

that the selected option has better robustness to uncertainties and system reliability.

7.4.4 Comparison among the three design methods

Table 7.7 shows the design option of robust optimal design, uncertainty-based design

and conventional design. Compared with conventional design and uncertainty-based

optimal design, the total cost under robust optimal design ($4,222 \times 10^3$HKD) is reduced

by about 26% and 11.4% respectively when the penalty ratio is 10 HKD/kW. To achieve

the minimum annual total cost, the option with 4 constant-speed chillers (1300 kW) and

1 variable-speed chiller (1100 kW) can be selected as the optimum selection for the

design. This best option also has the minimum total cost, which may indicate that it has

good robustness considering the uncertainties of design inputs and reliability of system

components.

Table 7.7 Optimal options using different design methods (penalty ratio:10HKD/kW)

	Total cooling capacity (kW)	Best option (size (kW) × number)	Availability risk cost (10^3HKD)	Operation cost (10^3HKD)	Total cost (10^3HKD)
Robust optimal design	6,300	1300×4CSD+ 1100×1VSD	131	3,463	4,222
Uncertainty-based design	5100	1400×3CSD+ 900×1VSD	656	3,495	4,765
Conventional design	5100	1700×3CSD	992	4,318	5,703

7.5 Summary

This chapter presented a robust optimal design method, which is based on a minimized life-cycle cost to ensure the high performance of chiller plant and achieve the minimum annual total cost considering uncertainties of inputs and system reliability. It is realized by optimizing the total cooling capacity and numbers/sizes of chiller plant. A case study is given as an example to test and demonstrate the proposed method. Conclusions can be made as follows:

- Quantification of uncertainties of design inputs is very important in determining the cooling load distribution of required accuracy.

- Based on the cooling load distribution, the searching range of total cooling capacity of chiller plant can be determined by the cooling capacities with numbers of hours.

The minimum cooling capacity is 5100 kW and the maximum cooling capacity is 6600 kW.

- Markov method can be effectively used to obtain the probability distribution of system state (health) for high accuracy and fast computation time. In this study, the failure rate different between constant-speed chillers and variable-speed chillers is considered. Results show that the probability distribution of chiller plant can be divided into the states of constant-speed chiller and the states of variable-speed chillers.

- Compared with the chiller plant option with two variable-speed chillers, the chiller plant with one variable-speed chiller might operate at lower efficiency at part load conditions when the variable-speed chiller could not work. Given that the variable-speed chiller is more expensive than the constant-speed chiller, using one variable-speed chiller is economical in spite of the lower operating efficiency.

- The design option of the chiller plant can be selected by achieving the minimum total cost when considering uncertainties and system reliability. The selected chiller plant can perform well under various possible cooling load conditions and have the good robustness towards the system reliability. The results of the case study show that the total cost of optimized chiller plant can be reduced significantly (26% and 11.4%) compared with the conventional design and uncertainty-based optimal design respectively.

- It is worth noticing that the optimization output may be slightly different from the best one in principle as not all options/combinations are tested due to the chosen test interval in computation and available chillers sizes in practice.

CHAPTER 8 ROBUST OPTIMAL DESIGN OF CHILLED WATER SYSTEM

This chapter presents a life-cycle based robust optimal design method of chilled water systems. It can ensure that the designed chilled water systems could operate at high energy performance and the minimum total life-cycle cost could be achieved under various possible cooling load conditions considering the uncertainties of design inputs and reliability of the components. In this study, the chilled water pumps are assumed to be identical in parallel and thus they have the same failure rate. A series of so-called uncertainty "scenarios" generated by Monte Carlo simulation, is used for obtaining the accurate cooling load distribution and accurate hydraulic resistance distribution. Markov method is used to obtain the steady probability distribution of each state of the pump system considering the reliability. Effective pump models and three typical control methods are considered for evaluating the effectiveness and robustness of the proposed design method. In order to achieve the minimum total cost, trials of simulations on different design flows and different nominal flows are conducted to obtain the optimum chilled water pump system.

Section 8.1 gives a brief introduction of the chilled water pump system. Section 8.2 describes the objective of robust optimal design for chilled water systems. Section 8.3 presents the method of the robust optimal design for chilled water pump systems. Section 8.4 shows a case study on the robust optimal design of the chilled water pump system of a building in Hong Kong. A summary of this chapter is given in Section 8.5.

8.1 Introduction

There are two main types of chilled water systems i.e. primary-secondary pump system and primary only pump system for distributing the chilled water from chillers to terminal users (air handling unit) (Tirmizi et al. 2012). For primary-secondary pump systems, constant-speed pumps are usually used to circulate the water in the primary loop whereas variable-speed pumps are usually employed for varying the water circulation in the secondary loop depending upon the cooling demands of terminal users. For a primary only pump system, variable-speed pumps are used to circulate the chilled water through the entire system, and the chilled water flow rate varies corresponding to building load.

In this chapter, a typical primary only pump system as shown in Fig. 8.1 is used for developing the robust optimal design method. Identical variable-speed pumps are employed to circulate the chilled water through the entire system and the chilled water flow rate varies corresponding to the load. Bypass is used to maintain the minimum flow rate for safety, and the cooling demands of three terminal users are similar.
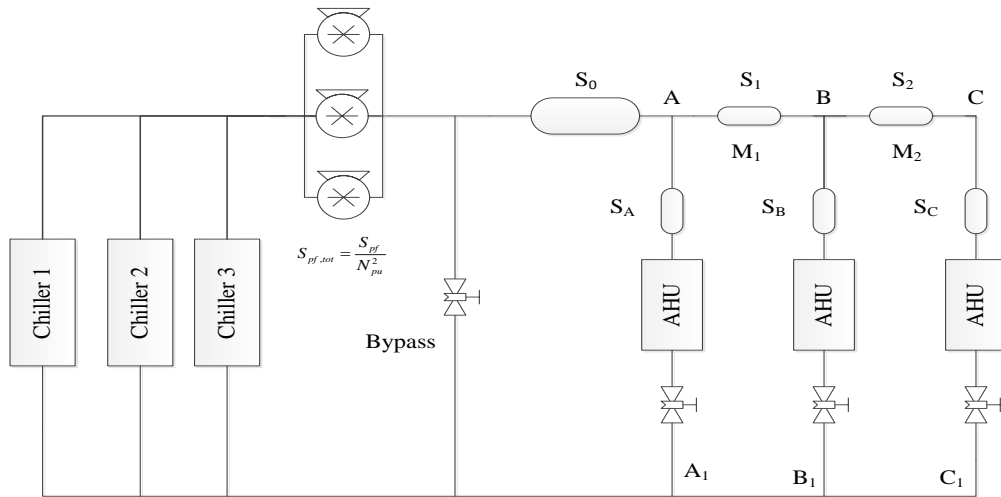
Fig.8.1 Scheme of primary only pump system

8.2 Objective of the Design Optimization Method

The objective of the proposed method is to ensure that the system operates at high efficiency over the entire cooling season and achieve the minimum annual total cost considering uncertainties and system reliability. The annual total cost (TC_n) consists of three parts: annualized capital cost (CC_n), annual operation cost (OC_n) and annual availability risk cost (RC_n). Annualized capital cost includes the expense in purchasing/installing the pumps and associated components (equipment cost) and the spaces for accommodating them (space cost), which is determined by the number and size of pumps. Annual operational cost is the cost electricity consumed by the pumps in operation, which is mainly associated to the annual cooling load distribution and the pump energy efficiency. Availability risk cost is the "expense" or service sacrifice which should be considered when the cooling demands cannot be fulfilled. Fig. 8.2 illustrates the conceptual relationship between the costs and system total capacity under the optimized pump head. It is well-known that large system capacity means higher system reliability. The capital cost increases as the system capacity increases. Under the optimal

configuration of chilled water pumps system, the operation cost may change slightly as the system capacity increases. On the other hand, the availability risk cost decreases as the system total capacity increases. The total life-cycle cost is comprised of the capital cost, operation cost and availability risk cost, as shown in Equation (8.1). According to Fig. 6.2, there should be a comprised system capacity to achieve the minimum total life-cycle cost, at which a comprised level of reliability is achieved (Billinton et al. 2001).

$$TC_n = CC_n + OC_n + RC_n \tag{8.1}$$
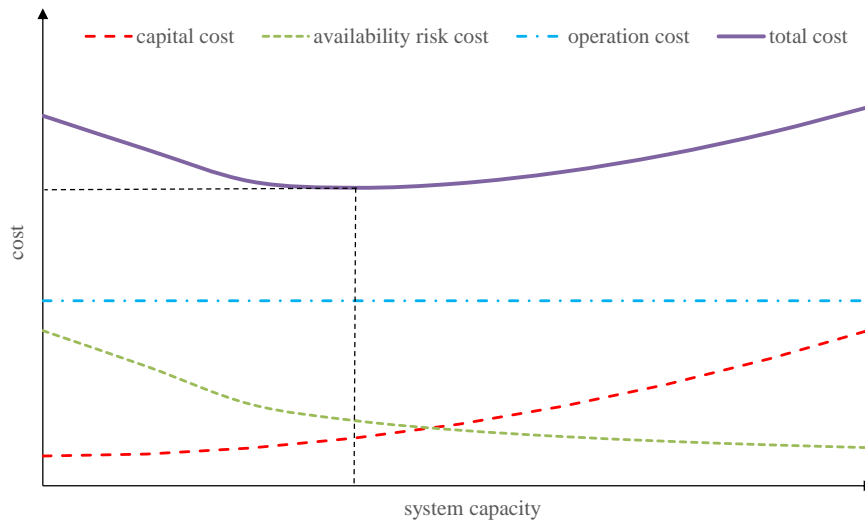
Fig.8.2 Total cost *vs* system capacity

8.3 Optimal Design Method for Chilled Water Pump System

The robust optimal design is performed by four steps as shown in Fig. 8.3. Details of the four steps are explained as follows.

I.   *Uncertainty quantification:* generate the cooling load distribution involving uncertainties and determine the design flow; then generate the hydraulic resistance distribution and determine the design pressure head;

II. *Reliability quantification:* obtain the probability distribution of each state of chilled water pumps;

III. *Modeling and control methods of chilled water pumps:* obtain the pump models on the calculation of electricity consumption; determine the basic, medium and advanced control methods of chilled water pumps.

IV. *Trials of simulations on the total flow and nominal flow:* determine the searching range of total pump flow capacity and conduct trials on each design flow step by step; obtain the operation cost, capital cost and availability risk cost under different pump numbers on each design flow; obtain the optimal chilled water pumps under each design flow.
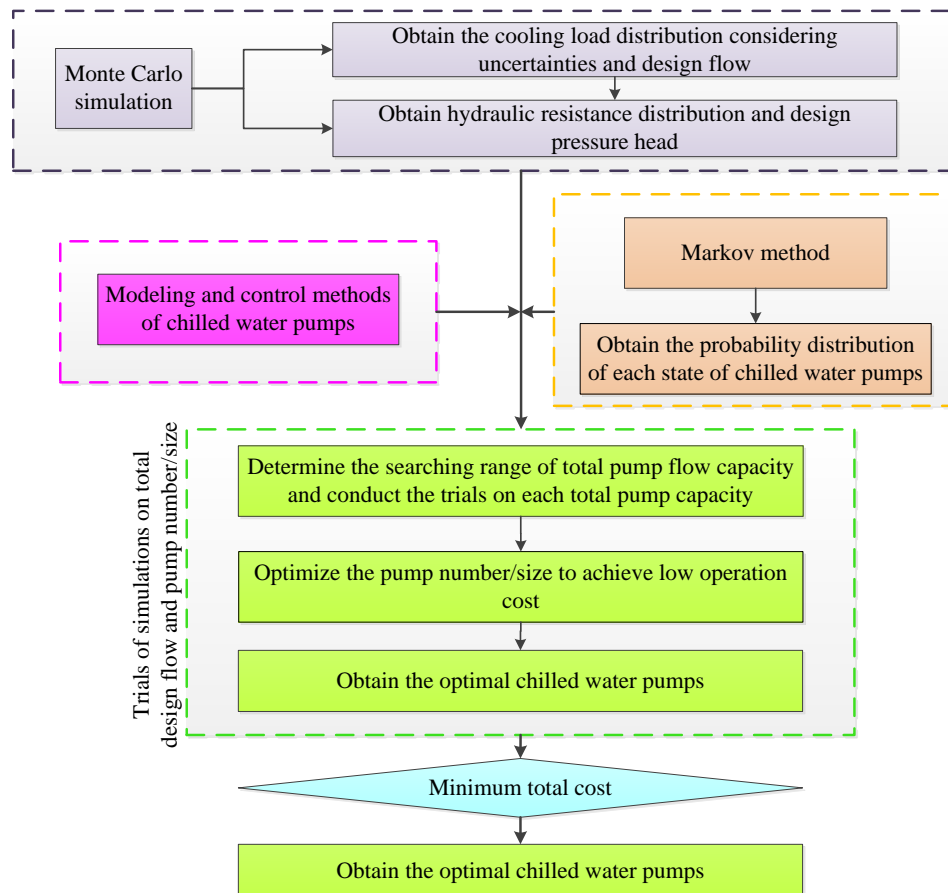
Fig.8.3 Procedure of the proposed robust optimal design

8.3.1 Modeling of chilled water pumps and control methods

The charging for the electricity consumption of chilled water system, also regarded as the operation cost, is one of the most important aspects in selecting the optimum chilled water pumps. The electricity consumption of the system (also called operation cost OC_{pu}) mainly depends on the pressure drop (H_{pu}), the water flow rate (m_w), pump efficiency (η_{pu}) and VFD (variable frequency drive) efficiency (η_{VFD}), which can be computed by Equation (8.2) (Wang et al. 2001).

$$OC_{pu} = \frac{m_w H_{pu}}{102 \eta_{pu} \eta_{VFD}}$$

(8.2)

The three efficiencies of variable speed pumps can be modeled using a series of polynomial approximations (Bahnfleth et al. 2006). The characteristics of pump efficiency and VFD efficiency are based on the manufacturers' data at the full speed operation and extended to the variable speed operation using the pump affinity laws. Pump efficiency is modeled using Equation (8.3), which is a function of the fraction of the nominal flow (Rishel et al. 2006). VFD efficiency is modeled using Equation (8.4), which is a function of the fraction of the nominal speed (Hansen 1995). The coefficients in these polynomials can be regressed using the pump performance data or performance curves and VFD efficiency curve provided by the manufacturers.

$$\eta_{pump} = \eta_{design} \cdot (e_0 + e_1 x + e_2 x^2 + e_3 x^3)$$

(8.3)

$$\eta_{VFD} = f_0 + f_1 y + f_2 y^2 + f_3 y^3$$

(8.4)

where, η_{design} is design pump efficiency, x is the fraction of nominal flow, y is the fraction of the nameplate brake horsepower or the nominal speed, e_0–e_3 and f_0–f_3 are coefficients.

The pressure head of chilled water pump systems depends on the control method. In this study, three levels of control optimization methods, i.e. basic level, medium level and advanced level, are proposed for determining the pressure set-point in operation and then the operation cost of systems, as shown in Fig. 8.4. Users can select them based on the expected level of the control optimization of the system to be optimized. The basic level method is that the pressure set-point of the chilled water loop $\Delta p_{set,b}$ (a major part of the pump pressure head) in the building is assumed to be a constant value regardless of the water flow rate as shown in Fig. 8.4 and Equation (8.5). The medium level method is that the pressure set-point of the chilled water loop $\Delta p_{set,m}$ in the building is assumed to be linear to the water flow rate (m_w) as shown in Fig.8.4 and Equation (8.6). The advanced level method is that the pressure set-point of the chilled water loop $\Delta p_{set,a}$ in the building is assumed to be square to the water flow rate (m_w) as shown in Fig. 8.4 and Equation (8.7). The minimum pressure set-point is assumed to be 30% of design pump pressure head. The chilled water flow rate in the building is assumed to be linear to cooling load and the minimum water flow rate is assumed to be 20% of design flow rate.

$$\Delta p_{set,b} = p_D \tag{8.5}$$

$$\Delta p_{set,m} = p_{\min} + \frac{\alpha \cdot m_w}{m_D} \tag{8.6}$$

$$\Delta p_{set,a} = p_{\min} + \beta \left(\frac{m_w}{m_D} \right)^2 \tag{8.7}$$

where, p_D is design pressure head, m_D is design flow rate, α and β are coefficients.
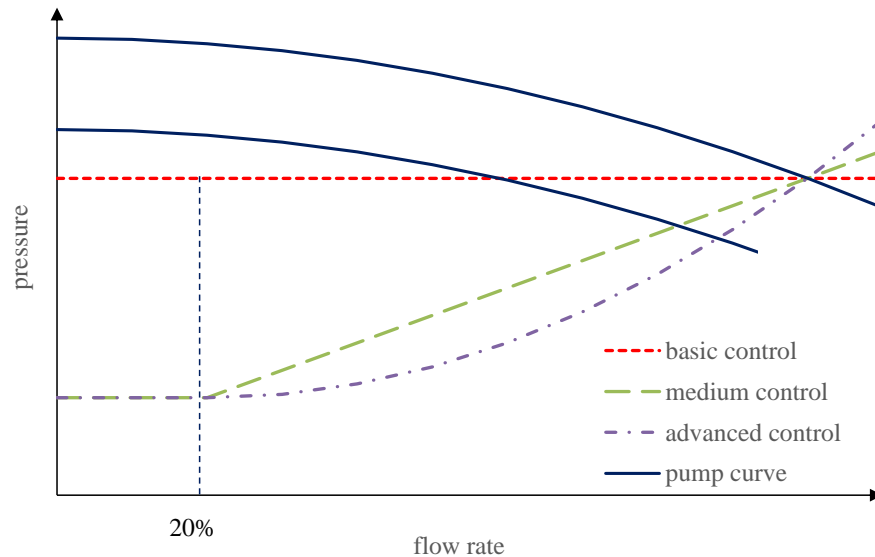
Fig.8.4 Pressure set-point of chilled water loop *vs* flow rate

8.3.2 Determination of design flow and pressure head involving uncertainties

To conduct the proposed robust optimal design, the first step is to obtain the cooling load distribution involving uncertainties and then determine the design flow, the second step is to obtain the hydraulic resistance distribution involving uncertainties and determine the design pressure head.

Module 1 – Obtain the cooling load distribution and design flow

In order to generate the cooling load distribution considering uncertainties and then obtain the design flow, Monte Carlo simulation is employed. In this study, the uncertainties of the design inputs are computed by Matlab. Three types of distributions (including normal distribution, tri-angular distribution and uniform distribution) are used to describe the uncertainties of inputs (Cheng et al. 2015; Gang et al. 2015). Table 3.2 shows an example of the settings of uncertainties of the inputs. Combining the output uncertainties from Matlab, the TRNSYS building model is used to generate the

building cooling load distribution considering the uncertainties based on the determined simulation number. The required trials of Monte Carlo simulations are determined by a statistic method (Cheng et al. 2015). After conducting the required trials of Monte Carlo simulations, the cooling load distribution involving uncertainties is determined. In this study, about 780 times of Monte Carlo simulations are used to generate the cooling load distribution (Cheng et al. 2015). Then, the designers can determine the design cooling capacity based on their specific requirements.

Besides, the design flow is determined by the temperature difference and design cooling load. In practice, the designers tend to choose a constant temperature difference in the design of cooling systems (i.e., the supply chilled water temperature is 7℃ and the return chilled water temperature is 12℃). The flow required is then calculated by Equation (8.8). Where, m_D is the design flow, CL_D is the design cooling load, c_p is the specific heat of chilled water and Δt is the temperature difference.

$$m_D = \frac{CL_D}{c_p \cdot \Delta t} \tag{8.8}$$

Module 2 – Obtain the hydraulic resistance distribution and pressure head

In practice, the pressure head is determined by the overall pressure drop of the "worst case circuit". Fig.8.1 presents the simplified structure of the pressure-flow balance model for the chilled water network at the primary pump only system, in which only three terminal units are included as examples. The bypass is used to maintain the actual flow rate above the minimum flow rate of chilled water through chillers (i.e., 60% of the design flow rate of an individual chiller). The overall pressure drop of the entire

system, i.e., along the sub-branch C-C$_1$, can be mathematically described as in Equation (8.9), which includes the pressure drop on the chillers, the pressure drop on the fittings around pumps (including the pressure drop on the headers that direct the flow into and from each pump and the pressure drop on the valves in the pump headers), the pressure drops on main supply and return pipelines, the pressure drop across the sub-branch (i.e., C-C$_1$) and the pressure drops on the pipeline sections of A-B and B-C.

$$\Delta p_{pump} = \frac{S_{ch}}{N_{ch}}m_0^2 + \frac{S_{pu}}{N_{pu}}m_0^2 + S_0 k_c m_0^2 + S_1 k_c m_1^2 + (S_2 k_c + S_C)m_2^2 \qquad (8.9)$$

where, ΔP_{pump} is the pressure drop of the entire chilled water loop. S_{ch} and S_{pu} are the coefficients of chillers and pumps. S_0, S_1 and S_2 are the coefficients of pipeline. S_C is the coefficient of AHU. m_0, m_1 and m_2 are the flow rate of chilled water.

The pump pressure head is also affected by the hydraulic resistance coefficients, chilled water distribution in each terminal unit and aging factor of the pipelines as well as the fluctuation of the chilled water flow. For a given design cooling load, the design chilled water flow is influenced by the fluctuation (i.e. uncertainty) of the difference between return and supply chilled water temperatures. The flow of chilled water in each terminal unit usually fluctuates around the design flow considering the uncertainty of its heat transfer performance. The flow of chilled water in each terminal unit is assumed to be subject to normal distribution. Uniform distribution is used to describe the uncertainties of the hydraulic resistances of components. In addition, an artificial aging factor is adopted to account for a decrease in pipe diameter as the system ages. According to Equation (8.9), the distribution of pressure head can be generated and the design pressure head is assumed to be 99.6 percentile of the distribution.

8.3.3 Probability distribution of each state considering system reliability

Markov method is used in this chapter because of its wide application in reliability analysis of multi-state systems (Lisnianski and Levitin 2003). The aim of using Markov method is to obtain the probability of each state of a multi-state system at a specific period and then the performance of the system and capability can be estimated. It is assumed that the state probabilities at a future instant do not depend on the states occurred in the past. The system either keeps current state or transfer to other states at the next time step. Several steps are required using Markov method (Gang et al. 2015), including:

- List all the possible states of the chilled water pump system;

- Determine the state transition density matrix;

- Obtain how much is required to reach the steady state;

- Obtain the probability of each state of the system;

- Calculate the mean steady performance and capability under each state.

A chilled water system is comprised of n chilled water pumps. It is assumed that each pump has two states only: normal (0) and failure (1). Totally the system has n states (i.e., each states contains several situations) considering the reliability of pumps, as shown in Fig. 8.5 (Lisnianski et al. 2012). It can be observed that state 0 symbolizes that no pump fail and state k symbolizes that k ($1 \leq k \leq n$) pumps fail. From state 0 to state n, the failure rate λ is used to represent the probability from one state to another. From state n to state 0, the repair rate μ is used to represent the probability from one state to another. The transition probability is determined by a state transition density matrix A (Equation

(8.10)), which only involves the repair rate and failure rate of pumps (Lisnianski et al. 2007). Probability distribution of the system at each state at time t can be represented with a vector $P(t)$ (Equation (8.11)). It can be deduced from the initial state by Equation (8.12) and Equation (8.13). When the time approaches to infinity, $P(\infty)$ will keep stable (Equation (8.14)). Then the steady state probabilities can be obtained by solving the linear algebraic equations (Equation (8.15) and Equation (8.16)).
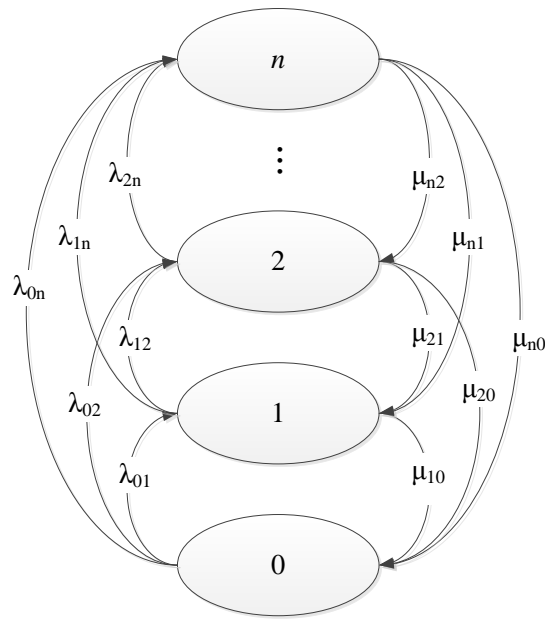
Fig.8.5 States of a n-pump system and possible transitions

$$A = \begin{bmatrix} a_{00} & a_{01} & a_{02} & ... & a_{0n} \\ a_{10} & a_{11} & a_{12} & ... & a_{1n} \\ \vdots & \vdots & \vdots & \vdots & \vdots \\ a_{n0} & a_{n1} & a_{n2} & ... & a_{nn} \end{bmatrix} \tag{8.10}$$

$$P(t) = \begin{bmatrix} p_0(t), \ p_1(t), ..., \ p_n(t) \end{bmatrix} \tag{8.11}$$

$$P(0) = \begin{bmatrix} 1, 0, 0, ..., 0 \end{bmatrix} \tag{8.12}$$

$$P(n) = P(n-1)A = P(0)A^n \tag{8.13}$$

$$P(\infty) = \lim_{n \to \infty} P(n) = \lim_{n \to \infty} P(0)A^n \tag{8.14}$$

$$P(\infty) = P(\infty-1)A = P(\infty)A \tag{8.15}$$

$$\begin{cases} p(0) = a_{00}p(0) + a_{10}p(1) + \cdots + a_{n0}p(n) \\ p(1) = a_{01}p(0) + a_{11}p(1) + \cdots + a_{n1}p(n) \\ \quad \vdots \qquad\qquad\qquad\qquad \vdots \\ p(n) = a_{0n}p(0) + a_{1n}p(1) + \cdots a_{nn}p(n) \\ \displaystyle\sum_{i=0}^{n} p(i) = 1 \end{cases} \qquad (8.16)$$

However, the key issue for using Markov method is to determine the transition density matrix A. As mentioned above, transition density matrix is related to the failure rate and repair rate of pump only. When the repair rate and failure rate are regarded as time-independent, these two variables can be obtained by Equation (8.17) and (8.18) (Tian et al. 2009). Considering that each state (i.e. same number of failure pumps) may contain several situations (i.e. different combinations of failure pumps), the probability that the situations in a state transfer to those in another state in various possible conditions should be obeyed to the law of combinations, as shown in Equation (8.19).

$$\lambda = 1 / MTTF \qquad (8.17)$$

$$\mu = 1 / MTTR \qquad (8.18)$$

$$a_{ij} = \begin{cases} C_n^i \cdot C_{n-i}^{j-i} \lambda & , \quad i < j \\ 1 - a_{i0} - \cdots - a_{i(j-1)} - a_{i(j+1)} - \cdots - a_{in} & , \quad i = j \\ C_n^i \cdot C_{n-i}^{i-j} \mu & , \quad i > j \end{cases} \qquad (8.19)$$

where, λ is failure rate, μ is repair rate, $MTTF$ is mean time to failure, $MTTR$ is mean time to repair, a_{ij} is the probability from state i to state j.

8.3.4 Trials of simulation on total pump flow capacities and pump sizes

Different from previous research that is mainly based on the BEP, in this study, the cooling load distribution are selected to determine the optimal chilled water pumps, which could improve the total operating efficiency and reduce the operation cost.

Considering that pumps are only manufactured in certain size, trials of simulations on different total pump flow capacities and different and discrete pumps sizes are conducted to select the optimal pump system. At start, the searching range of total pump flow capacity should be determined to facilitate the trials on design flow. In this study, the searching range of total pump flow capacity is assumed to be about 1~2 times of the design flow and the interval of total pump flow capacity is 2.5% of the design flow.

After the searching range and interval of total pump flow capacity are determined, the trials of simulations on each total pump flow capacity based on the cooling load distribution can be implemented as shown in Fig. 8.6. The option which has the lowest total cost under each total pump flow capacity is selected. Eventually, among the options corresponding to various total pump flow capacities, the option which has the minimum total cost is selected as the optimum design for a building.
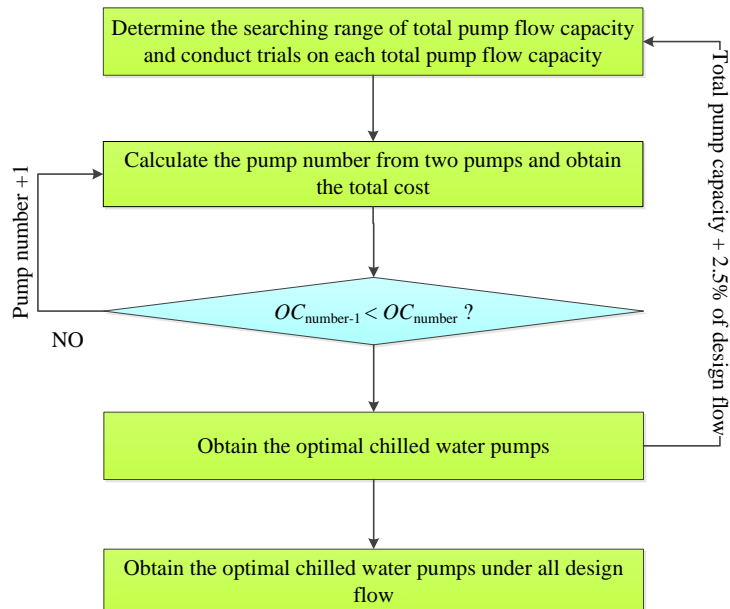
Fig.8.6 Trials of simulation to select optimum pump design

The main step in this searching process is "Calculate the pump number/size from two

pumps and obtain the total cost". Under each total pump flow capacity, simulation trials start from two pumps (minimum two is assumed concerning the basis requirement for reliability and maintenance) until the operation cost begins to increase. At the same time, the capital cost and availability risk cost are determined. Identical variable-speed pumps are assumed in this study, which is typical particularly when chillers of identical capacity are selected.

The overall efficiency of pump systems is determined by the pump efficiency and VFD efficiency, as shown in Equation (8.20). It is well known that for a given building, if the number of pumps used is larger, the nominal flow of individual pumps is lower, the design pump efficiency is lower (Harvey 2012), and the VFD efficiency and load ratio of pumps are larger in operation because they can operate near their full load. Fig. 8.7 presents the relationship between the rated pump efficiency and pump capacity in this study. It can be observed that the rated pump efficiency increases when the pump capacity increase.

$$\eta_e = \eta_{pu} \cdot \eta_{VFD} \tag{8.20}$$
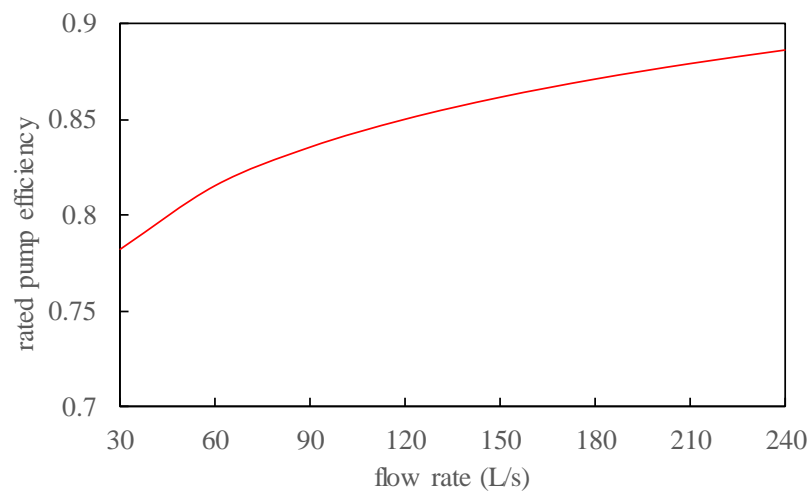
Fig.8.7 Rated pump efficiency vs. pump capacity

Fig. 8.8 shows the conceptual relationship between the number of pumps and overall pumps efficiency. When the number of pumps is small, the increase of pump number may result in the increase of overall efficiency because the VFD efficiency and load ratio of pumps increase significantly along with the decrease of the design efficiency of pumps. When the number of pumps is large, the increase of pump number may result in the decrease of overall efficiency because the VFD efficiency and load ratio of pumps have no obvious further improvement. Since at least two pumps are assumed, the number of pumps is tested starting from two until the operation cost begins to increase. Equation (8.21) presents the typical pump efficiency profiles of a variable-speed pump (120L/s) according to the data from a pump manufacturer. In this study, under the same part load ratio, the pump efficiency of variable-speed pumps is assumed to be proportional to their capacity. The operation cost is calculated using Equation (8.22), the capital cost and availability risk cost are calculated using Equation (8.23) and (8.24). Where, $p_i(t)$ and OC_i are the probability and operation cost under the cooling load CL_i. n is the number of pumps, EC_{ind} is the equipment cost of individual pump, and SC_{ind} is the space cost of accommodating an individual pump. RC_i is the availability risk cost under the cooling load CL_i.

$$\eta_{pu} = 0.85 * \left[0.2455 + 1.509 * \left(\frac{m_w}{m_D} \right) - 1.671 * \left(\frac{m_w}{m_D} \right)^2 + 1.275 * \left(\frac{m_w}{m_D} \right)^3 \right] \tag{8.21}$$

$$OC = \sum_{i=0}^{n} p_i(t) \cdot OC_i \tag{8.22}$$

$$CC = n \cdot (EC_{ind} + SC_{ind}) \tag{8.23}$$

$$RC = \sum_{i=0}^{n} p_i(t) \cdot RC_i \tag{8.24}$$
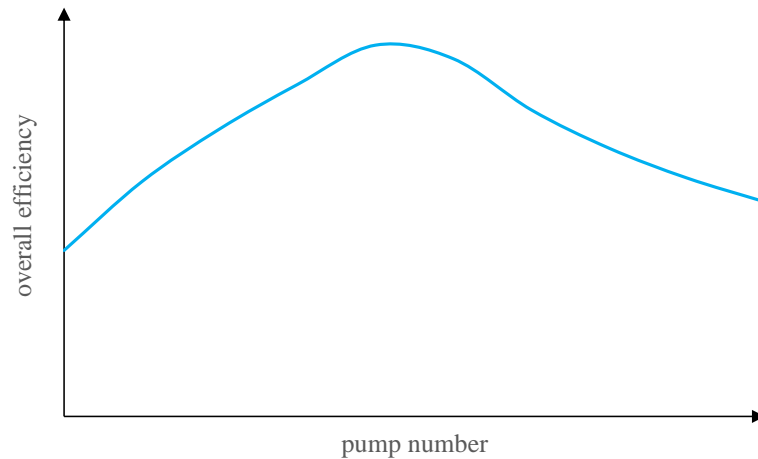
Fig.8.8 pump number *vs.* overall efficiency

8.4 Case Study and Results

A case study on the chilled water pump system design for a building in Hong Kong is conducted to test and evaluate the proposed robust optimal design. At first, Monte Carlo simulation is used to generate the cooling load distribution profile and the design flow is determined based on the cooling load distribution. Then, the hydraulic resistance distribution and design flow are determined according to the cooling load distribution profile. Reliability assessment of the pump system is conducted to obtain the probability of each state under different pump number. Combining the pump models and control methods, the trials of simulations on different total pump flow capacities and pump sizes are conducted to select the optimum chilled water pump system which has the minimum total cost.

8.4.1 Probability distribution of each state of chilled water system

It is essential to obtain the probability distribution of each steady state under various pump numbers. Table 8.1 shows the probability distribution of each steady state under

different pump numbers. It can be observed that the probability of state 0 decreases as

the increase of pump number.

Table 8.1 Probability distribution of steady states of pumps

state	pumps						
	2	3	4	5	6	7	8
0	0.9222	0.8906	0.8494	0.7951	0.7289	0.6575	0.5711
1	0.0605	0.0809	0.1114	0.1517	0.1973	0.2381	0.2913
2	0.0173	0.02	0.0247	0.0327	0.0462	0.0666	0.0865
3	-	0.0085	0.0096	0.0115	0.0146	0.0198	0.0273
4	-	-	0.0049	0.0057	0.0068	0.0084	0.0106
5	-	-	-	0.0033	0.0039	0.0047	0.0057
6	-	-	-	-	0.0024	0.0029	0.0036
7	-	-	-	-	-	0.0019	0.0023
8	-	-	-	-	-	-	0.0016

8.4.2 Implementation of proposed design method of chilled water system

Obtain the cooling load distribution and design chilled water flow

To conduct the Monte Carlo simulations for obtaining the cooling load distribution, it

is essential to select the parameters of uncertainties of the design inputs (Cheng et al.

2015). Combining the output uncertainties from Matlab, the TRNSYS building model

is used to generate the building cooling load involving the uncertainties. After

conducting 780 times of Monte Carlo simulations (Cheng et al. 2015), the cooling load

distribution is obtained, as shown in Fig. 8.9. The reference case is the normal cooling

load distribution without considering the uncertainties. It can be seen that the cooling

load distribution profile of 780 simulation trials is smoother than that of reference case

because more cooling load conditions are considered. The design cooling capacity can be sized based on the load of 5100 kW according to the design standard "50 unmet hours" (Cheng et al. 2015).
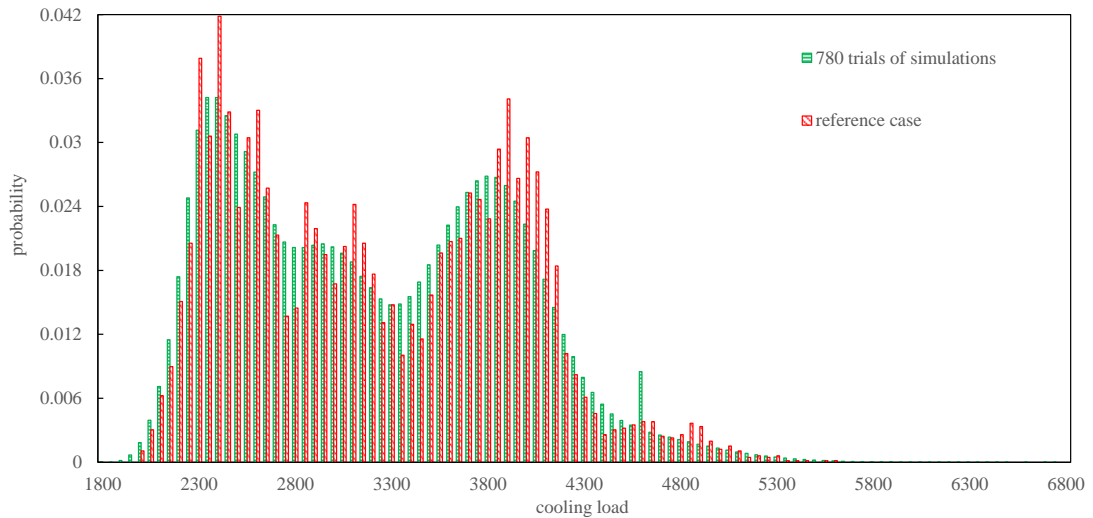
Fig.8.9 Distribution of cooling load considering uncertainties

The design chilled water flow is determined by the design capacity and temperature difference. In practice, designers tend to assume that chilled water supply temperature is 7℃, chilled water return temperature is 12℃ and then the temperature difference is 5℃. According to Equation (8.1), the design chilled water flow is 240L/s.

Obtain the probability distribution of pump pressure head

The pump pressure head is determined by chilled water flow rate, hydraulic resistance coefficient, chilled water distribution in each terminal unit and aging factor of the pipeline. Table 8.2 shows the pressure drops of components, water distribution in each terminal unit and aging factor (Rishel et al. 2006). In this study, three AHUs are used to serve three zones of the same cooling demand and the aging factor of pipes is assumed to be 15% as a constant. According to Equation (8.2), the distribution of pump pressure

head can be generated as shown in Fig. 8.13. The design pump pressure head is assumed

to be about 26m, which is equivalent to 99.6% of the distribution of hydraulic resistance.

Table 8.2 Settings of hydraulic parameters

Parameters	Pressure drop of fittings (m)	Uncertainty
Chiller	5.8	$U(0.9,1.1)$
Pump	7.2	$U(0.9,1.1)$
Pipe (main)	5.7	$U(0.9,1.1)$
Pipe (branch)	2.9	$U(0.9,1.1)$
AHU	4.5	$U(0.9,1.1)$
Valve	4.4	$U(0.9,1.1)$
Chilled water flow rate	-	$1+N(0,0.05)$
Chilled water flow in each branch	1/3 of the total	$1+N(0,0.05)$
Aging factor of pipes	15%	-
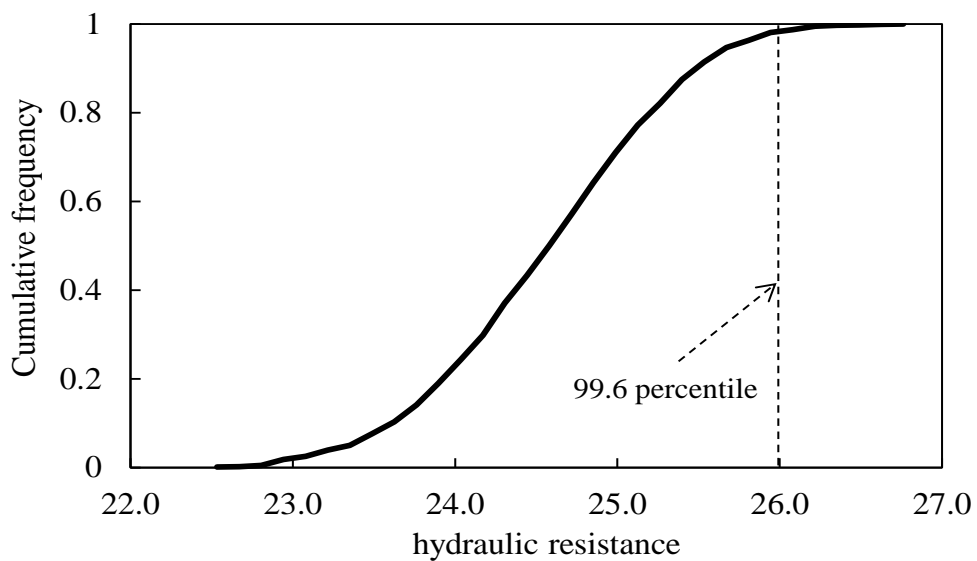
Fig.8.10 Accumulative probability distribution of the overall hydraulic resistance

Trials of simulations on the total pump flow capacity and pump size

At the previous steps, the design chilled water flow and pump pressure head are determined to be 240L/s and 26m respectively. To conduct the trials of simulation on the total pump flow capacity and pump size, it is essential to determine the searching range of total pump flow capacity. As mentioned above, the searching range of total pump flow capacity is assumed to be 1~2 times of design flow and the searching interval is selected to be 2.5% in this study. Trials of simulations are conducted on the 41 total pump flow capacities respectively (i.e. 240L/s, 246L/s, …, 474L/s and 480L/s).

For example, it is assumed that total pump flow capacity is 336L/s. According to Fig. 8.9, the overall efficiency increases when the number of pumps increases in certain range and it decreases when the number of pumps increases further. According to Section 8.3.4, the evaluation of the number of pumps on the operation cost is conducted. The electricity price used in this study is 1 HKD/kW, which is the typical rate in Hong Kong. The results are shown in Table 8.3. It can be observed that the operation costs under basic and medium levels of control optimization decrease when the pump number increases from 2 to 7 and they increase when the pump number increases to 8. Under the advanced level of control optimization, the operation cost does not have obvious change when the number of pumps is 3 or more. In this paper, the detailed results the case study under medium level of control optimization are presented to demonstrate the design process. The design option comprised of 7 pumps has the lowest operation cost compared with the other options.

Table 8.3 Annualized capital cost of different design options

Option (size (L/s)× number)	Operation cost (10^3HKD)			EC (10^3HKD)	SC (10^3HKD)	CC (10^3HKD)
	Basic	Medium	Advanced			
168×2	579	452	380	60	10	70
112×3	547	439	364	77	15	92
84×4	517	435	366	92	20	112
67×5	511	433	366	105	25	130
56×6	493	431	362	117	30	147
48×7	485	424	366	128	35	163
42×8	483	431	366	139	40	179
Remarks: EC- equipment cost, *SC-* space cost, *CC-* capital cost						

Annualized capital cost contains the equipment cost and space cost. The life cycle of the chilled water pump system is assumed to be 10 years. Equipment cost of variable-speed pump (26m, 60L/s) is 150×10^3HKD, referring to the data from a manufacture. As for the equipment cost of other variable-speed pumps, they are estimated using Equation (8.25) (Taal et al. 2003; Guthrie 1969).

$$EC = EC_0 \cdot \left(C / C_0 \right)^{\alpha} \tag{8.25}$$

where, EC_0 is the equipment cost of a reference pump with the capacity C_0. EC is equipment cost of pump with the capacity C. α is the coefficient, which set to be 0.15 in this study (Biegler et al. 1997; Seider et al. 2009). The annualized capital costs under the different design options are estimated using Equation (8.22) and presented in Table

8.3. From Table 8.3, the annualized capital cost increases when pump number increases at a given design flow.

Availability risk cost is the "expense" or service sacrifice which should be considered when the cooling demands cannot be fulfilled. Table 8.4 shows the annual availability risk costs and total costs of different pump numbers under three different penalty ratios (i.e., 1, 10 and 100 HKD/kW). It can be seen that, when the pumps number is small, the annual availability risk cost decreases rapidly when the pump number increases. The annual availability risk cost of options having 2, 3, 4 and 5 pumps is very sensitive to the penalty ratio when the pump number is small, but it is not sensitive any more when the number of pumps is 6 or more. It can also be observed that the total cost decreases when the pump number increases in certain range and it increases when the pump number increases further. Since the availability risk cost is high when the pump number is small and the capital cost is high when the pump number is large, there is a comprised pump number/size which has the minimum total cost. In this study, the penalty ratio is assumed to be 10HKD/kW. Among these options, the option 56L/s×6 pumps has the minimum total cost $586×10^3$HKD, which is not sensitive to the penalty ratio. Therefore, it can be considered as the best option under the total pump capacity 336L/s. If the penalty ratio is 1HKD/kW, the best option under the total pump capacity is 67L/s×5 pumps. The designers can select the best option based on their specific requirement of penalty ratio.

Table 8.4 Annual availability risk cost (10³HKD) and total cost (10³HKD) of different

pump design options

Penalty ratio (HKD/kW)	1		10		100	
Option (size(L/s)×number)	*RC*	*TC*	*RC*	*TC*	*RC*	*TC*
168×2	1,377	1,900	13,770	14,294	13,7700	13,8240
112×3	442	973	4,420	4,951	4,4200	44,729
84×4	96	643	963	1,510	9,630	10,179
67×5	10	573	100	662	1000	1,559
56×6	1	578	**9**	**586**	92	669
48×7	0	587	0	587	0	587
42×8	0	609	0	609	0	609
Remarks: RC- availability risk cost, *TC*- total cost.						

After conducting the trials on other total pump flow capacities, the minimum total costs
are computed and presented in Table 8.5. It can be observed that the options comprised
of more pumps may have lower operation cost compared with those design options
comprised of less pumps. When the total pump flow capacity increases from 240L/s to
336L/s, the availability risk costs of the best options decrease rapidly and the total costs
are also reduced. When the total pump flow capacity is over 384 L/s (i.e. 384 L/s to
480L/s), the availability risk cost of the best option is almost equal to 0. When the total
pump capacity is low, more number of pumps is required to reduce the availability cost

resulting in high capital cost. When the total pump capacity is large, less number of pumps is sufficient to keep low availability risk cost while the capital cost is low. It can be seen that the option with 78 L/s×5 pumps has the minimum total cost 569×10³ HKD compared with other options. It means that the selected option has better robustness to uncertainties and system reliability.

Table 8.5 Best pump design options under different total pump flow capacities

(penalty ratio:10HKD/kW)

Total capacity (L/s)	Best option (size (L/s) × number)	Availability risk cost (10³HKD)	Operation cost (10³HKD)	Total cost (10³HKD)
240	30×8	588	431	1,181
264	33×8	142	432	740
288	36×8	25	431	626
312	45×7	11	428	598
336	48×7	0	424	587
360	72×5	24	430	587
384	77×5	3	431	574
390*	*78×5*	*1*	*432*	*569*
408	82×5	0	438	572
432	86×5	0	438	579
456	114×4	5	446	574
480	120×4	0	456	581

8.4.3 Comparison among the three design methods

Table 8.6 shows the results of robust optimal design, uncertainty-based design and conventional design. It can be seen that the total cost under conventional design (698×10^3HKD) is close to that (700×10^3HKD) under uncertainty-based optimal design. Compared with conventional design and uncertainty-based optimal design, the total cost under robust optimal design (569×10^3HKD) is reduced by about 18.6% when the penalty ratio is 10 HKD/kW. To achieve the minimum annual total cost, the option with 5 variable-speed pumps (78L/s) can be selected as the optimum selection for the design. Compared with conventional design (OC=461×10^3HKD) and uncertainty-based design (OC=431×10^3HKD), the proposed robust optimal design (OC=432×10^3HKD) could achieve a relatively low operation cost. This best option also has the minimum total cost (569×10^3HKD), which may indicate that it has good robustness considering the uncertainties of design inputs and reliability of system components.

Table 8.6 Best pump design options under different total pump flow capacities and optimal options using different design methods (penalty ratio:10HKD/kW)

	Total capacity (L/s)	Best option (size (L/s) × number)	Availability risk cost (10^3HKD)	Operation cost (10^3HKD)	Total cost (10^3HKD)
Robust optimal design	390	78×5	1	432	569
Uncertainty-based design	280	40×7 (including 1 standby pump)	116	431	700
Conventional design	400	100×4 (including 1 standby pump)	116	461	698

8.5 Discussion

Table 8.7 shows the results under all the three levels of control methods. The optimal design option is 50 L/s×7 pumps under the basic level of control and its total cost is $643×10^3$ HKD. The optimal design option is 79 L/s×5 pumps under the advanced level of control and its total cost is $501×10^3$HKD. The users can choose the preferred option based on their specific level of control methods.

Table 8.7 Minimum total cost under different levels of control methods

	Control level	Best option (size (L/s) × number)	Total capacity (L/s)	Operation cost (10^3 HKD)	Total cost (10^3 HKD)
Robust optimal design	Basic	50×7	350	478	643
	Medium	78×5	390	432	569
	Advanced	79×5	395	365	501
Uncertainty-based design	Basic	40×7	280	480	749
	Medium	40×7	280	431	700
	Advanced	40×7	280	378	647
Conventional design	Basic	100×4	400	527	761
	Medium	100×4	400	461	698
	Advanced	100×4	400	368	602

8.6 Summary

This chapter presented a robust optimal design method that is based on a minimized life-cycle cost to ensure the high performance of chilled water pump systems and achieve the minimum annual total cost considering uncertainties of inputs and system reliability. It is realized by optimizing the pump pressure head, the total pump flow capacity and number of chilled water pumps. A case study is presented as an example to test and demonstrate the proposed method. Conclusions can be made as follows:

- Annual average cooling load varies largely when considering uncertainties. If the sizing of design cooling capacity is based on the cooling load without considering

uncertainties, the design cooling capacity and design chilled water flow will be very likely oversized. If the pump head is determined without considering the uncertainties of hydraulic resistance and water flow distribution, the oversize of pump head will be greatly increased.

- Markov method can be effectively used to obtain the probability distribution of system state (health) for high accuracy and fast computation time. In this study, the iteration time under different repair rate and failure rate is obtained. Results show that the iteration time is less when more pumps are used and when the ratio of repair rate to failure rate is small.

- In this study, the design cooling capacity is that corresponding to the capacity under "50 unmet hours". According to this design capacity, the design chilled water flow and searching range of total pump flow capacity are determined. If different design cooling capacity is selected, the design chilled water flow and the searching range of total pump flow capacity will change accordingly. Then, the optimal option may also change.

- The design option of the chilled water pump system can be selected by achieving the minimum total cost when considering uncertainties and system reliability. The selected pump system can perform well under various possible cooling load conditions and have the good robustness towards the system reliability. The results of the case study show that the total cost of optimized pump system can be reduced significantly (totally 18.6%) compared with the conventional design and

uncertainty-based optimal design.

The robust optimization is conducted by separating optimizing trials into two steps, i.e. the determination of design chilled water flow and pump head, the optimization of total pump flow capacity and number/size of pumps. It is worth noticing that the optimization output may be slightly different from the best one in principle as not all options/combinations are tested due to the chosen test interval in computation and available pumps sizes in practice.

CHAPTER 9 ROBUST OPTIMAL DESIGN OF COOLING WATER SYSTEMS BASED ON SEQUENTIAL MONTE CARLO SIMULATION

This chapter presents a sequential Monte Carlo simulation-based robust optimal design method of cooling water system. In this chapter, sequential Monte Carlo simulation is used for the quantification of reliability of equipment and components. In order to achieve the minimum total cost, trials of simulations on different cooling water flows and different number/size of cooling water pump and cooling tower are conducted to obtain the optimum cooling water system. A series of so-called uncertainty "scenarios" generated by Monte Carlo simulation, is used for obtaining the accurate average cooling load and average "unmet cooling load". Several indices are developed for the convergence assessment of average cooling load and average "unmet cooling load". Average cooling load is used to evaluate the operation cost of cooling water system. "Unmet cooling load" is used to evaluate the availability risk cost of cooling water system.

Section 9.1 presents an introduction of cooling water system. Section 9.2 describes the objective of robust optimal design for cooling water system. Section 9.3 presents the method of the robust optimal design for cooling water systems. Section 9.4 shows a case study on the proposed robust optimal design of the cooling water system of a building in Hong Kong. A summary of this chapter is given in Section 9.5.

9.1 Introduction

Fig.9.1 shows the schematic of a cooling water loop. Identical constant-speed pumps are used to circulate the cooling water through the entire system and the pumps are assumed to work at the rated power. Identical cooling towers are used to reject the heat load to the ambient. Variable speed fans are used in the cooling towers.
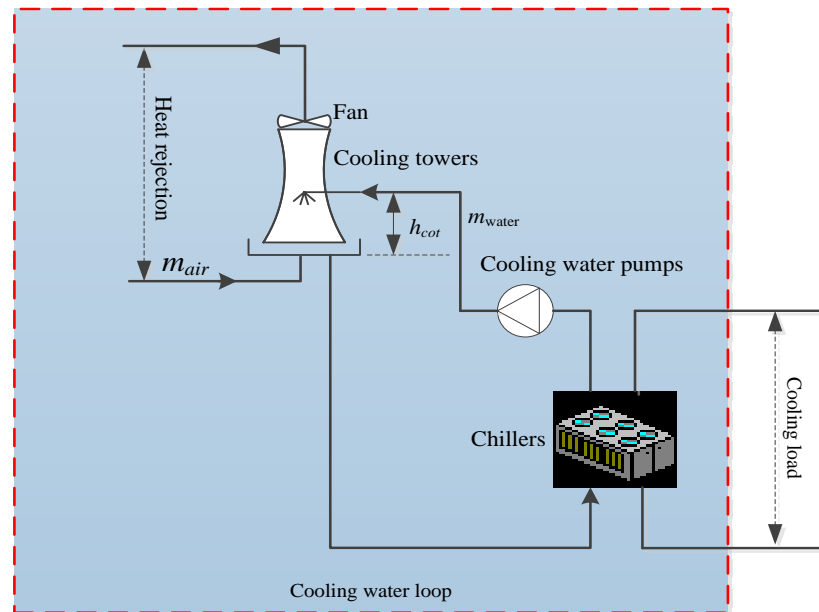
Fig.9.1 Scheme of a typical cooling water loop

In a cooling water loop, the energy balance is shown in Equation (9.1) and (9.2).

$$CL + Q_{compression} = \sum_{i=1}^{n} m_{fluid} \cdot c_{fluid} \cdot \left(T_{fluid,in} - T_{fluid,out}\right) \qquad (9.1)$$

$$Q_{compression} = CL / COP_{chiller} \qquad (9.2)$$

where, CL is cooling load, $Q_{compression}$ is heat of compression, m_{fluid} is the cooling water flow rate, c_{fluid} is the specific heat of water, $T_{fluid,in}$ is the return cooling water temperature, $T_{fluid,out}$ is the supply cooling water temperature.

The total heat load rejected by the cooling towers is determined by the cooling load and

the COP of chillers. Under the given range (i.e. the temperature difference between the supply cooling water temperature and return cooling water temperature) and approach temperature (i.e. the temperature difference between supply cooling water temperature and wet-bulb temperature of inlet air), the design cooling flow rate is determined by the total heat load.

9.2 Objective of this Design Optimization Method

The objective of the proposed method is to ensure that the cooling water system operates at high efficiency over the entire cooling season and achieve the minimum total cost considering uncertainties of inputs and reliability of system components in operation. The total cost (TC_n) consists of annualized capital cost (CC_n), annual operation cost (OC_n) and annual availability risk cost (RC_n). Annualized capital cost includes the expense in purchasing/installing the pumps and cooling towers and associated components (equipment cost) and the spaces for accommodating them (space cost), which is determined by the number and size of pumps and cooling towers. Annual operational cost is the cost of electricity consumed by the pumps and fans in cooling towers in operation, which is mainly associated to the annual cooling load distribution and the energy efficiency of pumps and fans. Availability risk cost is the "expense" or service sacrifice penalty that should be considered when the cooling demands cannot be fulfilled. In the cooling water loop, the overall total cost contains the total cost of cooling towers and the total cost of cooling water pumps, as shown in Equation (9.3). Fig.9.2 illustrates the conceptual relationship between the costs and system total capacity. It is well-known that a larger system capacity means higher system reliability.

The capital cost and operation cost increase as the system capacity increases. On the other hand, the availability risk cost decreases as the system total capacity increases. The total life-cycle cost is comprised of the capital cost, operation cost and availability risk cost, as shown in Equation (9.4) and (9.5). According to Fig.9.2, there should be a comprised system capacity to achieve the minimum total life-cycle cost, at which a comprised level of reliability is achieved.

$$TC_{n,all} = TC_{n,cot} + TC_{n,cwp} \tag{9.3}$$

$$TC_{n,cot} = CC_{n,cot} + OC_{n,cot} + RC_{n,cot} \tag{9.4}$$

$$TC_{n,cwp} = CC_{n,cwp} + OC_{n,cwp} + RC_{n,cwp} \tag{9.5}$$
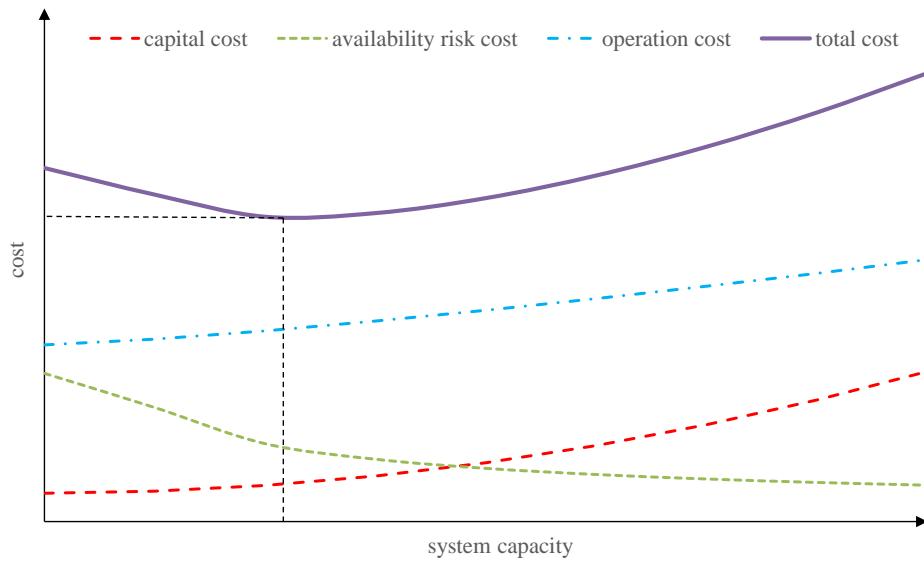
Fig.9.2 Total cost *vs* system capacity

9.3 Computing Procedure of the Robust Optimal Design Method

9.3.1 Procedure outline

Fig.9.3 shows the overall procedure of the proposed robust optimal design. It mainly addresses the determination of design cooling water flow, the pump head of cooling

water pumps and number/size of cooling towers and cooling water pumps. Considering that the cooling towers and cooling water pumps are only manufactured in certain discrete sizes, trials on different design cooling water flow rates and different numbers/sizes of cooling towers and cooling water pumps are conducted to select the optimal cooling water system.
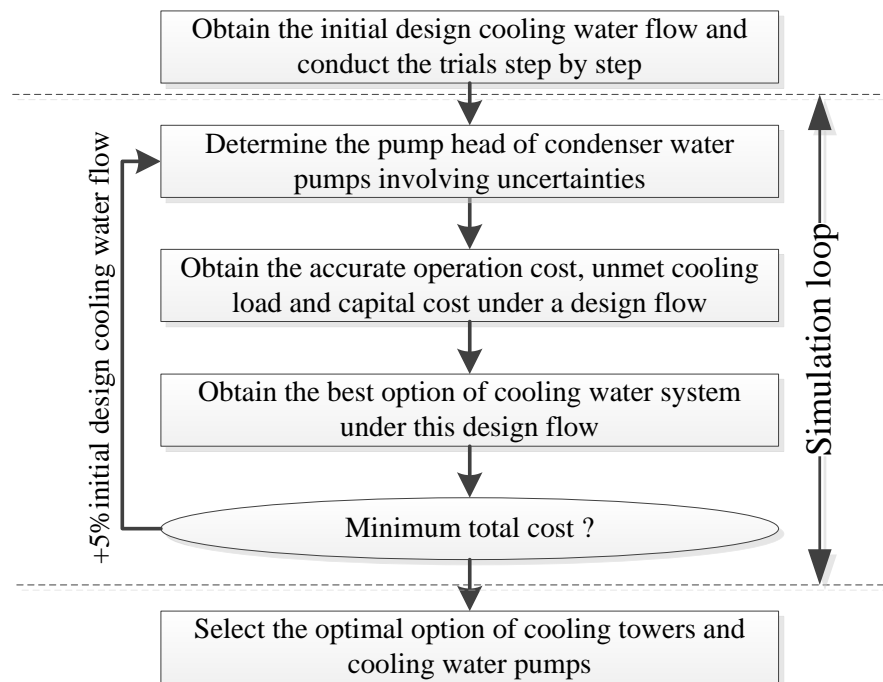
Fig.9.3 Design optimization procedure of cooling water system

Searching range of design cooling water flow rate is assumed to be 1 to 2 times of the minimum design cooling water flow. The minimum design cooling water flow is equivalent to the required cooling water flow based on the design cooling capacity and the rated COP of chillers concerned. Under a given design cooling water flow rate, the pump head is determined by the hydraulic resistance distribution involving uncertainties. Then, the operation cost, unmet cooling load and capital cost are obtained under different numbers/sizes of cooling tower and cooling water pump. Under this given

design cooling water flow rate, the optimal option of cooling water system is selected based on the minimized total costs of the cooling water pumps and cooling towers. Simulation trials of cooling water pumps start from two pumps (the minimum of two is assumed concerning the basic requirement for reliability and maintenance) until the total cost of pumps begins to increase. For the same reason, simulation trials of cooling towers also start from two cooling towers until the total cost of cooling towers in the life-cycle begins to increase. Eventually, among the options corresponding to various design cooling water flow rates, the option that has the minimum total cost is selected as the optimum design for application.

Equation (9.6) formulates the optimization problem for selecting the total design cooling water flow rates and numbers/sizes of cooling towers and cooling water pumps. Where, TC is the total cost, M is the design cooling water flow, m_{cot} is the individual capacity of cooling water, n_{cot} is the number of cooling towers, m_{cwp} is the individual capacity of cooling water pump, n_{cwp} is the number of cooling water pumps, M_{min} is the minimum design cooling water flow.

$$\text{find} \quad M, m_{\text{cot}}, n_{\text{cot}}, m_{cwp}, n_{cwp}$$

$$\text{minimize} \quad TC_{n,all}(M_i, m_{\text{cot}}, n_{\text{cot}}, m_{cwp}, n_{cwp})$$

$$\text{constraint} \quad M_i \geq M_{\min}, M_i \leq 2M_{\min} \tag{9.6}$$

$$M_i = m_{\text{cot}} \cdot n_{\text{cot}} = m_{cwp} \cdot n_{cwp}$$

$$n_{\text{cot}} \geq 2, n_{cwp} \geq 2$$

9.3.2 Sequential Monte Carlo simulation

Fig.9.4 shows the simulation procedure for obtaining the cooling load distribution, average operation cost and average "unmet cooling load". Cooling load distribution is generated by the TRNSYS building energy model based on the uncertainties of design inputs. Average operation cost and average "unmet cooling load" are determined by the cooling load conditions, heat of compression and available cooling capacity. Unmet cooling load is the load difference when the available cooling capacity is less than the actual cooling load conditions. Available cooling capacity is determined by the uncertainties of health states of components in the system, which can be calculated by the component reliability model. When some cooling towers fail, the capacity of cooling towers might not be able to meet the capacity of chiller plant. Heat of compression is determined by the COP of chiller plant. The COP is affected by the condensing temperature which depends on the cooling water temperature. Convergence assessment is conducted to verify the cooling load distribution, average operation cost and average "unmet cooling load". If not, more Monte Carlo sampling times of simulation are conducted until these three values converge.
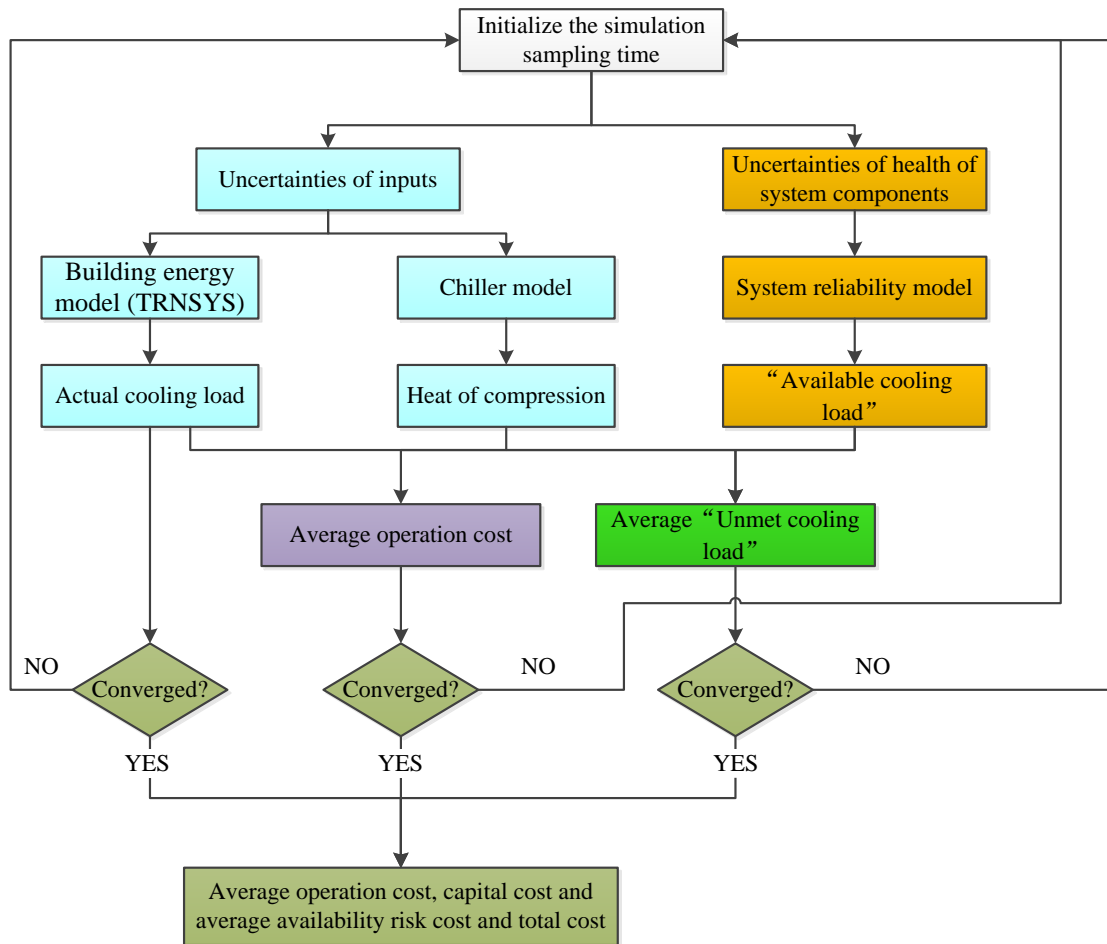
Fig.9.4 Simulation procedure for obtaining the accurate cooling load distribution,

average operation cost and average "unmet cooling load"

9.3.3 Implementation flowchart of the proposed design method

Quantification of pump head of cooling water pump

The simplified model structure for the pressure-flow balance of the cooling water loop

is presented earlier in Fig.9.1. The overall pressure drop of the system can be

mathematically described as in Equation (9.7), which consists of five parts of pressure

drops, including (1)   the pressure drop on the condensers of chillers, (2) the pressure

drop on the fittings around pumps (including the pressure drop on the headers that direct

the flow into/from each pump and the pressure drop on the valves), (3) the pressure

drops on main supply and return pipelines, (4) the pressure drop measured from the operating water level in the cold water basin to the spray system (i.e. nozzle) and, (5) the pressure drop of nozzle required to effect proper distribution of the water to the fill.

$$\Delta p = \frac{S_{con}}{N_{chiller}} \cdot m_w^2 + \frac{S_{cwp}}{N_{cwp}} \cdot m_w^2 + S_{pipe} \cdot k_c \cdot m_w^2 + H_{cot} + S_{noz} \cdot m_w^2 \qquad (9.7)$$

Where, Δp is the pressure drop of the entire cooling water loop, S_{con} is the coefficient of chiller condenser, $N_{chiller}$ is the number of chillers, S_{cwp} is the coefficient of cooling water pumps, N_{cwp} is the number of pumps, S_{pipe} is the coefficient of pipelines, k_c is the aging factor of pipes, H_{cot} is the height from the operating water level in the cold water basin to the spray system, S_{noz} is the coefficient of nozzles, m_w is the cooling water flow rate.

The pump pressure head is then determined by the hydraulic resistance coefficients and aging factor of the pipelines as well as the fluctuation of the cooling water flow. For a given design cooling load, the cooling water flow is influenced by the fluctuation (i.e. uncertainty) of the difference between return and supply cooling water temperatures. The cooling water flow usually fluctuates around the design cooling water flow considering the uncertainty of its heat transfer performance. The cooling water flow is assumed to be subject to normal distribution. Uniform distribution is used to describe the uncertainties of the hydraulic resistances of components. In addition, an artificial aging factor is adopted to account for the decrease in pipe diameter as the system ages. According to Equation (9.7), the distribution of pressure head can be generated and the design pressure head is assumed to be 99.6 percentile of the distribution.

Quantification of cooling load conditions

Monte Carlo simulation is employed to obtain a representative and reasonable cooling load distribution considering uncertainties. The calculation process can be illustrated by Equation (9.8). With the inputs $x_1, x_2,…, x_n$ (e.g., the outdoor temperature, ventilation rate), the output y (the cooling load) can be obtained. In this study, the uncertainties of the design inputs are computed by Matlab. Three types of distributions (including normal distribution, tri-angular distribution and uniform distribution) are used to describe the uncertainties of inputs. Combining the output uncertainties from Matlab, the TRNSYS building model is used to obtain the cooling load conditions.

$$Y = [y_1, y_2,..., y_{8760}] = f(x_1, x_2,..., x_n) \tag{9.8}$$

Model of heat of compression

Heat of compression is the amount of heat added to refrigerant during the compression process, which depends on the actual cooling load and the operating COP of chillers COP_{op}. Usually, the COP_{op} of chiller varies depending on the part load ratio (PLR). It is well understood that the larger the PLR, the higher COP, as shown in Equation (9.9):

$$COP_{op} = \frac{273.15 + T_{eva}}{T_{con} - T_{eva}} \times \left(D_0 + D_1 \cdot PLR + D_2 \cdot PLR^2 + D_3 \cdot PLR^3\right) \tag{9.9}$$

where, T_{eva} and T_{con} are evaporating and condensing temperature (°C), respectively; D_0-D_3 are the correlation coefficients that can be identified from chiller catalogues or field measurement data. The outlet water temperature of the evaporator ($T_{eva,out}$) is set to be 7℃ in simulation tests, and the inlet water temperature of condenser ($T_{con,in}$) is assumed to have a difference of 5 K with the wet-bulb temperature of the cooling tower inlet air ($T_{wb,in}$) as shown in Equation (9.10).

$$T_{con,in} = T_{wb,in} + 5 \qquad\qquad (9.10)$$

Model of available cooling capacity

Fig.9.5 is a reliability and maintainability history chart of a three-state machine. The state "Operate" indicates that the equipment currently resides in a working state (i.e. State 1). The lengths of this state are the holding times of being in working state. The holding time is random and determined by analysis of historical reliability and maintainability data. In practice, the mean time to failure ($MTTF$, $1/\lambda$) is often used to represent this holding time, as shown in Equation (9.11). The state "Maintenance" and "Failure" (i.e. State 0) indicate that the equipment currently resides in an inoperative (i.e. failure or maintenance) state. The lengths of these state are the holding times of being in this state. In practice, the mean time to repair ($MTTR$, $1/\mu$) is often used to represent this holding time, as shown in Equation (9.12). Given a reliability and maintainability history chart, the reliability indices, such as availability, $p_{availability}$ (percentage of time staying in a working state) and unavailability, $p_{unavailability}$ (percentage of time staying in a failure and maintenance state) can be calculated from the reliability and maintainability history chart above by Equation (9.13) and (9.14). Where, $t_{operate}$, t_{main} and t_{fail} are the total operation time, the total maintenance time, and the total failure time respectively in an entire period. λ is failure rate, μ is repair rate.
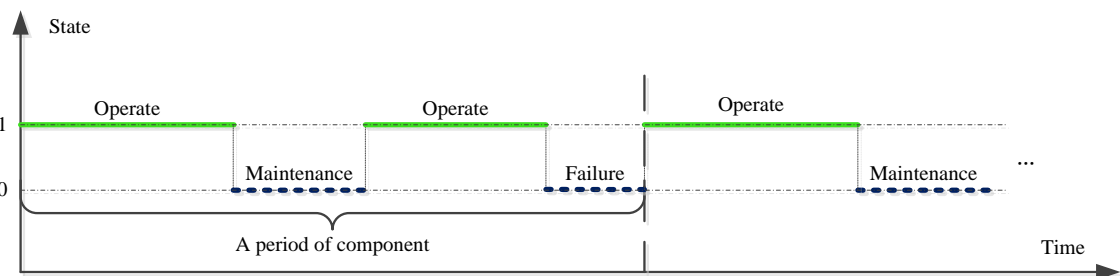
Fig.9.5 Health states of a component in the life cycle

$$MTTF = \frac{1}{\lambda} = \sum t_{operate} \tag{9.11}$$

$$MTTR = \frac{1}{\mu} = \sum t_{main} + \sum t_{fail} \tag{9.12}$$

$$p_{availability} = \frac{MTTF}{MTTF + MTTR} \tag{9.13}$$

$$p_{unavailability} = \frac{MTTR}{MTTF + MTTR} \tag{9.14}$$

With the assumption that each component is independent and has no relationship with the other components, the probability of cooling water pump and cooling tower are assumed to be subject to the binary distribution, as shown in Equation (9.15) and (9.16). The total available cooling load of cooling water pumps and cooling towers are calculated by Equation (9.17) and (9.18). The unmet cooling load of cooling water pumps and cooling towers are calculated by Equation (9.19) and (9.20). Where, $p_{availablility,cot}$ and $p_{availability,cwp}$ are the availabilities of cooling towers and cooling water pumps. $f_{cot}(i)$ and $f_{cwp}(i)$ are the states of cooling tower and cooling water pump. $CL_{available,cwp}$ and $CL_{available,cot}$ are the available cooling load of cooling water pumps and cooling towers, $CL_{ind,cwp}$ and $CL_{ind,cot}$ are the nominal capacity of cooling water pumps and cooling towers. $CL_{unmet,cot}$ and $CL_{unmet,cwp}$ are the unmet cooling loads of cooling towers and cooling water pumps. CL_{actual} is the annual cooling load.

$$f_{cot}(i) = B(1, p_{availability,cot}) \tag{9.15}$$

$$f_{cwp}(i) = B(1, p_{availability,cwp}) \tag{9.16}$$

$$CL_{available,cwp} = CL_{ind,cwp} \cdot \sum_{i=1}^{n_{cwp}} f_{cwp}(i) \tag{9.17}$$

$$CL_{available,cot} = CL_{ind,cot} \cdot \sum_{i=1}^{n_{cot}} f_{cot}(i) \tag{9.18}$$

$$CL_{unmet,cot} = Max(CL_{actual} - CL_{available,cot}, 0) \tag{9.19}$$

$$CL_{unmet,cwp} = Max \left(CL_{actual} - CL_{available,cwp}, 0 \right) \tag{9.20}$$

Model of condenser water loop

Pump model

Cooling water pumps are constant speed pumps and they are assumed to work at their rated powers. Their electricity consumptions depend on the pressure drop (Δp_{cwp}), the cooling water flow rate (m_w) and pump efficiency (η_{cwp}) as shown by Equation (9.21). In this study, the pressure drop of the cooling water loop is equivalent to the pressure head of cooling water pump. The pump efficiency depends on the pump capacity.

$$OC_{pu} = \frac{m_w \Delta p_{cwp}}{102 \eta_{pu}} \tag{9.21}$$

Cooling tower model

The electricity consumption of cooling towers is calculated based on the design efficiency of fan and load ratio of fan (Equation (9.22)). The fans of cooling towers are equipped with variable speed drives. The cooling tower model (TYPE510) in TRNSYS is used in this study. The air at tower outlet is assumed to be saturated air. The load ratio of fan (γ_{air}) can be then calculated by Equation (9.23) and (9.24). Where, P_{fan} and $P_{fan,rated}$ are the power consumption of fans and the rated power consumption of fans. γ_{air} is the load ratio. g_0-g_3 are the correlation coefficients provided by the manufacturer. h_{sat} is the enthalpy of saturated air, h_{air} is the enthalpy of air.

$$P_{fan} = P_{fan,rated} \cdot \left(g_0 + g_1 \cdot \gamma_{air} + g_2 \cdot \gamma_{air}^2 + g_3 \cdot \gamma_{air}^3 \right) \tag{9.22}$$

$$h_{sat} = h_{air}\left(T_{air,in}\right) + \frac{c_{fluid} \cdot m_{fluid} \cdot \left(T_{fluid,in} - T_{fluid,out}\right)}{m_{air} \cdot \left(1 - \exp\left[- \lambda_{design} \cdot \gamma_{air}^{-0.4}\right]\right)} \tag{9.23}$$

$$\lambda_{design} = \ln \left[\frac{h_{sat}\left(T_{fluid,out,design}\right) - h_{air}\left(T_{air,in,design}\right)}{h_{sat}\left(T_{fluid,out,design}\right) - h_{air}\left(T_{air,out,design}\right)} \right] \qquad (9.24)$$

Convergence of Monte Carlo simulation

As mentioned above, the cooling load distribution, the operation cost and available cooling capacity are generated by a sequential Monte Carlo simulation. For the purpose of checking the convergence and terminating the sampling process, there are several different types of stop criteria in literature, such as coefficient of variance, maximum number of iterations and convergence band (i.e. also called as threshold). Among these criteria, the threshold is used to evaluate the uncertainty and reliability in this study.

As mentioned above, the convergence assessment needs to be conducted on the average cooling load distribution, average operation cost and average unmet cooling load. Two convergence criteria are applied as follows:

- The deviation of the cooling load distribution profile should be within its threshold B_w over a number of simulation trials (i.e. over convergence band length B_L).

- The deviations of the dimensionless operation cost and unmet cooling load should be within their threshold B_w over the same convergence band length B_L.

The profile deviation $f(n+i,n)$ is defined as the difference between average cooling load distribution profiles over $(n+i)$ number of simulations and n number of simulations respectively, as shown in Equation (9.25) and Fig.9.6 .

$$f(n+i,n) = \frac{\sum_1^k \left[|p_{n+i}(j) - p_n(j)| \cdot \Delta CL_j \right]}{\sum_1^k \left[p_n(j) \cdot \Delta CL_j \right]} \qquad (9.25)$$

where, $p_n(j)$ is the probability at the load CL_j over n trials of simulations, $p_{n+i}(j)$ is the

162

probability at the load CL_j over $n+i$ trials of simulations. $\triangle CL_j$ is the cooling load

interval and k is the total number of intervals.
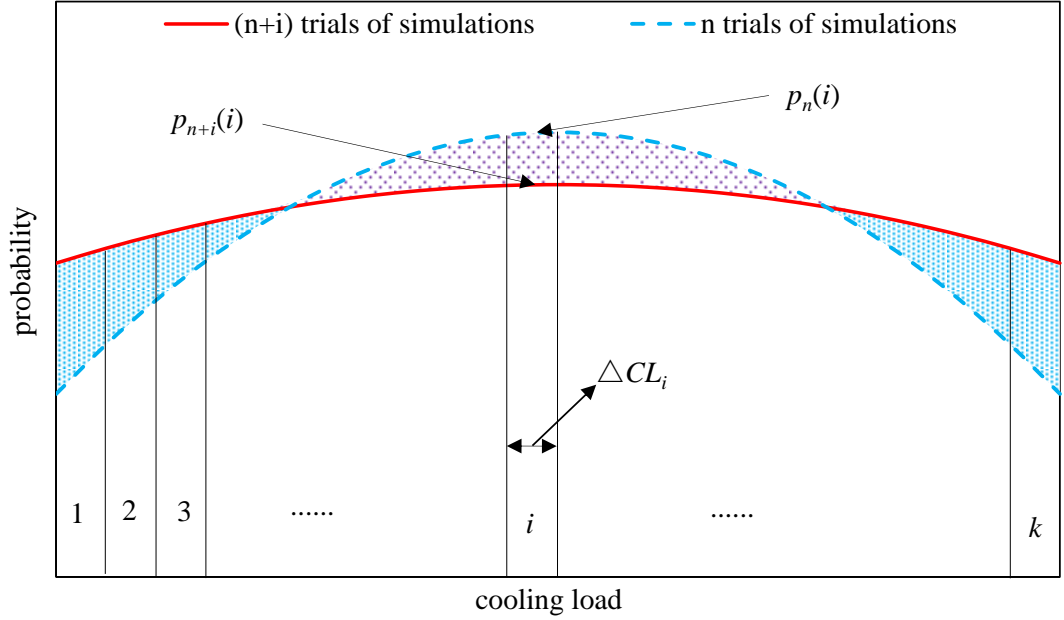
Fig.9.6 Difference between cooling load distributions over simulation of two different

simulation numbers

The deviation $\Delta y(n+i,n)$ is defined as the difference between the average value of $(n+i)$

number of simulations and the average value of n number of simulations respectively,

as shown in Equation (9.26). This deviation is used to evaluate the convergence of the

dimensionless operation cost and unmet cooling load.

$$\Delta y(n+i,n) = \frac{\left| y_{n+i} - y_n \right|}{y_n} \tag{9.26}$$

where, y_n is the average value over n trials of simulations, y_{n+i} is the average value over

$(n+i)$ trials of simulations.

9.4 Case study and evaluation of the proposed design optimization method

A case study on the cooling water system design for a building in Hong Kong is conducted to test and evaluate the proposed robust optimal design method. The performance of the system designed using the proposed robust optimal design method is compared with that using conventional design method, conventional optimal design method and uncertainty-based design method.

9.4.1 Outline of implementation

The main steps of design method implementation are summarized as follows:

• At first step, the minimum design cooling water flow rate and searching range of design cooling water flow rate are determined;

• Under each given design cooling water flow rate, the pressure head of cooling water pumps is determined by the hydraulic resistance distribution involving uncertainties;

• Then, the trials of different number of cooling towers and cooling water pumps on each given design cooling water flow rate are conducted;

• A sequential Monte Carlo simulation is used to obtain the cooling load distribution profile, operation cost and unmet cooling load;

• The optimal option under each design cooling water flow rate is selected based on the minimized total cost;

- Among these options, the option which has the minimum total cost is selected as the best option used in the building energy system.

9.4.2 Determination of cooling load distribution and head of cooling water pumps

According to Equation (9.1) and (9.2), the minimum design cooling water flow rate is 285L/s. The searching range of design cooling water flow rate is assumed to be 285~420L/s and the interval of the trials is 15L/s. The failure rates of pump and cooling tower are 0.0001/hour and 0.00001/hour respectively, which means that the total working time of cooling water pumps and cooling towers are 10,000 hours and 100,000 hours during an entire period (see Fig.9.5). The repair rates of both pumps and cooling towers are 0.002/hour, which means that totally 500 hours are needed to repair or maintain each of the pumps and cooling towers during the same period. Therefore, the availabilities of pumps and cooling towers are 0.9524 and 0.995 respectively.

For example, when the design cooling water flow rate is assumed to be 330L/s, the annual cooling load profile and annual unmet cooling load of cooling towers under five years can be obtained as shown in Fig.9.7. It can be observed that the annual cooling load profile is different over the five years and the annual unmet cooling load varies greatly under different years. Therefore, sufficient sampling is required to obtain the accurate cooling load distribution, operation cost and unmet cooling load.
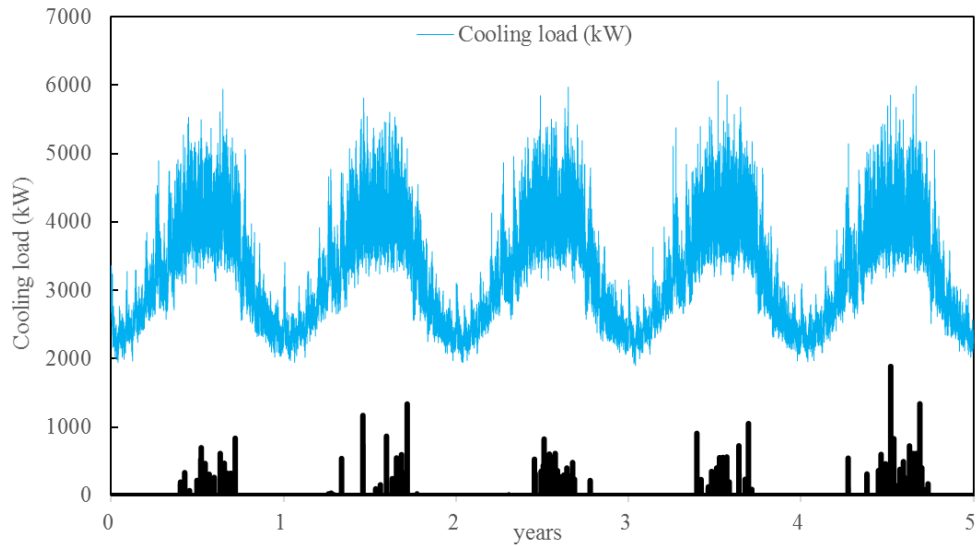
Fig.9.7 Annual cooling load and unmet cooling load of cooling towers

The pressure head of cooling water pumps is determined by the cooling water flow rate, hydraulic resistance coefficient and aging factor of the pipelines. Table 9.1 shows the settings of pressure drops of components and aging factor, which are selected referring to the literature. According to Equation (9.7), the distribution of pump pressure head can be generated as shown in Fig.9.8. The design pump pressure head is assumed to be 25.5m, which is equivalent to 99.6% of the distribution of the hydraulic resistance.

Table 9.1 Settings of hydraulic parameters

Parameters	Pressure drop of fittings (m)	Uncertainty
Condenser of Chiller	5.8	U (0.9,1.1)
Pump	7.2	U (0.9,1.1)
Pipe	5.7	U (0.9,1.1)
Nozzle	4.4	U (0.9,1.1)
Height	2.6	-
Cooling water flow	-	$1+N(0,0.05)$
Aging factor of pipes	15%	-
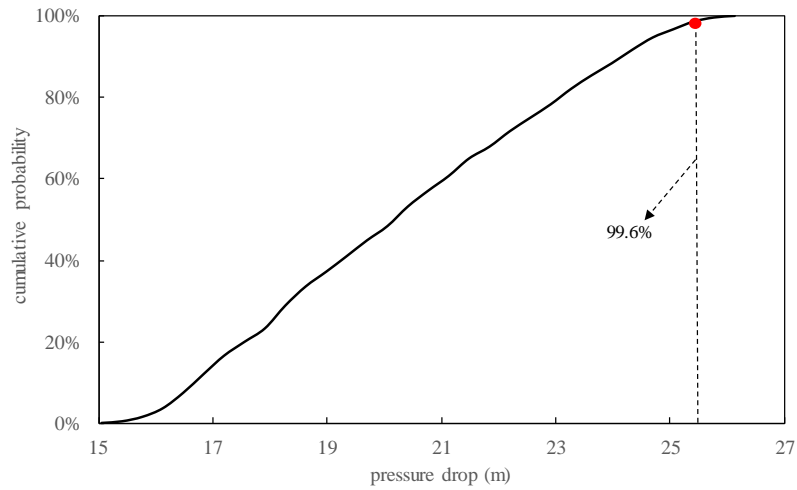
Fig.9.8 Accumulative probability distribution of the overall pressure drop

Then, the trials on different numbers/sizes of cooling towers and cooling water pumps are conducted based on the minimized total cost respectively. The cooling load distribution depends on the uncertainties of inputs and it is independent from the design cooling water flow rate. After conducting 780 times of Monte Carlo simulations, a cooling load distribution of sufficient accuracy is obtained based on the convergence assessment, as shown in Fig.9.9. The reference case is the cooling load distribution in the typical year without considering uncertainties.
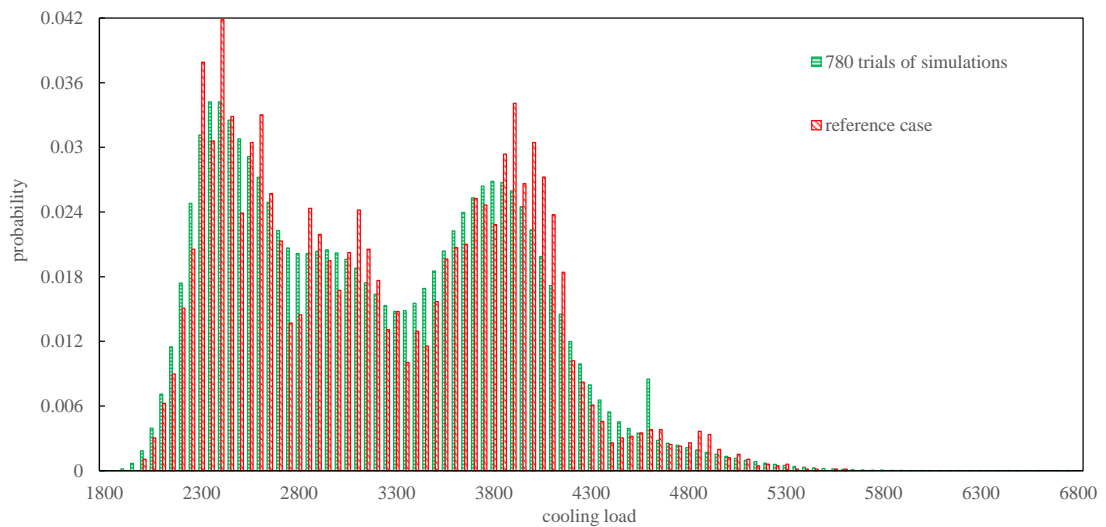
Fig.9.9 Distribution of annual cooling load

9.4.3 Sequential Monte Carlo simulation for quantifying unmet cooling load

Fig.9.10 shows the average unmet cooling loads when using 3, 5 and 7 cooling towers using sequential Monte Carlo simulation. It is obvious that the average unmet cooling load is getting smaller when the number of cooling tower increases. Fig.9.10 (a) shows the average unmet cooling load when using 3 cooling towers under different simulation trials. The average unmet cooling load varies greatly when the simulation trial is less than 250. About 530 sampling times (years) are needed to obtain the accurate average unmet cooling load and the average unmet cooling load fluctuates around the converged value 7330kWh. Fig.9.10 (b) shows the average unmet cooling load when using 5 cooling towers under different simulation trials. About 530 sampling times (years) are needed to obtain the accurate average unmet cooling load and the average unmet cooling load fluctuates around the converged value 814kWh. Fig.9.10 (c) shows the average unmet cooling load when using 7 cooling towers under different simulation trials. About 480 sampling times (years) are needed to obtain the accurate average unmet cooling load and the average unmet cooling load fluctuates around the converged value 100kWh. Therefore, Monte Carlo simulation approach is capable of providing more comprehensive information, such as the detailed changes of unmet cooling load.

Table 9.2 shows the converged average unmet cooling load under different options of cooling towers. It can be seen that the converged average unmet cooling load decreases rapidly when the number of cooling towers increases. When the number of cooling towers is large, further increase of the number will not result in obvious change of the average unmet cooling load any more.
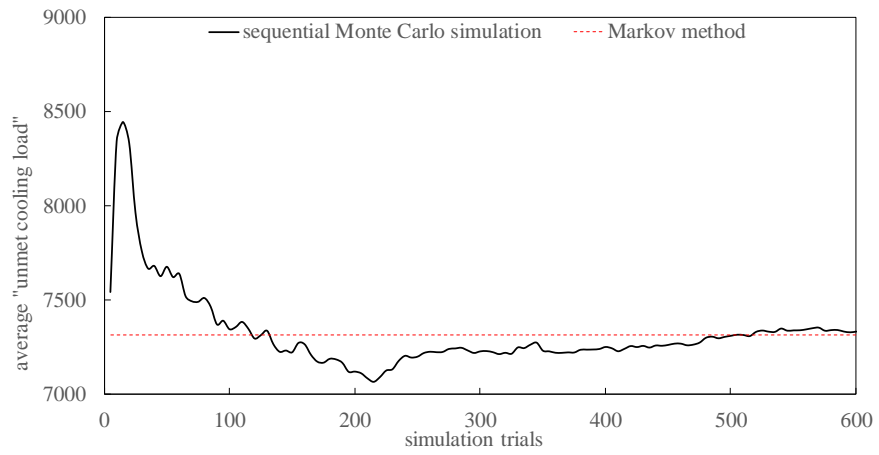
(a) 3 cooling towers
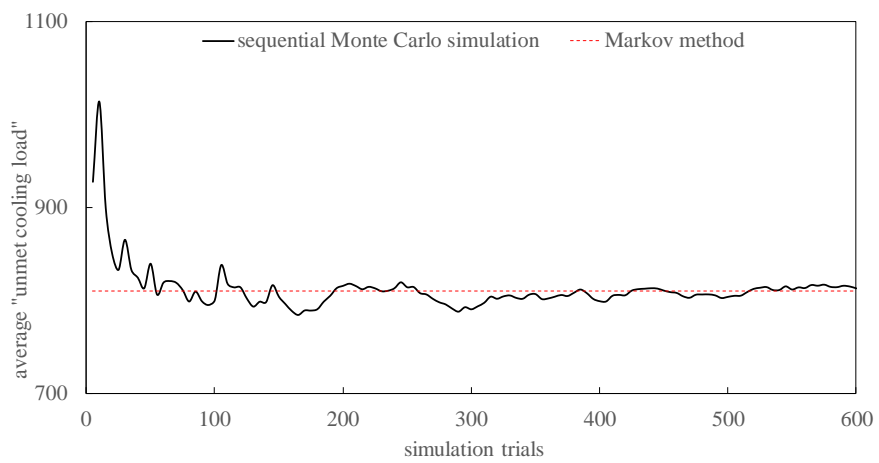
(b) 5 cooling towers
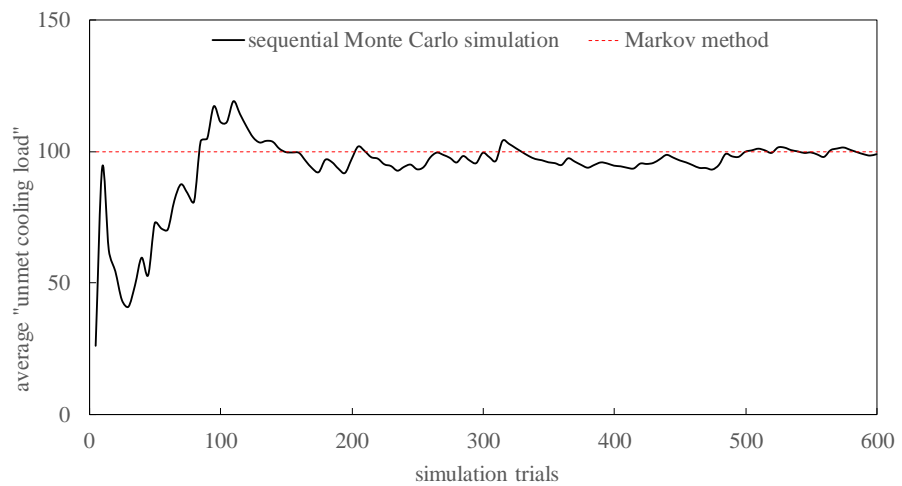
(c) 7 cooling towers

Fig.9.10 Average unmet cooling load vs number of simulation trials when using

different tower numbers

Table 9.2 Converged average unmet cooling load and average operation cost of

different cooling tower options

Options (Size (L/s) ×number)	165×2	110×3	83×4	66×5	55×6	47×7	41×8
Average unmet cooling load (kWh)	26504	7341	1961	814	325	100	60
Operation cost (10^3 HKD)	570	620	643	661	676	688	698

The electricity price used in this study is 1 HKD/kWh, which is within the range of the
typical rate in Hong Kong. Fig.9.11 shows the average operation costs when using 3, 5
and 7 cooling towers. It is obvious that the average operation cost is larger when more
cooling towers are used. Fig.9.11 (a), (b) and (c) show the average operation costs when
using 3, 5 and 7 cooling towers under different numbers of simulation trials respectively.
It can be seen that the average operation costs have no obvious change under different
simulation trials. The converged average operation costs when using 3, 5 and 7 cooling
towers are $6.2×10^5$, $6.62×10^5$ and $6.88×10^5$ respectively. Table 9.2 shows the converged
average operation costs using different design options of cooling towers. It can be seen
that the converged average operation cost increases when the number of cooling towers
increases.
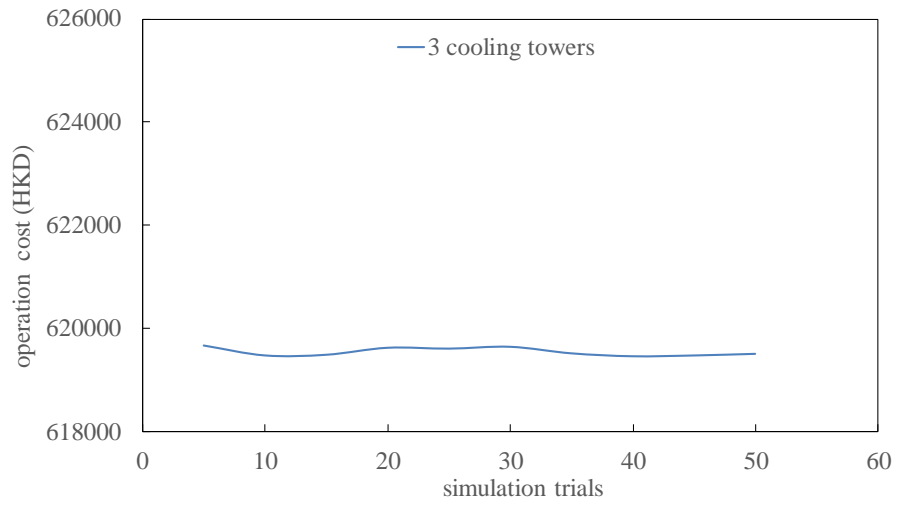
(a)
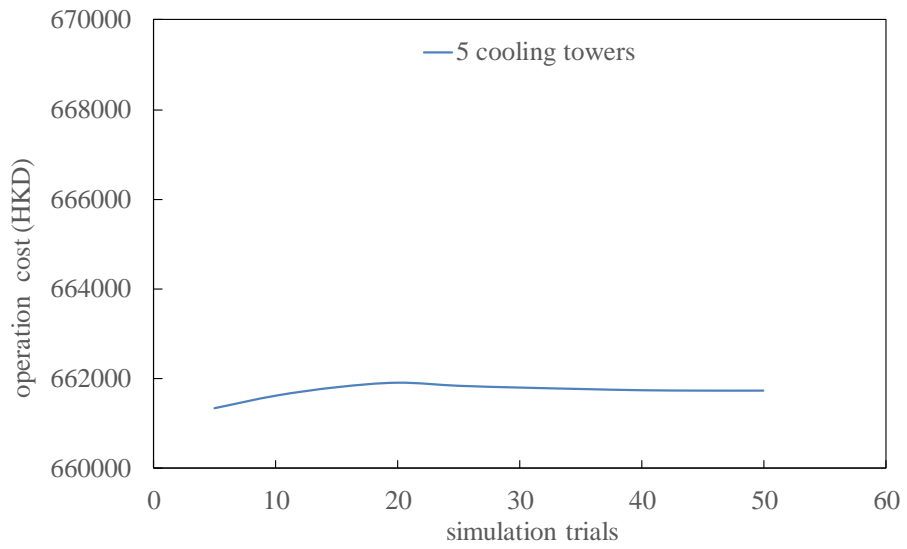
(b)
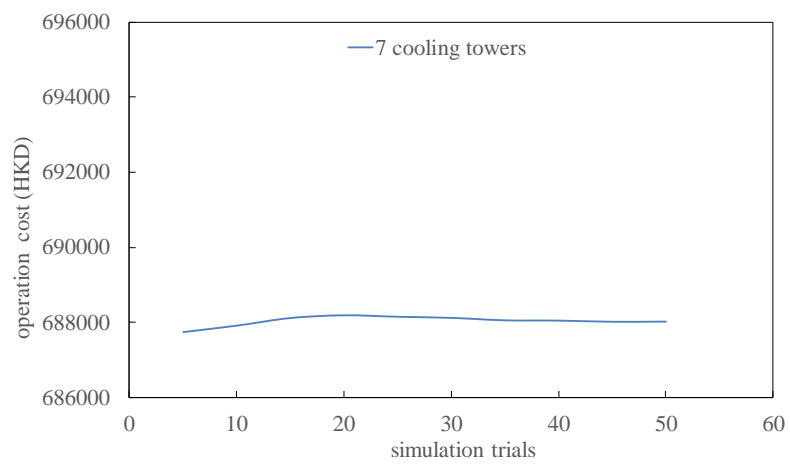
(c)

Fig.9.11 Average operation cost under different simulation trials

9.4.4 Optimal configuration of cooling water system

Annualized capital cost contains the equipment cost and space cost. The lifespan of the cooling water system is assumed to be 10 years. Equipment cost of cooling tower (110L/s) is 110,000HKD, referring to the data from a manufacturer. The cooling tower cost of other sizes are estimated using Equation (9.28).

$$EC = EC_0 \cdot (C / C_0)^{\alpha} \tag{9.28}$$

where, EC_0 is the equipment cost of the reference cooling tower with the capacity C_0. EC is equipment cost of cooling tower with the capacity C. α is the coefficient, which set to be 0.15 in this study. The space cost of cooling tower is assumed to be 5000HKD/unit/year.

Table 9.3 shows the capital costs, annual availability risk costs and total costs of different numbers of cooling towers under three penalty ratios (i.e., 1, 10 and 100 HKD/kWh). It is obvious that the annualized capital cost becomes larger when the number of cooling tower increases. It can be seen that, when the number of cooling towers is small, the annual availability risk cost decreases rapidly when the number of cooling tower increases. It can also be observed that the total cost decreases when the number of cooling tower increases in certain range and increases when the number of cooling tower increases further. Since the availability risk cost is high when the number of cooling towers is small and the capital cost and operation cost is high when the number of cooling towers is large, there is a comprised number/size of cooling tower which has the minimum total cost. In this study, the penalty ratio is assumed to be 10HKD/kWh. Among options assessed, the option, 83L/s×4 cooling towers, has the

minimum total cost 1.035×10^6 HKD, which can be considered as the best option under the design cooling water flow, 330L/s. If the penalty ratio is 1HKD/kWh, the best cooling tower option under the design cooling water flow is 165L/s×2. If the penalty ratio is 100HKD/kWh, the best cooling tower option under the design cooling water flow is 55L/s×6. The designers can select the best option based on their specific concern on the predefined penalty ratio.

Table 9.3 Annual availability risk cost (10^3HKD) and total cost (10^3HKD) of different cooling tower design options

Penalty ratio (HKD/kWh)	1			10			100		
Option (size (L/s)×number)	*CC*	*RC*	*TC*	*CC*	*RC*	*TC*	*CC*	*RC*	*TC*
165×2	313	26.5	910	313	265	1148	313	2650	3534
110×3	345	7.3	972	345	73.3	1038	345	733	1698
83×4	371	2	1017	***371***	***19.6***	***1035***	371	196	1211
66×5	393	0.81	1055	393	8.1	1063	393	81	1136
55×6	412	0.3	1090	412	3.3	1093	412	33	1122
47×7	430	0	1118	430	1	1119	430	10	1128
41×8	446	0	1144	446	1	1145	446	6	1150
Remarks: CC- capital cost*, RC-* availability risk cost*, TC-* total cost									

Table 9.4 shows the capital costs, annual availability risk costs and total costs of different numbers of pumps under three penalty ratios (i.e., 1, 10 and 100 HKD/kWh).

It is also obvious that the annualized capital cost becomes larger when the number of pumps increases. It can be seen that the annual availability risk cost of pumps is larger than that of cooling towers because of the larger failure rate of pumps. It can also be observed that the total cost decreases when the number of cooling tower increases. Among these options, the option 41L/s×8 pumps has the minimum total cost 1.119×10^{6}HKD, which can be considered as the best option in principle under the design cooling water flow of 330L/s. In practice, the number of cooling water pumps should be integer times of the number of chillers for the convenient capacity control when the cooling water pumps are constant speed pumps. Therefore, the option 41L/s×6 pumps may be considered as the best design option under the design cooling water flow 330L/s. If the penalty ratio is 1HKD/kWh, the best option under the design cooling water flow is 110L/s×3 pumps. If the penalty ratio is 100HKD/kWh, the best option under the design cooling water flow is 55L/s×6 pumps. The designers can select the best option based on their specific concern on the penalty ratio. Therefore, the best option of the cooling water system consists of 83L/s×4 cooling towers and 55L/s×6 pumps under the design cooling water flow rate 330L/s.

Table 9.4 Annual availability risk cost (10^3HKD) and total cost (10^3HKD) of different

pump design options

Penalty ratio (HKD/kWh)	1			10			100		
Option (size (L/s)×number)	CC	RC	TC	CC	RC	TC	CC	RC	TC
165×2	70	325	1129	70	3250	4054	70	32500	33298
110×3	91	114	978	91	1140	2003	91	11400	12249
83×4	111	55.3	962	111	553	1460	111	5530	6441
66×5	129	35.4	977	129	354	1296	129	3540	4480
55×6	146	20.1	994	*146*	*201*	*1175*	146	2010	2982
47×7	162	12.4	1016	162	124	1127	162	1240	2243
41×8	178	8.9	1039	178	89	1119	178	890	1923
Remarks: CC- capital cost*, RC-* availability risk cost, *TC-* total cost									

After conducting the trials on other design cooling water flow rates within the range
between 285 L/s and 420 L/s, the minimum total costs are computed corresponding to
each design flow rate respectively as shown in Table 9.5. When the design cooling water
flow rate increases from 285L/s to 375L/s, the total cost of cooling tower increases, the
total cost of pumps decreases and the total cost of the cooling water system decreases.
When the design cooling water flow rate is over 375 L/s (i.e. 375 L/s to 420L/s), the
total costs of both the cooling towers and pumps increase, which result in the increase
of total cost of the cooling water system. Among the options assessed, the option with

120L/s×3 cooling towers and 60L/s×6 pumps has the minimum total cost (i.e. 2.166×10^6 HKD) compared with other options. This option selected therefore has better robustness to uncertainties and system reliability.

Table 9.5 Best design options of cooling water system under different design cooling water flow rates (penalty ratio:10HKD/kW)

Design cooling water flow (L/s)		300	330	345	*360*	375	390
Cooling towers	Best options (size (L/s) ×number)	60×5	83×4	115×3	*120×3*	125×3	130×3
	Total cost (10^3HKD)	1,026	1,035	1,067	*1,076*	1,098	1,130
Cooling water pumps	Best options (size (L/s) ×number)	50×6	55×6	58×6	*60×6*	63×6	65×6
	Total cost (10^6HKD)	1.422	1.175	1.107	*1.090*	1.087	1.113
Total cost (10^6HKD)		2.448	2.210	2.178	*2.166*	2.185	2.243

9.4.5 System performance using different design methods

Table 9.6 shows the results of uncertainty-based design, conventional design and robust optimal design. It can be seen that the unmet cooling load of uncertainty-based design is much larger than that of conventional design and robust optimal design. Compared

with the total costs of conventional design (2.801×10^6HKD) and uncertainty-based optimal design (4.65×10^6HKD), the total cost under robust optimal design (2.166×10^6HKD) is reduced by about 22.7% and 53.4% respectively when the penalty ratio is 10 HKD/kW. To achieve the minimum annual total cost, the option with 120L/s×3 cooling towers and 60L/s×6 cooling water pumps can be selected as the optimum design option. This option has the minimum total cost and it also has good robustness considering the uncertainties of design inputs and reliability of system components.

Table 9.6 Best options using different design methods (penalty ratio:10HKD/kW)

		Conventional design	Uncertainty-based design	Robust optimal design
Design cooling water flow (L/s)		345	285	360
Cooling towers	Best options (size (L/s) ×number)	115×3	95×3	120×3
	Total cost (10^6HKD)	1.067	1.122	1.076
Cooling water pumps	Best options (size (L/s) ×number)	115×4 (one standby)	95×4 (one standby)	60×6
	Total cost (10^6HKD)	1.734	3.528	1.090
Total cost (10^6HKD)		2.801	4.650	2.166

9.5 Discussion

Table 9.7 shows the best design options under different repair rates. It can be observed that the required design cooling water flow rate decreases when the repair rate increases (i.e. the availabilities of cooling tower and pump increase). Users can choose the preferred repair rate based on their specific level or efficiency of handling the problems such as maintenance and failure.

Table 9.7 Best design options under different repair rates

Repair rate		0.001	0.002	0.003	0.004	0.005
Design cooling water flow (L/s)		375	360	345	315	315
Cooling towers	Best options (size (L/s) ×number)	125×3	120×3	115×3	79×4	105×3
	Total cost (10^3HKD)	1,072	1,076	1,044	1,009	1,001
Cooling water pumps	Best options (size (L/s) ×number)	63×6	60×6	58×6	53×6	53×6
	Total cost (10^3HKD)	1,284	1,090	1,020	999	975
Total cost (10^3HKD)		2,355	2,166	2,064	2,013	1,975

9.6 Summary

This chapter presented a robust optimal design method of cooling water system, which is based on a sequential Monte Carlo simulation to achieve the minimum annual total

cost of cooling water system considering both uncertainties of design inputs and reliability of system components in operation. It is realized by optimizing the design cooling water flow rate, the number/size of cooling towers and the number of cooling water pumps. The design method is tested and evaluated by conducting a case study. Based on the results, conclusions can be made as follows:

- Annual average cooling load and annual unmet cooling load varies largely when considering uncertainties. Sufficient sampling times are required to obtain the accurate cooling load distribution, operation cost and unmet cooling load. Sequential Monte Carlo simulation can be effectively used to obtain the accurate cooling load distribution, operation cost and unmet cooling load by quantifying the uncertainties of design inputs and the reliability of system components.

- Using Markov method can obtain accurate unmet cooling load and consume less computation time compared to sequential Monte Carlo simulation. However, Monte Carlo simulation approach is capable of providing more comprehensive information than Markov methods such as the detailed changes of unmet cooling load.

- The penalty ratio and repair rate can affect the determination of design cooling water flow rate and thus the selected best option. The optimal design cooling water flow rate is larger at the higher penalty ratio. The results also show that the design cooling water flow reduces when the repair rate increases.

- The design option of cooling water systems can be selected by achieving the

minimum total cost when considering uncertainties and system reliability. The selected cooling water system has the good robustness towards the uncertainties of design inputs and system reliability. The results of the case study show that the total cost of optimized system can be reduced significantly (totally 22.7%) compared with the conventional design.

It is worth noticing that the optimization output may be slightly different from the best one in principle as not all options/combinations are tested due to the interval selected in the tests and limitations on the available sizes of cooling towers and pumps in practice.

CHAPTER 10 CONCLUSIONS AND FUTURE WORK

In this chapter, main contributions of this thesis are summarized. Conclusions are made based on the above studies. Recommendations for future work are also presented.

10.1 Main Contributions of This Study

This study addresses the design optimization of HVAC systems (including chiller plant, chilled water system and cooling water system) considering uncertainties of design inputs and reliability of system components in operation. Main contributions are summarized as follows:

i. An uncertainty-based optimal design method for chiller plant is developed. Performance of the chiller plant using the proposed method is analyzed and compared with that using the conventional design method.

ii. Robust optimal design methods considering both uncertainty and reliability are developed and implemented in HVAC system (including chiller plant, chilled water system and cooling water system). The performance of HVAC systems using the robust optimal design method is evaluated and compared with that using the conventional method and uncertainty-based method.

iii. The uncertainties of the design inputs are quantified. Monte Carlo simulation is used for the quantification of uncertainty.

iv. The reliabilities of system components are quantified. Markov method and sequential Monte Carlo simulation are used for the quantification of reliability.

Markov method contains the Markov method with the same failure rate and Markov method with different failure rates.

v. A probabilistic approach is developed to determine the minimum sufficient number of Monte Carlo simulation. This approach is used to obtain the cooling load distribution of required accuracy considering the uncertainties of inputs.

10.2 Conclusions

Conclusions from the uncertainty-based optimal design method of chiller plant

i. An uncertainty-based optimal design method considering uncertainties of inputs is developed. It can ensure that the high performance and the minimum annual total cost of chiller plants could be achieved by optimizing the capacity and configuration of chiller plants.

ii. Annual average cooling load varies largely when considering uncertainties. It can be seen that the cooling load distribution profile of 780 simulation trials is smoother than that of reference case because more cooling load conditions are considered.

iii. The optimum configuration of the chiller plant can be selected by achieving the minimum total cost when considering uncertainties. The results of the case study show that the total cost of optimized chiller plant can be reduced significantly (i.e. 17.7%) compared with the conventional design.

Conclusions from the robust optimal design method of chiller plant

i. Quantification of uncertainties of design inputs is very important in determining the cooling load distribution of required accuracy. Based on the cooling load distribution, the searching range of total cooling capacity of chiller plant can be determined by the cooling capacities corresponding to different number of unmet hours.

ii. Markov method can be effectively used to obtain the probability distribution of system state (health) for high accuracy and fast computation time. In this study, different failure rates are considered for constant-speed chillers and variable-speed chillers.

iii. Compared with the chiller plant option with two variable-speed chillers, the chiller plant with one variable-speed chiller might operate at lower efficiency at part load conditions when the variable-speed chiller could not work. Given that the variable-speed chiller is more expensive than the constant-speed chiller, using one variable-speed chiller is economical in spite of the lower operating efficiency.

iv. The optimum design option of the chiller plant can be selected by achieving the minimum total cost when considering uncertainties and system reliability. The results of the case study show that the total cost of optimized chiller plant can be reduced significantly (totally 26% and 11.4%) compared with the conventional design and uncertainty-based optimal design.

Conclusions from the robust optimal design method of chilled water system

i. Annual average cooling load varies largely when considering uncertainties, which greatly affects the design of chilled water system. If the sizing of design cooling capacity is based on the cooling load without considering uncertainties, the design cooling capacity and design chilled water flow will be very likely oversized. If the

pump head is determined without considering the uncertainties of hydraulic resistance and water flow distribution, the oversize of pump head will be greatly increased.

ii.   Markov method can be effectively used to obtain the probability distribution of system state (health) for high accuracy and fast computation time.

iii.   The design option of the chilled water pump system can be selected by achieving the minimum total cost when considering uncertainties and system reliability. The results of the case study show that the total cost of optimized pump system can be reduced significantly (totally 18.6%) compared with the conventional design and uncertainty-based optimal design.

Conclusions from the robust optimal design method of cooling water system

i.   Sufficient sampling times are required to obtain the accurate cooling load distribution, operation cost and unmet cooling load. Sequential Monte Carlo simulation can be effectively used to obtain the accurate cooling load distribution, operation cost and unmet cooling load by quantifying the uncertainties of design inputs and the reliability of system components.

ii.   The penalty ratio and repair rate can affect the determination of design cooling water flow rate and thus the selected best option. The optimal design cooling water flow rate is larger at the higher penalty ratio. The results also show that the design cooling water flow reduces when the repair rate increases.

iii.   The design option of cooling water systems can be selected by achieving the

minimum total cost when considering uncertainties and system reliability. The results of the case study show that the total cost of optimized system can be reduced significantly (totally 22.7%) compared with the conventional design.

Conclusions from the probabilistic approach for generating the cooling load distribution

i.   Determining the minimum simulation number is very important for obtaining the accurate peak cooling load and cooling load distribution. The minimum simulation number required depends on the required accuracy. 780 simulation trials are found and used and to achieve an accuracy of 0.5% for both the peak cooling load and the cooling load distribution.

Conclusions from the reliability quantification methods

i.   The transition hours of Markov method could be ignored during the lifespan of a HVAC system. About 1500 hours (i.e., 83 days if the system works 18 hours daily) is required to achieve the steady state 0 when the Markov method is used.

ii.   The advantages of the Markov method include high accuracy and relatively fast computation time; the disadvantages are the inability to provide more reliability information (i.e. this method can only provide the average probability distribution of steady state of system).

iii.   Compared with Markov method, the sequential Monte Carlo simulation is capable of providing more comprehensive results than Markov method. However, the computation time using sequential Monte Carlo simulation is much longer than that using Markov method.

10.3 Further Work

This thesis answers several important questions about the robust optimal design of HVAC system but many other problems still need to be solved. Following points are recommended for further studies:

i. The selection of uncertainties may influence the final sizing of HVAC system. If a larger range of uncertainties is used, the total design capacity of HVAC system may be larger to reduce the availability risk cost and thus the optimal option may be different. Further study on the proper selection of uncertainties needs to be conducted.

ii. Effective and accessible tools are necessary to implement the proposed design methods in HVAC systems considering uncertainty and reliability. It will be helpful if such tools can be integrated with popular building energy simulation tools such as EnergyPlus, TRNSYS, etc. Similar tools for building energy systems are available such as GURA-Workbench. However, for the central cooling plant, such tools are still needed to be developed.

iii. Probability density functions to quantify the uncertainties of design inputs (except that representing the weather condition) in this study are mainly determined based on experiences or assumptions. It is necessary and important to develop more reliable methods to obtain probability density functions as reasonable/accurate as possible.

iv. The robust optimal design method can determine the optimal design of the HVAC system effectively in terms of the human effort of programming for implementing the method. It is worth noticing that the optimization output may not the perfect one as not all options/combinations are tested. It is necessary and significant to make a software package to implement the proposed design method with a small interval, which could include the design options as many as possible.

v. In this study, the chilled water pumps, cooling water pumps and cooling towers are assumed to be identical in parallel respectively, which can facilitate the control and maintenance in operation. Further study needs to be conducted on the optimization of the sizes of them, which could reduce the annual operation cost.

vi. The robust optimal design method is used for the design optimization of chiller plant, chilled water system and cooling water system. The quantifications of reliability of each subsystem are considered individually Further study needs to be conducted on the robust optimal design of HVAC system as a whole. Sequential Monte Carlo simulation can be effectively used to quantify the reliability of the whole HVAC system.

REFERENCES

Aguilar O., Kim J. K., Perry S., Smith R. 2008. Availability and reliability considerations in the design and optimization of flexible utility systems. Chemical Engineering Science 63(14): 3569-3584.

Ahlgren R C E 2001. Why did I buy such an oversized pump?. ASHRAE Transactions 107: 566.

Allan R.N. 2013. Reliability evaluation of power systems. Springer Science & Business Media.

Almeida R M S F, Ramos N M M, Manuel S 2015. Towards a methodology to include building energy simulation uncertainty in the Life Cycle Cost analysis of rehabilitation alternatives. Journal of Building Engineering 2: 44-51.

Anderson E L, Hattis D 1999. Foundations. Risk analysis 19(1): 47-68.

ASHRAE Handbook 2000. HVAC systems and equipment, Atlanta, GA.

ASHRAE Handbook 2004. HVAC systems and equipment, Atlanta, GA.

ASHRAE Handbook 2008. HVAC systems and equipment, Atlanta, GA.

ASHRAE Handbook 2009. Fundamentals. Atlanta, GA.

ASHRAE Handbook 2012. HVAC systems and equipment, Atlanta, GA.

Ashouri A, Petrini F, Bornatico R, Ben MJ 2014. Sensitivity analysis for robust design of building energy systems. Energy 76: 264-275.

Ata M Y 2007. A convergence criterion for the Monte Carlo estimates. Simulation Modelling Practice and Theory 15(3): 237-246.

Augenbroe G., Zhang Y., Khazaii J., Su H., Sun Y., Lee B. D., Wu C. J. 2013. Implications of the uncoupling of building and HVAC simulation in the presence

of parameter uncertainties. Proceedings of BS2013: 13th Conference of International Building Performance Simulation Association: 3169-3176.

Au-Yong C P, Ali A S, Ahmad F 2014. Improving occupants' satisfaction with effective maintenance management of HVAC system in office buildings. Automation in Construction 43: 31-37.

Bahnfleth W.P., Peyer E. 2006. Energy use and economic comparison of chilled-water pumping systems alternatives, ASHRAE Transaction 112 (2): 198–208.

Bai X., Asgarpoor S. 2004. Fuzzy-based approaches to substation reliability evaluation. Electric Power Systems Research 69(2): 197-204.

Bernier M.A. 1995. Thermal performance of cooling towers. ASHRAE journal 37(4).

Beven K 2010. Environmental modelling: an uncertain future?. CRC Press.

Biegler L T, Grossmann I E, Westerberg A W 1997. Systematic methods for chemical process design.

Billinton R, Chen H, Ghajar R 1996. A sequential simulation technique for adequacy evaluation of generating systems including wind energy. Energy Conversion, IEEE Transactions, 11(4): 728-734.

Billinton R, Zhang W 2001. Cost related reliability evaluation of bulk power systems. International journal of electrical power & energy systems 23(2): 99-112.

Blanchard A, Roy B.N 1998. Savannah River Site Generic Data Base development Savannah WSRC-TR-93-262. REV.1. Westinghouse Safety Management. Aiken (SC).

Booth A. T., Choudhary R., Spiegelhalter D. J. 2012. Handling uncertainty in housing stock models. Building and Environment 48: 35-47.

Braun J E, Klein S A, MITCEL J W 1989. Applications of optimal control to chilled water systems without storage. ASHRAE transactions 95: 663-675.

Brohus H., Frier C., Heiselberg P., Haghighat F. 2011. Quantification of uncertainty in predicting building energy consumption: A stochastic approach. Energy and Buildings 55: 127-140.

Burhenne S, Tsvetkova O, Jacob D 2013. Uncertainty quantification for combined building performance and cost-benefit analyses. Building and Environment 62: 143-154.

Burhenne S, Jacob D, Henze G P 2010. Uncertainty analysis in building simulation with Monte Carlo techniques. SimBuild 2010 Fourth National Conference of IBPSA-USA.

Carey J M, Burgman M A 2008. Linguistic uncertainty in qualitative risk analysis and how to minimize it. Annals of the New York Academy of Sciences 1128(1): 13-17.

Celuch J 2001. Hybrid chilled water plant. ASHRAE journal 43(7): 34-35.

Chang Y.C., Chen W.H. 2009. Optimal chilled water temperature calculation of multiple chiller systems using Hopfield neural network for saving energy. Energy 34(4):448-456.

Chang Y C, Lin J K, Chuang M H 2005. Optimal chiller loading by genetic algorithm for reducing energy consumption. Energy and Buildings 37(2): 147-155.

Cheng Q., Wang S.W., Yan C.C. 2016. Robust optimal design of chilled water systems in buildings with quantified uncertainty and reliability for minimized life-cycle cost. Energy and Buildings 126: 159-169.

Cheng Qi, Wang Shengwei, Yan Chengchu, Xiao Fu 2015. Probabilistic approach for

uncertainty-based optimal design of chiller plants in buildings. Applied Energy; http://doi:10.1016/j.apenergy.2015.10.097.

Chinese D., Nardin G., Saro O. 2011. Multi-criteria analysis for the selection of space heating systems in an industrial building. Energy 36(1): 556-565.

Crowther H, Furlong J 2004. Optimizing chillers & towers. ASHRAE Journal 46(7): 34.

CSD 1998. Hong Kong energy statistics, annual Report.

Cullen A C, Frey H C 1999. Probabilistic techniques in exposure assessment: a handbook for dealing with variability and uncertainty in models and inputs. Springer.

DeST.   2011. http://dest.tsinghua.edu.cn/chinese/default1.asp?accessdenied=%2Fchinese%2Fdefault%2Easp#.

De Wit S., Augenbroe G. 2002. Analysis of uncertainty in building design evaluations and its implications. Energy and Buildings 34(9): 951-958.

Djunaedy E., Van Den Wymelenberg K., Acker B., Thimmana H. 2011. Oversizing of HVAC system: Signatures and penalties. Energy and Buildings 43(2–3): 468-475.

DOE-2. 2009. Building Energy Use and Cost Analysis Tool. http://doe2.com/doe2/index.html.

Domínguez-Muñoz F, Cejudo-López J M, Carrillo-Andrés A 2010. Uncertainty in peak cooling load calculations. Energy and Buildings 42(7): 1010-1018.

Eisenhower B, O'Neill Z, Fonoberov VA, Mezić 547 I 2011. Uncertainty and sensitivity decomposition of building energy models. Journal of Building Performance Simulation 5(3):171-184.

EMSD 2012. Hong Kong energy end-use data.

EnergyPlus energy simulation software. 2015. http://apps1.eere.energy.gov/buildings/energyplus/?utm_source=EnergyPlus&utm_medium=redirect&utm_campaign=EnergyPlus%2Bredirect%2B1.

Fiksel J 2003. Designing resilient, sustainable systems. Environmental science & technology 37(23): 5330-5339.

Finkel A M 1990. Confronting Uncertainty in Risk Management: A Guide for Decision-makers: a Report. Center for Risk Management, Resources for the Future.

Fowlkes W Y, Creveling C M 1995. Engineering methods for robust product design. Addison-Wesley.

Frangopoulos C. A., Dimopoulos G. G. 2004. Effect of reliability considerations on the optimal synthesis, design and operation of a cogeneration system. Energy 29(3): 309-329.

Gang W.J., Augenbroe G., Wang S.W., Fan C., Xiao F. 2016. An uncertainty-based design optimization method for district cooling systems. Energy 102: 516-527.

Gang W, Wang S, Shan K 2015. Impacts of cooling load calculation uncertainties on the design optimization of building cooling systems. Energy and Buildings 94: 1-9.

Gang W.J., Wang S.W., Xiao F, Gao D.C. 2015. Robust optimal design of building cooling systems considering cooling load uncertainty and equipment reliability. Applied Energy 159: 265-275.

Gang W.J., Wang S.W., Yan C.C., Xiao F 2015. Robust optimal design of building cooling systems concerning uncertainties using mini-max regret theory. Science

and Technology for the Built Environment 21(6): 789-799.

Ge H., Asgarpoor S. 2011. Parallel Monte Carlo simulation for reliability and cost evaluation of equipment and systems. Electric Power Systems Research 81(2): 347-356.

Gentle J E 2003. Random number generation and Monte Carlo methods. Springer.

Gidwani B N 1987. Optimization of chilled water systems. Energy Engineering.

Gillund F, Kjølberg K A, Krayer von Krauss M 2008. Do uncertainty analyses reveal uncertainties? Using the introduction of DNA vaccines to aquaculture as a case. Science of the total environment 407(1): 185-196.

Gorter J L 2012. HVAC Equipment right-sizing: Occupant comfort and energy savings potential. Energy Engineering 109(1): 59-75.

Guthrie K.M. 1969. Capital cost estimating. Chemical Engineering 3:114–142.

Hansen E.G. 1995. Parallel operation of variable speed pumps in chilled water systems. ASHRAE Journal 37 (10): 34–38.

Hartman T 2001. All-variable speed centrifugal chiller plants. ASHRAE journal 43(9): 43-53.

Harvey D 2012. A handbook on low-energy buildings and district-energy systems: fundamentals, techniques and examples. Routledge.

Heiselberg P., Brohus H., Hesselholt A., Rasmussen H., Seinre E., Thomas S. 2009. Application of sensitivity analysis in design of sustainable buildings. Renewable Energy 34(9): 2030-2036.

Heising C. 1991. IEEE recommended practice for the design of reliable industrial and commercial power systems: IEEE Inc., New York.

Hong T, Yang L, Hill D 2014. Data and analytics to inform energy retrofit of high performance buildings. Applied Energy 126: 90-106.

Hopfe C J, Hensen J L M 2011. Uncertainty analysis in building performance simulation for design support. Energy and Buildings 43(10): 2798-2805.

Huang P., Huang G., Wang Y. 2015. HVAC system design under peak load prediction uncertainty using multiple-criterion decision making technique. Energy and Buildings 91: 26-36.

Jin G.Y., Cai W.J., Lu L., Lee E.L., Chiang A. 2007. A simplified modeling of mechanical cooling tower for control and optimization of HVAC systems. Energy conversion and management 48(2): 355-365.

Kaya A 1991. Improving efficiency in existing chillers with optimization technology. ASHRAE Journal 33(10).

Keith R. Hayes 2011. Uncertainty and uncertainty analysis methods. Issues in quantitative and qualitative risk modeling with application to import risk assessment ACERA project.

Kim J.K., Smith R. 2001. Cooling water system design. Chemical Engineering Science 56(12): 3641-3658.

Koury R N N, Machado L, Ismail K A R 2001. Numerical simulation of a variable speed refrigeration system. International Journal of Refrigeration 24(2): 192-200.

Kwak R.Y., Takakusagi A., Sohn J.Y., Fujii S., Park B.Y. 2004. Development of an optimal preventive maintenance model based on the reliability assessment for air-conditioning facilities in office buildings. Building and Environment 39(10): 1141-1156.

Lee P., Lam P., Yik F. W., Chan E. H. 2013. Probabilistic risk assessment of the energy saving shortfall in energy performance contracting projects–A case study. Energy and Buildings 66: 353-363.

Lee W L, Lee S H 2007. Developing a simplified model for evaluating chiller-system configurations. Applied energy 84(3): 290-306.

Lee W L, Yik F W H, Jones P 2001. Energy saving by realistic design data for commercial buildings in Hong Kong. Applied Energy 70(1): 59-75.

Lee W, Yik F W H, Burnett J 2001. Simplifying energy performance assessment in the Hong Kong building environmental assessment method. Building Services Engineering Research and Technology 22(2): 113-132.

Li DHW, Wong SL, Lam JC 2003. Climatic effects on cooling load determination in subtropical regions. Energy Conversion and Management 44(11):1831-1843

Li C Z, Shi Y M, Huang X H 2008. Sensitivity analysis of energy demands on performance of CCHP system. Energy Conversion and Management 49(12): 3491-3497.

Lisnianski A 2007. Extended block diagram method for a multi-state system reliability assessment. Reliability Engineering & System Safety 92(12): 1601-1607.

Lisnianski A, Levitin G 2003. Multi-state System Reliability: Assessment, Optimization and Applications. World Scientific.

Lisnianski A, Elmakias D, Laredo D, Haim HB 2012. A multi-state Markov model for a short-term reliability analysis of a power generating unit. Reliability Engineering & System Safety 98(1): 1-6.

Lu L., Cai W., Soh Y.C., Xie L., Li S. 2004. HVAC system optimization—condenser

water loop. Energy Conversion and Management 45(4): 613-630.

Lu Y.Q. 2008. Practical HVAC design manual. China Architecture & Building Press. (In Chinese).

Ma Z, Wang S 2011. Supervisory and optimal control of central chiller plants using simplified adaptive models and genetic algorithm. Applied Energy 88(1): 198-211.

Ma Z.J., Wang S.W. 2011. Enhancing the performance of large primary-secondary chilled water systems by using bypass check valve. Energy 36(1): 268-276.

Mansfield S K 2001. Oversized pumps--a look at practical field experiences. ASHRAE Transactions 107: 573.

Marley Cooling Tower Company 1983.Cooling tower fundamentals.

McCann R K, Marcot B G, Ellis R 2006. Bayesian belief networks: applications in ecology and natural resource management. Canadian Journal of Forest Research 36(12): 3053-3062.

Menassa C. C. 2011. Evaluating sustainable retrofits in existing buildings under uncertainty. Energy and Buildings 43(12): 3576-3583.

Milosavljevic N., Heikkilä P. 2001. A comprehensive approach to cooling tower design. Applied Thermal Engineering 21(9): 899-915.

Mohiuddin A.K.M., Kant K 1996. Knowledge base for the systematic design of wet cooling towers. Part I: Selection and tower characteristics. International Journal of Refrigeration 19(1): 43-51.

Morari M 1983. Flexibility and resiliency of process systems. Computers & chemical engineering 7(4): 423-437.

Morgan M G, Small M 1992. Uncertainty: a guide to dealing with uncertainty in

quantitative risk and policy analysis. Cambridge University Press.

Murray N 2002. Import risk analysis: animals and animal products. Import risk analysis: animals and animal products.

Myrefelt S 2004. The reliability and availability of heating, ventilation and air conditioning systems. Energy and Buildings 36(10): 1035-1048.

Nolte D 2004. Why efficiency matters. World Pumps 448: 27-29.

O'Neill Z., Eisenhower B. 2013. Leveraging the analysis of parametric uncertainty for building energy model calibration. Building Simulation 6(4): 365-377.

Panjeshahi M.H., Ataei A., Gharaie M., Parand R. 2009. Optimum design of cooling water systems for energy and water conservation. Chemical Engineering Research and Design 87(2): 200-209.

Park G J 2007. Analytic methods for design practice. Germany: Springer.

Peruzzi L, Salata F, De Lieto Vollaro A, De Lieto Vollaro R 2014. The reliability of technological systems with high energy efficiency in residential buildings. Energy and Buildings 68: 19-24.

Pettersen T. D. 1994. Variation of energy consumption in dwellings due to climate, building and inhabitants. Energy and Buildings 21(3): 209-218.

Phadke M S 1995. Quality engineering using robust design. Prentice Hall PTR.

Picón-Núnez M., Polley G.T., Canizalez-Dávalos L.,Medina-Flores J.M. 2011. Short cut performance method for the design of flexible cooling systems. Energy 36(8): 4646-4653.

Raftery P., Lee E., Webster T., Hoyt T., Bauman F. 2014. Effects of Furniture and Contents on Peak Cooling Load. Energy and Buildings 85: 445-457.

Rezaee R., Brown J., Augenbroe G. 2014. Building Energy Performance Estimation in Early Design Decisions: Quantification of Uncertainty and Assessment of Confidence. Construction Research Congress: 2195-2204.

Rishel JB, Durkin TH, Kincaid BL 2006. HVAC pump handbook. NY: McGraw-Hill Professional.

Rudoy W., Cuba J. F. 1979. Cooling and heating load calculation manual. American Society of Heating, Refrigerating and Air-Conditioning Engineers.

Sadeghi S A, Karava P 2014. Stochastic Model Predictive Control of Mixed-mode Buildings Based on Probabilistic Interactions of Occupants with Window Blinds.

Saltelli A, Tarantola S, Campolongo F 2004. Sensitivity analysis in practice: a guide to assessing scientific models. John Wiley & Sons.

Seider W D, Seader J D, Lewin D R 2009. Product & process design principles: synthesis, analysis and evaluation. John Wiley & Sons.

Shiming D 2002. Sizing replacement chiller plants. ASHRAE journal 44(6): 47-49.

Smith A, Luck R, Mago P J 2010. Analysis of a combined cooling, heating, and power system model under different operating strategies with input and model data uncertainty. Energy and Buildings 42(11): 2231-2240.

Stanford III H W 2011. HVAC water chillers and cooling towers: fundamentals, application, and operation. CRC Press.

Stapelberg RF 2009. Handbook of reliability, availability, maintainability and safety in engineering design. Springer.

Sun Y, Gu L, Wu C F 2014. Exploring HVAC system sizing under uncertainty. Energy and Buildings 81: 243-252.

Sun Y, Gu L, Wu C F J 2014. Sizing HVAC systems under uncertainty. ASHRAE/IBPSA-USA Building Simulation Conference, Atlanta, GA, September 10-12.

Sun YJ, Wang SW, Xiao F 2013. In situ performance comparison and evaluation of three chiller sequencing control strategies in a super high-rise building. Energy and Buildings 61: 333-343.

Taal M, Bulatov I, Klemeš J, StehlíK P 2003. Cost estimation and energy price forecasts for economic evaluation of retrofit projects. Applied Thermal Engineering 23(14): 1819-1835.

Tanner R A, Henze G P 2014. Stochastic control optimization for a mixed mode building considering occupant window opening behavior. Journal of Building Performance Simulation 7(6): 427-444.

Tassou S A, Qureshi T Q 1998. Comparative performance evaluation of positive displacement compressors in variable-speed refrigeration applications. International Journal of Refrigeration 21(1): 29-41.

Tian Z, Levitin G, Zuo M J 2009. A joint reliability–redundancy optimization approach for multi-state series–parallel systems. Reliability Engineering & System Safety 94(10): 1568-1576.

Tirmizi S A, Gandhidasan P, Zubair S M 2012. Performance analysis of a chilled water system with various pumping schemes. Applied Energy 100: 238-248.

Trane 2005. Plants with multiple chillers. Trane publications. http://www.trane.com/commercial/library/vol281/plants.asp [as at 31 December 2005].

TRNSYS 2004. TRNSYS 16 documentation. <http://sel.me.wisc.edu/trnsys>.

Transient System Simulation Tool. 2015. http://www.trnsys.com/.

United Nations Environment Program 2006. Energy Efficiency Guide for Industry in Asia.

Vanderhaegen F 2001. A non-probabilistic prospective and retrospective human reliability analysis method—application to railway system. Reliability Engineering & System Safety 71(1): 1-13.

Van Gelder L, Janssen H, Roels S 2013. Effective and robust measures for energy efficient dwellings: probabilistic determination. Building Simulation: 3465-3472.

Walker W E, Harremoës P, Rotmans J 2003. Defining uncertainty: a conceptual basis for uncertainty management in model-based decision support. Integrated assessment 4(1): 5-17.

Walski T, Zimmerman K, Dudinyak M, Dileepkumar P 2003. Some surprises in estimating the efficiency of variable speed pumps with the pump affinity laws. Proc. World Water and Environmental Resources Congress: 1-10.

Wang S.W., Burnett J. 2001. Online adaptive control for optimizing variable-speed pumps of indirect water-cooled chilling systems. Applied Thermal Engineering 21 (11): 1083–1103.

Wang S.W., Ma Z.J. 2008. Supervisory and optimal control of building HVAC systems: A review. HVAC&R Research 14(1): 3-32.

Wang S.W., Yan C.C., Xiao F 2012. Quantitative energy performance assessment methods for existing buildings. Energy and Buildings 55: 873-888.

Woradechjumroen D., Yu Y., Li H., Yu D., Yang H. 2014. Analysis of HVAC system

oversizing in commercial buildings through field measurements. Energy and Buildings 69: 131-143.

Yan Chengchu, Wang Shengwei, Xiao Fu 2012. A simplified energy performance assessment method for existing buildings based on energy bill disaggregation, Energy and buildings 55: 563-574.

Yan C.C., Wang S.W., Xiao F., Gao D.C. 2015. A multi-level energy performance diagnosis method for energy information poor buildings. Energy 83: 189-203.

Yıldız Y, Arsan Z D 2011. Identification of the building parameters that influence heating and cooling energy loads for apartment buildings in hot-humid climates. Energy 36(7):542 4287-4296.

Yik F W H, Lee W L, Burnett J 1999. Chiller plant sizing by cooling load simulation as a means to avoid oversized plant. HKIE Transactions 6(2): 19-25.

Yu F W, Chan K T 2007. Strategy for designing more energy efficient chiller plants serving air-conditioned buildings. Building and environment 42(10): 3737-3746.

Yu P C H, Chow W K 2000. Sizing of air-conditioning plant for commercial buildings in Hong Kong. Applied energy 66(2): 91-103.

Zang C, Friswell M I, Mottershead J E 2005. A review of robust optimal design and its application in dynamics. Computers & structures 83(4): 315-326.

Zhang Y., Augenbroe G. 2014. Right-sizing a residential photovoltaic system under the influence of demand response programs and in the presence of sysetm uncertainties. 2014 ASHRAE/IBPSA-USA Building Simulation Conference, September 10-12, Atlanta, GA, United States.

Zhou Z, Zhang J, Liu P 2013. A two-stage stochastic programming model for the

optimal design of distributed energy systems. Applied Energy 103: 135-144.